NKS-358
ISBN 978-87-7893-442-0

Effects of dynamic behaviour of Nordic marine environment to radioecological assessments

Iosjpe[1] M.
Isaksson[2] M.
Joensen[3] H. P.
Jonsson[4] G.
Logemann[5] K.
Roos[6] P.
Suolanen[7] V.
Thomas[2] R.

1 Norwegian Radiation Protection Authority, Norway
2 University of Gothenburg, Sweden
3 Fróðskaparsetur Føroya, Faroe Islands
4 Geislavarnir Rikisins, Iceland
5 University of Iceland, Iceland
6 Technical University of Denmark, Denmark
7 Technical Research Centre of Finland, Finland

February 2016

Abstract

The goal of the EFMARE project is an analysis of consequences of radioactive releases into marine environment with special attention to the effects of the dynamic behaviour of the Nordic seas to radioecological assessments.

The main goals for the EFMARE project is development and implementation of the bioaccumulation process into the models, improvement of the models, comparison with previous results and testing of the influence of the time of an accident for the radioecological consequences.

Results of implementation of the kinetic model for bioaccumulation processes into the NRPA box model and the DETRA computer code clearly demonstrated that there is a significant quantitative difference between the kinetic modelling approach and the approach based on the constant concentration rates.

Results of modelling were compared with experimental data on the basis of improved version of the NRPA box model for the Baltic Sea. It is clear demonstration that dynamic modelling of the bioaccumulation processes can provide a more correct description of the concentration of radionuclides in biota and, therefore, these results support the main goal of the EFMARE project.

It is shown that the improved modelling approach for radioecological assessment indicates significant differences between results based on constant concentration factors (CF) and the description of bioaccumulation process with a kinetic submodel. Also, kinetic modelling of bioaccumulation processes leads to a better harmonisation between the different end points calculations (for example, between doses to the critical group and concentrations in marine organisms for short-life radionuclides), and also to better logical explanations of the results.

With a numerical case study the temporal variability of pollutant dispersal in Icelandic waters was demonstrated and discussed. The results emphasize the necessity to use operational hydrodynamic ocean models in order to forecast pollutant dispersal in Icelandic waters.

The use of particle density can be used for comparison with simulations from the NRPA box model.

Key words

marine environment, hydrodynamic and box modelling, bioaccumulation submodel, accidents, radioecological consequences

NKS-358
ISBN 978-87-7893-442-0
Electronic report, February 2016

NKS Secretariat
P.O. Box 49
DK - 4000 Roskilde, Denmark
Phone +45 4677 4041
www.nks.org
e-mail nks@nks.org

Effects of dynamic behaviour of Nordic marine environment to radioecological assessments (EFMARE)

Final Report for the NKS-B EFMARE activity 2015
Contract AFT/B(14)12

Iosjpe Mikhail, Norwegian Radiation Protection Authority, Norway
Isaksson Mats, University of Gothenburg, Sweden
Joensen Hans Pauli, Fróðskaparsetur Føroya, Faroe Islands
Jonsson Gisli, Geislavarnir Rikisins, Iceland
Logemann Kai, University of Iceland, Iceland
Roos Per, Technical University of Denmark, Denmark
Suolanen Vesa, Technical Research Centre of Finland, Finland
Thomas Rimon, University of Gothenburg, Sweden

January 2016

Content

1. Introduction

The analysis of the consequences of some hypothetical NPP and submarine reactor accidents in the coastal Nordic marine environment (COSEMA, 2014) showes conclusively that it is possible to improve the present evaluation by a more detailed modelling of the key processes for radioecological assessment.

High concentrations of radionuclides in fish, detected long time after the Fukushima accident, have also supported a hypothesis about the necessity to include the dynamic ingestion of radionuclides by marine organisms into the radioecological assessment.

According to the proposed activity under the course of the EFMARE project, analysis of consequences of accidental radioactive releases to Nordic marine environment was provided with special attention to the effects of the dynamic behaviour of the Nordic marine environment to radioecological assessments.

The main hypotheses which are tested in the present project can be desctribed with following expressions: Is it true that the description of the bioaccumulation process, which is based on the use of constant concentration rates/factors can be significantly improved by involving a food web modelling approach? Is it especially important during the initial dynamic phase of an accident when no equilibrium conditions exist?

Radioecological assessment covers complex processes such as dispersion of radionuclides in oceanic space, transfer of radioactivity between seawater and sediments, uptake of radionuclides by biota and, finally, dose calculations for man and biota. The time of an accident can be a significant factor for the evaluation of the concentration of radionuclides in marine environment. Implementation of the variability / seasonality can be significant for many Nordic coastal sea areas, because their complex hydrodynamics often show a substantial seasonal variability. Evaluation of the seasonality with following implementation into the models is another task for the present project.

Evaluation of the dispersion of radionuclides in water and sediment phases with following effective dose calculation via marine food is performed on the basis of the improved version of the computer codes from the national institutes (Hydrodynamic model from University of Iceland, VTT’s Detra-code and NRPA compartment model).

2. Improvements and achievements in modelling of radionuclides dispersal.

2.1. Temporal variability of pollutant dispersal in Icelandic Waters – a numerical case study.

Maritime accidents can lead to a large variety of environmental threads. From oil slicks at the sea surface to dangerous material deposited at the sea floor, from dispersed molecules to drifting containers. Once an accident has happened the competent authorities will try to determine the risks for the ambient ocean area, particularly if the accident has happened in a coastal, economically important zone like the Icelandic waters. A crucial part of this risk assessment is the forecast of the particular pollutant's dispersal. Traditionally, estimated or assumed mean ocean current fields are used for these computations. However, meanwhile we obtained, based on refined measurements and numerical ocean simulations more information about the flow fields and found many indications of much more variable ocean dynamics than previously expected. The question arises whether and, if so, how this variability should be considered in those dispersal estimations. In this study we therefore examine the temporal variability of a fictive pollutant's dispersal in Icelandic waters with a set of numerical experiments based on the flow fields of an operational hydrodynamic model.

2.1.1. Experimental Setup

We selected the position 66.5°N, 25°W, northwest of Iceland within Denmark Strait as the location of a fictive accident. The ocean depth here is around 170 m which indicates that it is above the Icelandic continental slope. We assume a temporal constant source of pollution which is evenly spread throughout the whole water column. This pollution is simulated by the gradual release of 5000 particles during a time period of 3 months. I.e. the particle initial positions is randomly chosen at 66.5°N±0.125°, 25°W±0.25° in a depth between 0 and 170 m. Thereafter, the particles' passive drift with the ocean currents, including a parameterized random walk referring to non-resolved turbulence, is simulated based on the data given by the hydrodynamic model CODE (Logemann et al. 2013).

The temporal range of these three-months experiments cover the four seasons, i.e. from 1 January to 31 March, from 1 April to 30 June, from 1 July to 30 September and from 1 October to 31 December. These four seasonal experiments are repeated for 10 different years: from 2004 to 2013. Hence, an overall number of 40 experiments were performed.

2.1.2. Results

In order to analyse the simulated particle drift pattern we used the 5000 particle positions (latitude, longitude) at the end of each experiment and converted these into a continuous "particle density" field. Therefore, we counted the number of particles in a 5 nm (9.26 km) radius around each point of a spherical matrix with a 1' resolution (Fig. 1). Hence, the "particle density" describes the probability to find a particle at a given position. It can be also interpreted as the concentration of a pollutant emitted at the source position (point "S" in fig. 1).

All 40 experiments show a mainly eastward particle drift. However, also a south-westward drift onto the East-Greenland shelf can be detected (results of simulations can be found in the Appendix 1).

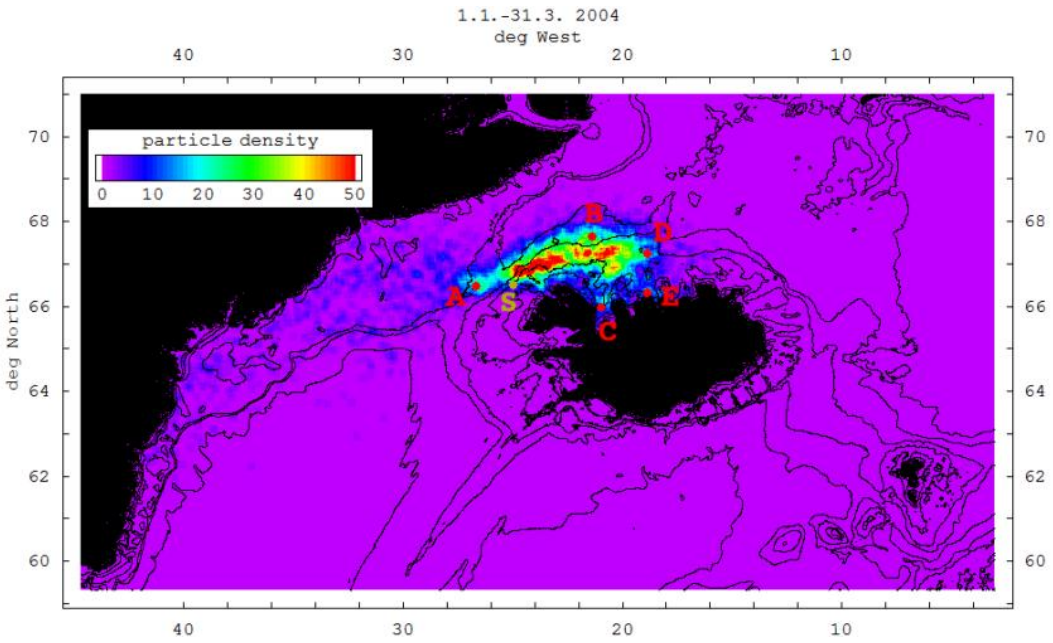

Fig. 1: Particle density at the end of the winter 2004 simulation. The point denoted with "S" shows the source position. The points "A", "B", "C", "D", and "E" denote the stations where time series were constructed.

Figure 1 shows the positions of five stations – A, B, C, D, E – where we extracted the particle density at the end of each experiments, this way obtaining five time series (tab. 1). The five time series show a generally high variability with values between 0 and 70 (Figures. 2 – 6).

Table 1: Positions and depth of the five stations where the particle time series were extracted.

Station	Latitude (°N)	Longitude (°W)	Depth (m)
A	66.4833	26.7000	506
B	67.6500	21.3667	703
C	65.9833	20.9500	178
D	67.2333	18.8667	460
E	66.3167	18.8667	172

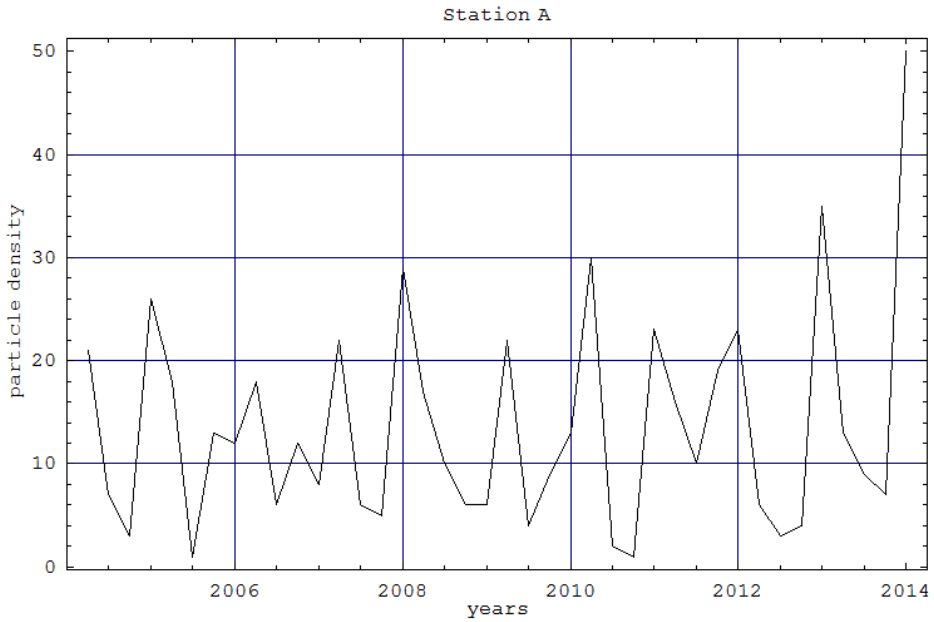

Fig. 2: Particle density time series at station A.

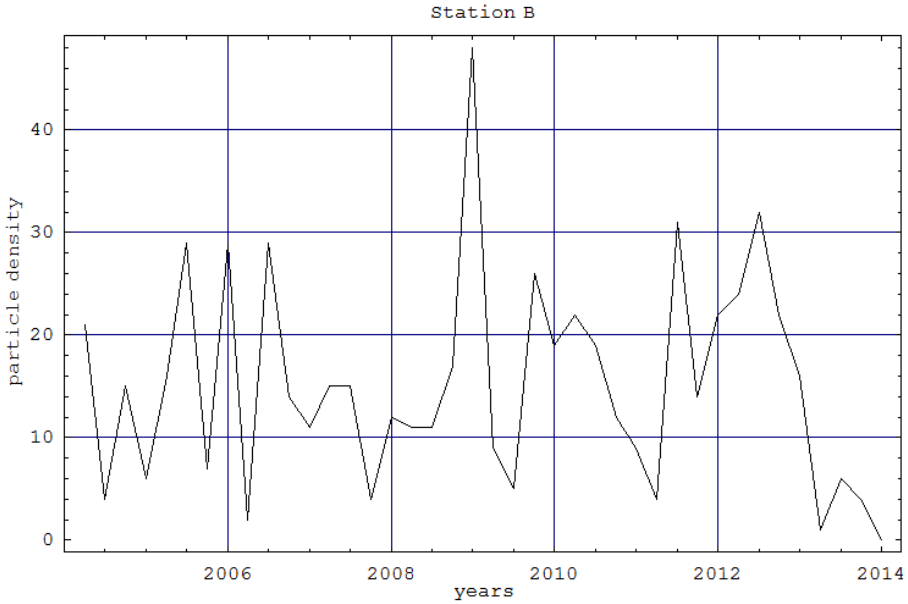

Fig. 3: Particle density time series at station B.

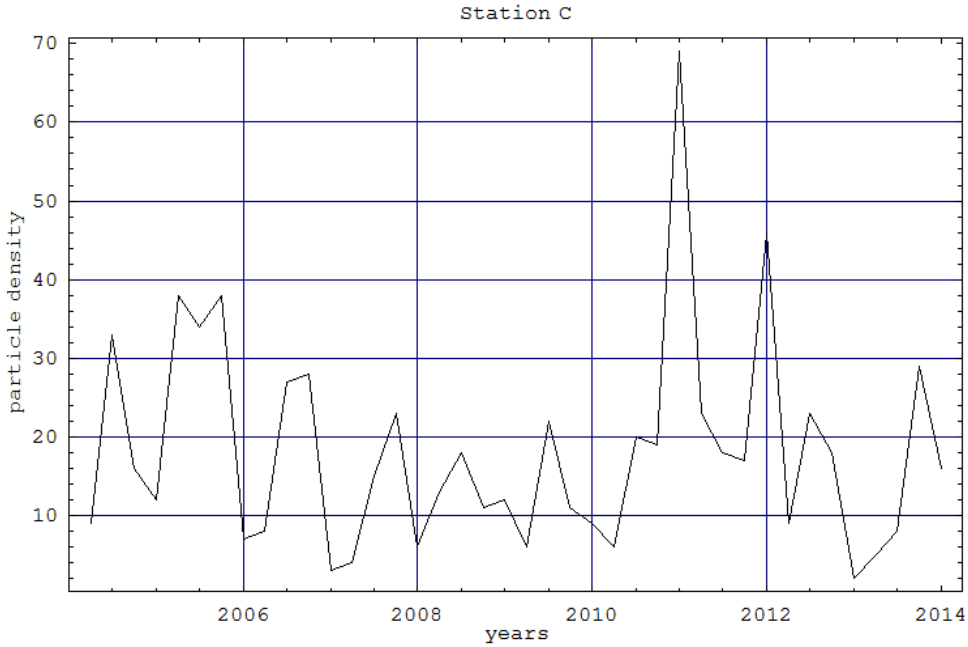

Fig. 4: Particle density time series at station C.

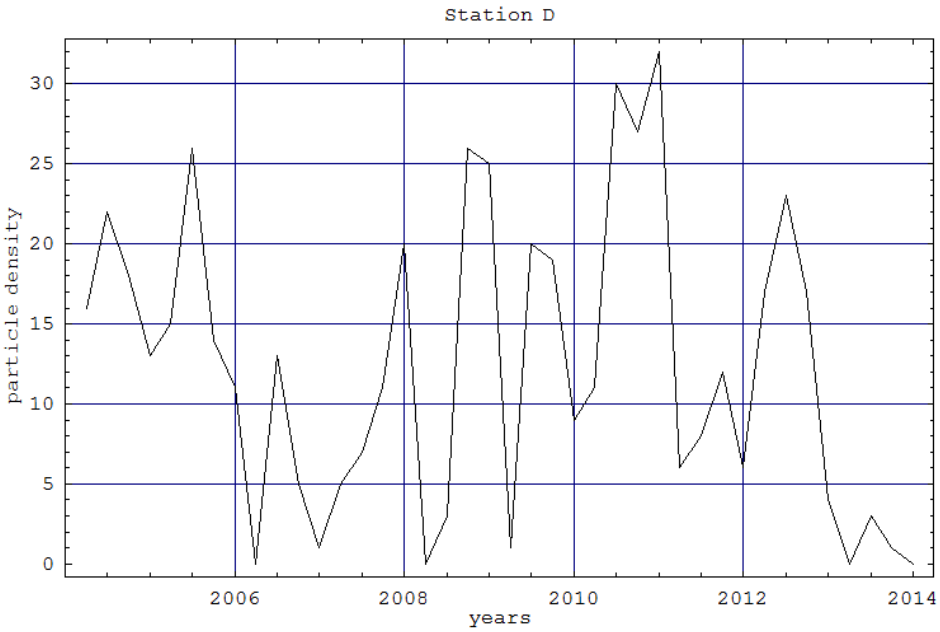

Fig. 5: Particle density time series at station D.

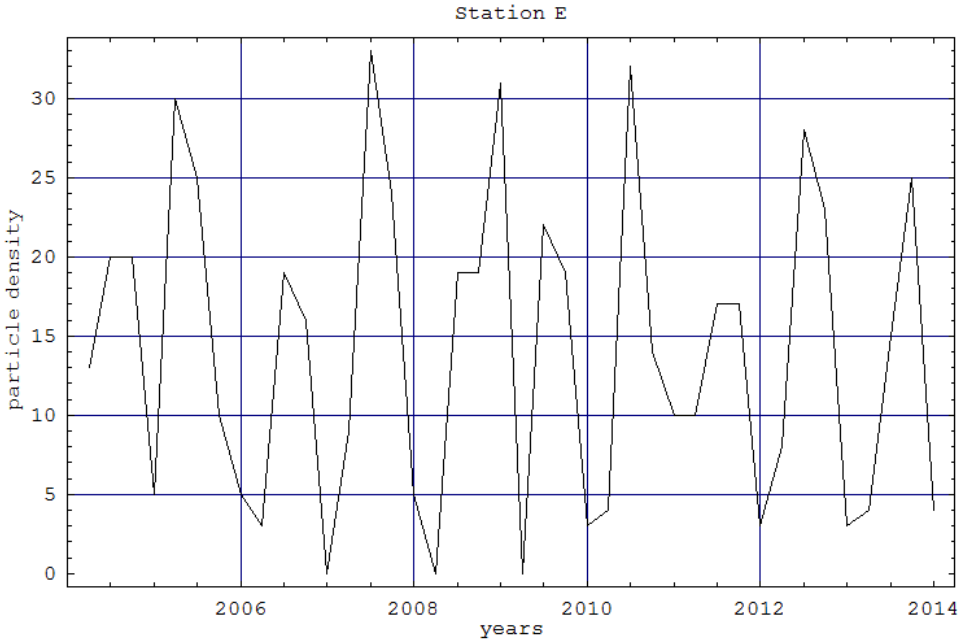

Fig. 6: Particle density time series at station E.

2.1.3. Discussion

The principal feature of the simulated pollutant dispersal is the eastward drift with the North Icelandic Irminger Current (NIIC), a flow of relatively warm and salty Atlantic Water northwards through Denmark Strait and further eastwards over the North Icelandic shelf. Therefore, at the end of the three-month simulation, the majority of the particles is found over the northern shelf between 25°W and 15°W.

The other pathway of particles, which is less established but equally persistent, leads to the south-west onto the East Greenland shelf. Here, even larger distances compared to the NIIC path are achieved, down to the southern tip of Greenland at 60°N. The explanation for this path is the turbulent entrainment of some particles near the source point into the southward flowing East Greenland Current. Between this cold and less saline current of polar origin and the Atlantic Water east of it exists an oceanic front, the Polar Front, and the dynamics involved explain the long distances reached by the particles. Another pathway, finally also leading to Greenland is an entrainment from the NIIC north of Iceland into the counter-directed North Icelandic Jet which carries the particle back to Denmark Strait into the southward flowing Arctic and Polar waters there.

However, though the eastward and the westward path are very persistent, we found large differences of the dispersal pattern among the individual 40 experiments (figs. A1 – A39). A striking example of this are the summer 2013 (fig. A38) and the autumn 2013 (fig. A39) experiment showing very different results, i.e. a strong westward transport during the first and a strong eastward transport during the latter period.

In order to analyse the dispersal's temporal variability we have constructed time series of the final particle density at five stations (A, B, C, D, E) based on the results of the 40 experiments, i.e. with a temporal resolution of three months. The stations were chosen to detect either the western branch (A) or the eastern branch over different parts of the north Icelandic shelf (B, C, D, E).

The frequency spectra of these time series, i.e. their discrete Fourier transformations, are show in figures 7 to 11. All spectra show a rather even distribution of periods between three months and ten years. This reflects the fact that changes of the dispersal pattern mainly depend on chaotic mesoscale atmospheric and oceanic fluctuations, i.e. on barotropic and baroclinic instabilities which in fact are highly likely to occur within the frontal areas west and north of Iceland where the Arctic ocean/atmosphere climate zone borders the sub-polar.

Only at station A and E a sharp maximum at the period of one year, i.e. a clear seasonal signal can be detected. Here, the correlation between the pure seasonal signal and the complete time series is 0.67 for station A and 0.70

for station E (figs. 12 and 13) whereas the analogue correlations for the station B (fig. 14), C and D are: 0.05, 0.25 and 0.33 respectively.

The seasonal signal at station A shows its maximum at the beginning of the year. We assume that the stronger wind field during autumn and winter causes higher turbulence north-west of Iceland and therefore an increased entrainment of particles into the southwards flowing East Greenland Current which finally carries them to station A.

However, the seasonal signal at station E shows maximum values at beginning of the summer, after a relatively calm period. Because station E is located close to the North Icelandic coast, we assume the coastal current to be responsible for the signal. This current is forced by the salinity gradient caused by river runoff, and this runoff shows a peak in spring caused by the annual snowmelt. Hence, the transport of the coastal current increases at that time, therefore entrains more particles from offshore waters and carries them to station E.

Returning to the initial question: How should a pollutant dispersal forecast be performed? Our results show that long-term mean or seasonal mean flow fields used for their computation in Icelandic waters can easily introduce substantial errors because of the temporal variability inherent to this system with its considerable proportion of chaotic behaviour.

For short-term forecasts, extending not longer than two weeks, flow fields extracted from the current data of operational ocean models like the CODE system used for this study should be used. If the forecast has to reach further the question arises of determining the best flow field approximation for this purpose. One way could be just the continuation of the atmosphere and ocean forecast run assuming the more sluggish ocean dynamics drift slower into unrealistic states than the atmospheric. Other approaches could use the simulated current state and keep it stationary during the forecast period. Maybe trends of the short term forecast could be included. Hence, a large variety of mathematical techniques and methods should be explored in future in order to be able to produce optimal pollutant dispersal forecasts for Icelandic waters.

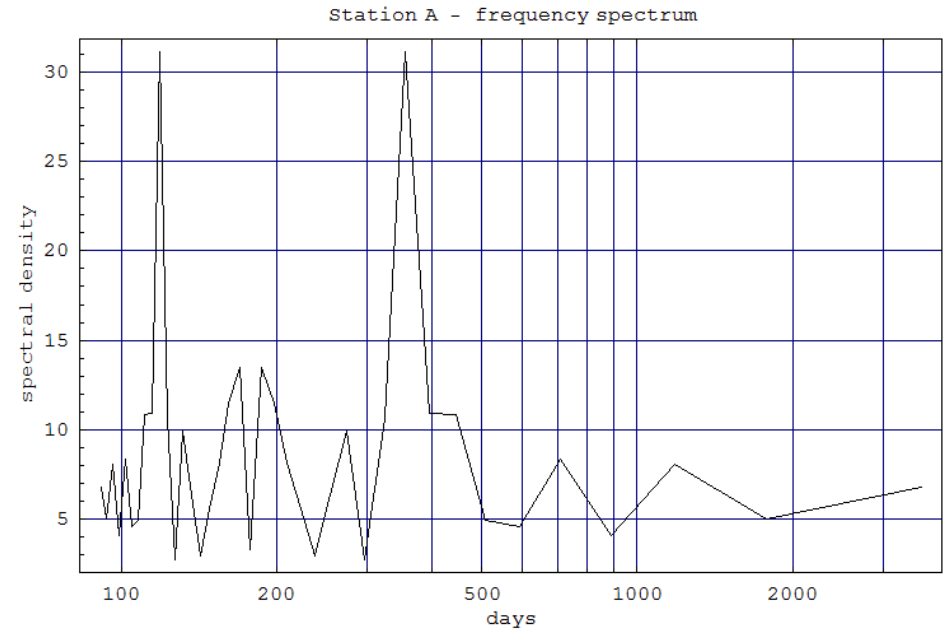

Fig. 7: Discrete Fourier transformation of the time series from station A.

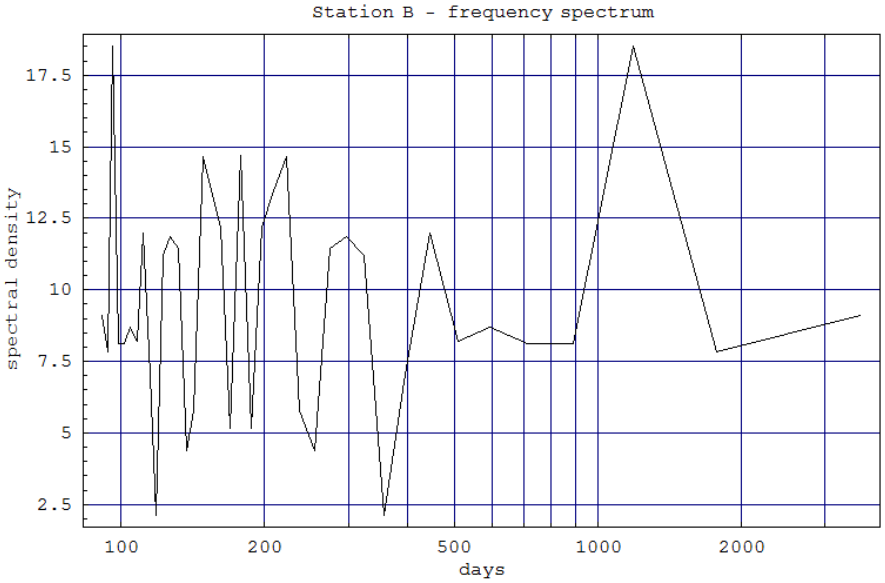

Fig. 8: Discrete Fourier transformation of the time series from station B.

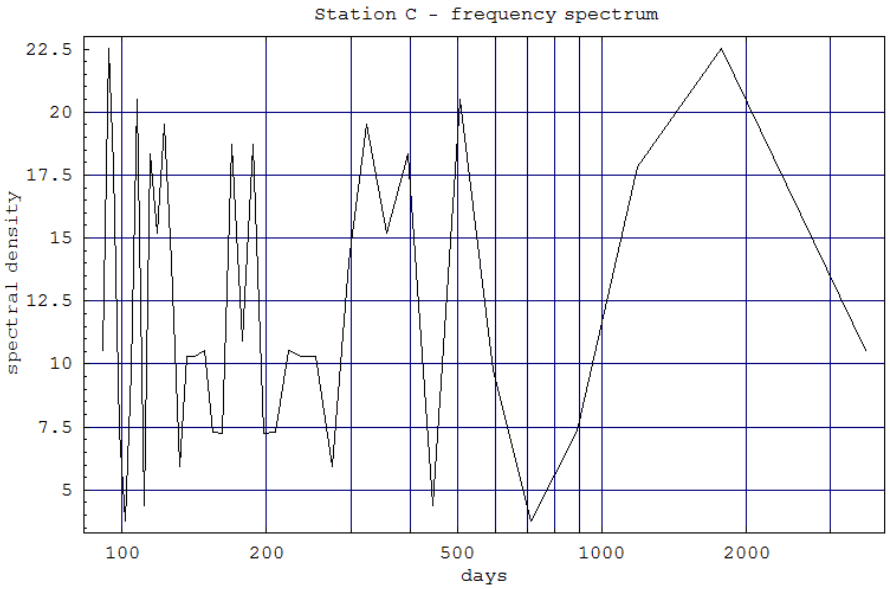

Fig. 9: Discrete Fourier transformation of the time series from station C.

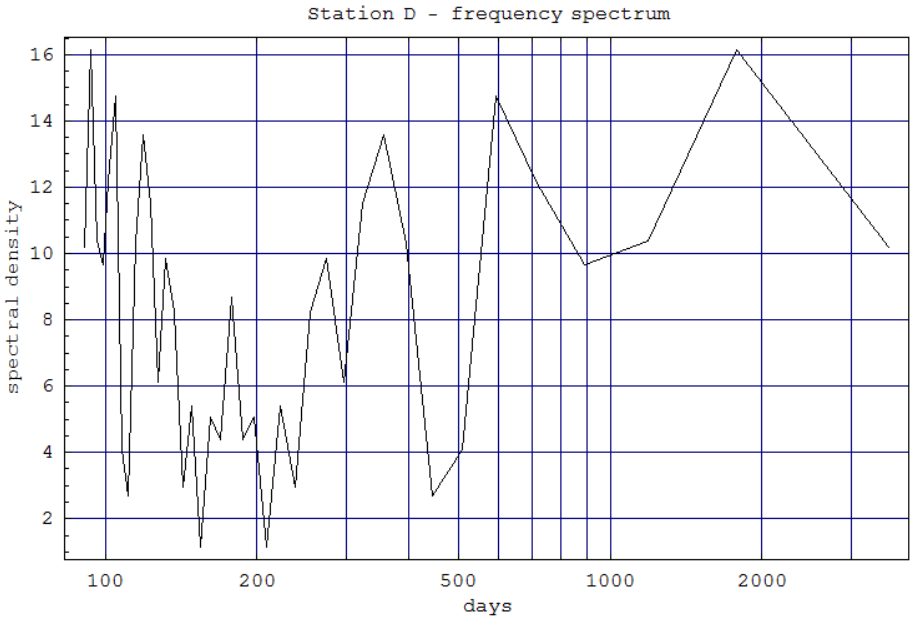

Fig. 10: Discrete Fourier transformation of the time series from station D.

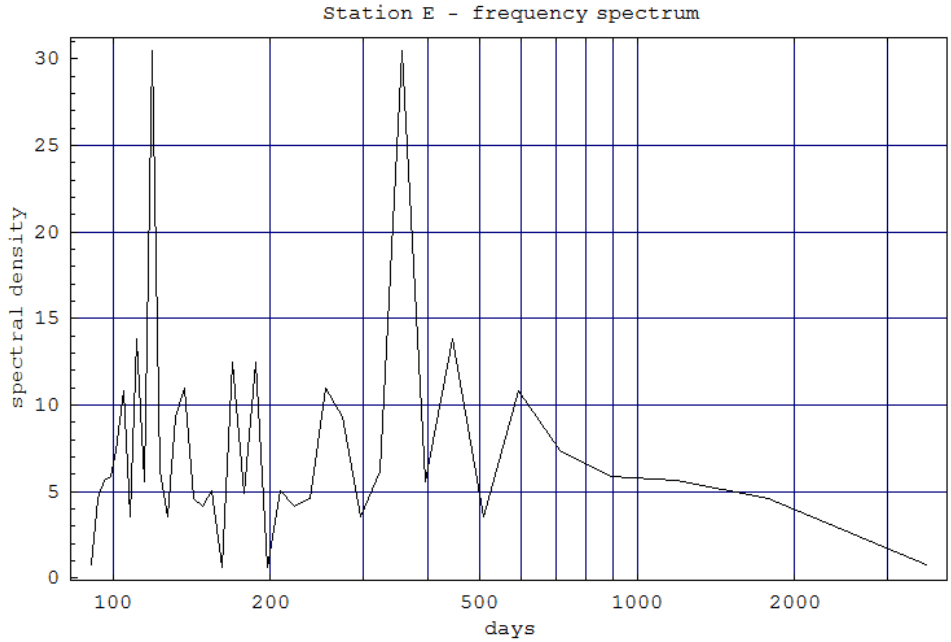

Fig. 11: Discrete Fourier transformation of the time series from station E.

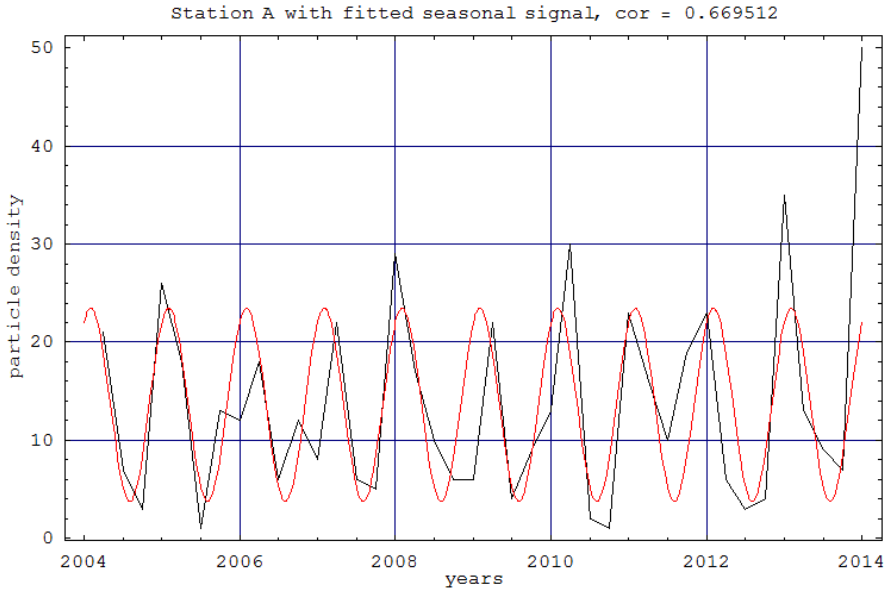

Fig. 12: Particle density time series at station A (black) and its mean seasonal signal (red).

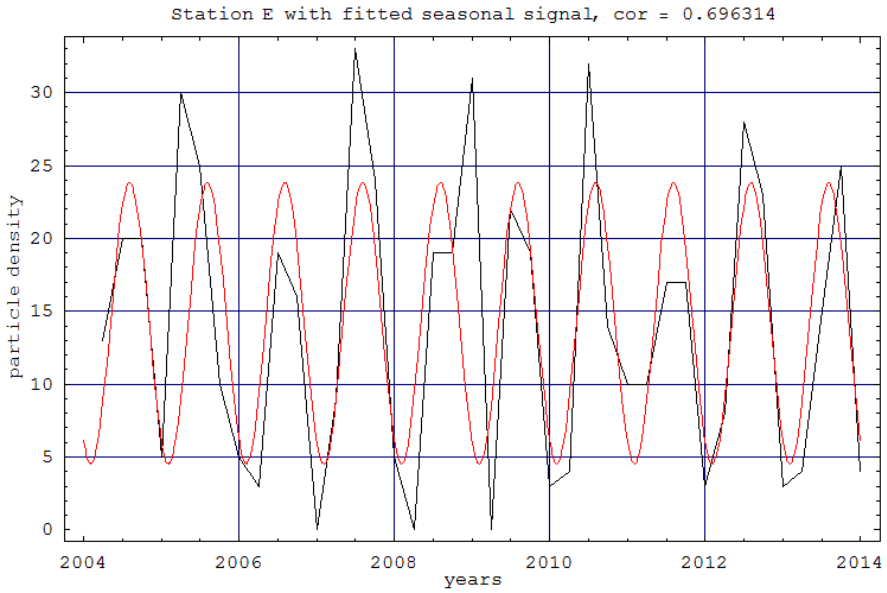

Fig. 13: Particle density time series at station E (black) and its mean seasonal signal (red).

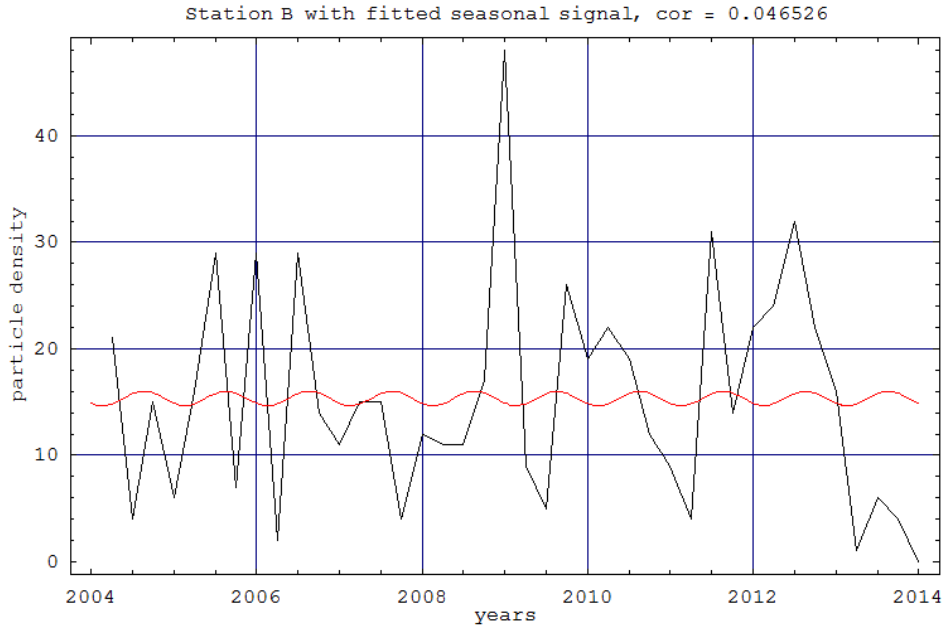

Fig. 14: Particle density time series at station B (black) and its mean seasonal signal (red).

2.1.4. Implementation to the NRPA regional box model for the Icelandic coastal waters

The above analysis shows that the temporal variability of the dispersion can be significant even on short time scales. Results for particle density at the point A are summarised in Figure 15. Each result corresponds to the particle density after three month of dispersion for real atmospheric and sea conditions for years 2004-2013. These calculations can be used for

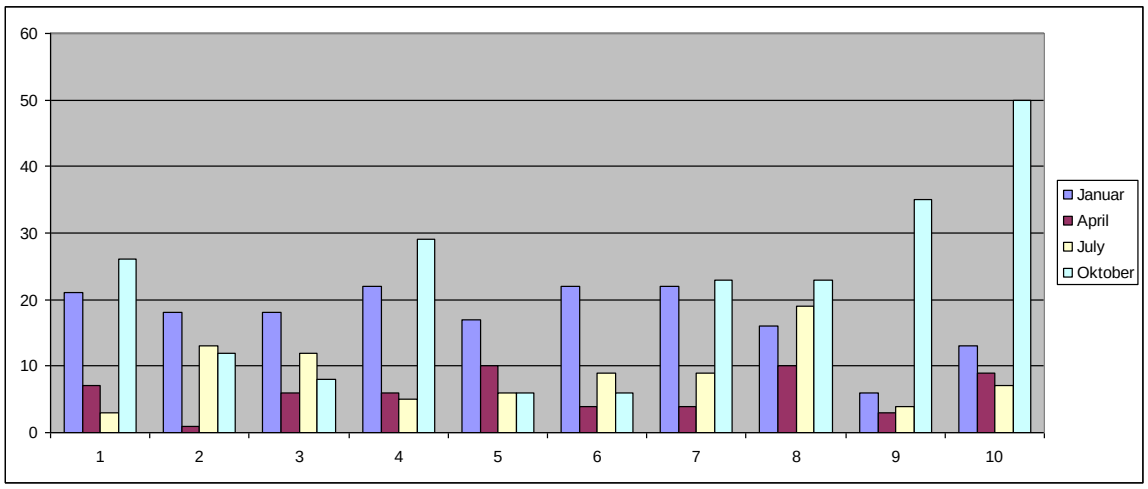

Fig. 15. Particle density, point A (2004-2013)

a harmonisation of the results between the hydrodynamic model CODE the NRPA box model for the Icelandic coastal waters.

Points “A” and “S” (the source position) are located in the box 2 (a red spot in Figure 16). Therefore, a particle density near the point A can be interpreted as a concentration of a conservative radionuclide with unit release into the box 2.

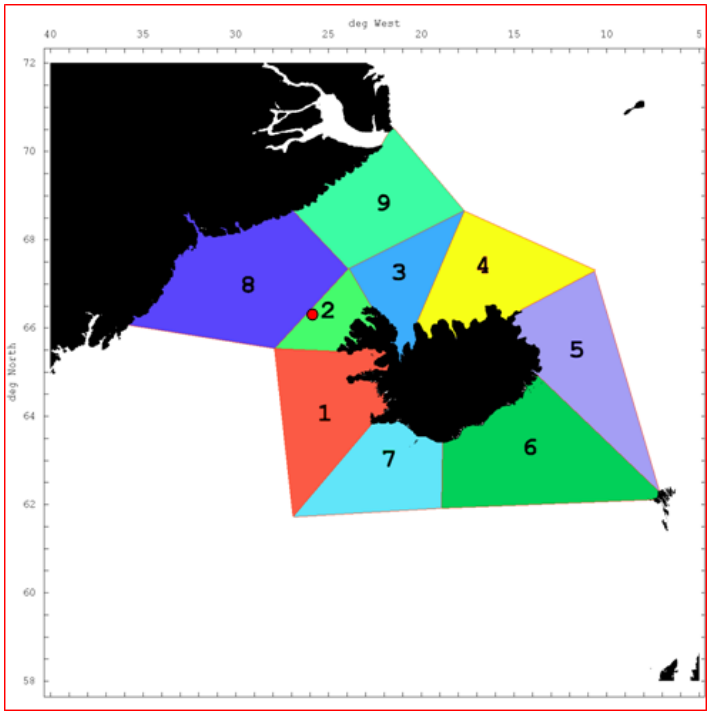

Fig. 16. Surface boxes for the NRPA bmodel for the Icelandic coastal waters.

Figure 17 shows the comparison and harmonisation between the CODE and NRPA box model output. Points in Figure 17 correspond to results of the CODE model at the point "A" after three months of dispersion referring to the different starting times during the period 2004-2013 (points are the same for both top and bottom figures). Lines in Figure 17 correspond to concentration of conservative radionuclide during one year dispersion in the box 2 after one unit release.

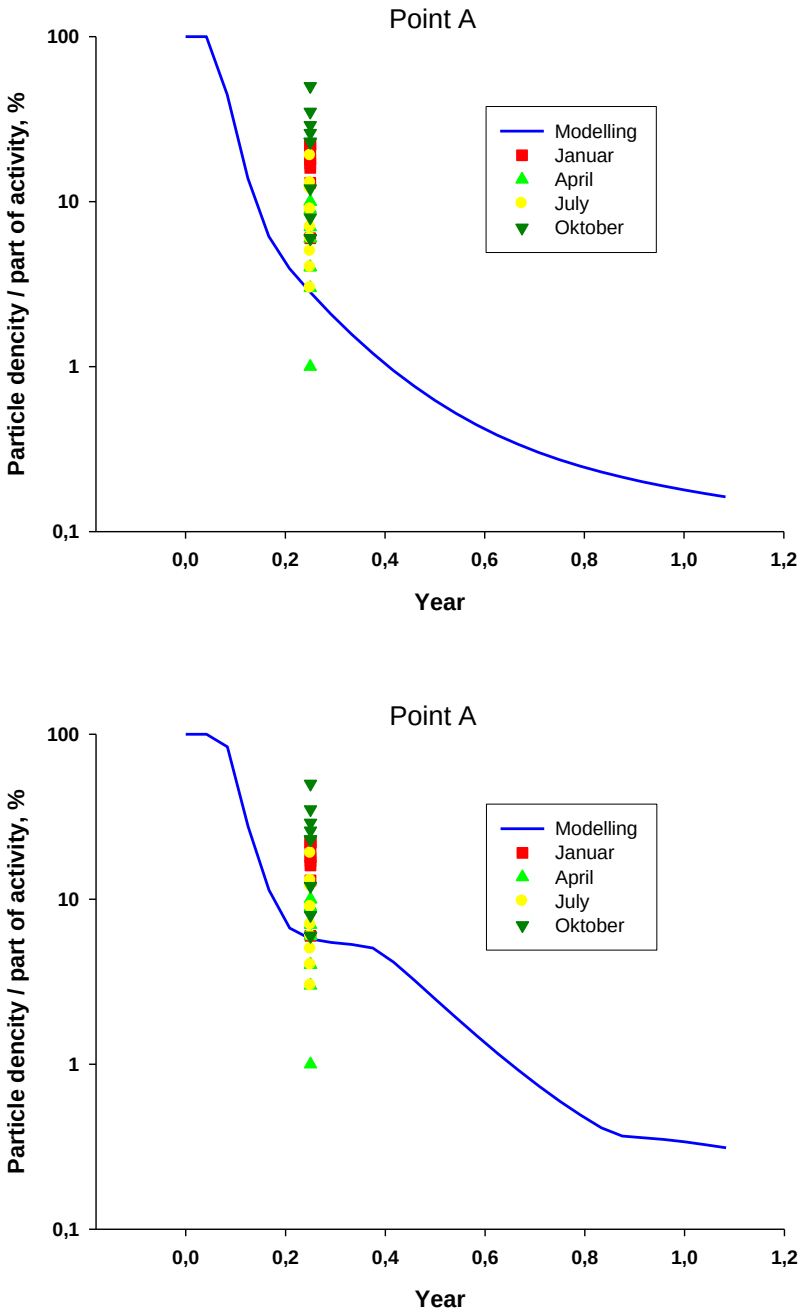

Fig. 17. Comparison and harmonisation between hydrodynamic CODE and NRPA box models

Since it was necessary to consider conservative radionuclides, the water-sediment interaction was not taken into account by calculating Figure 17 (parameters for suspended sediment load in water column *SSL*, sedimentation rate *RS* and sediment distribution coefficient K_d were equal to zero within the NRPA box model – see detailed description of model parameters in Appendix 2).

The advections of water between the boxes are the same for both top and bottom plots in Figure 17. Times of availability for box 2 (see detailed description of model parameters in Appendix 2) for the plot in the top figure are calculated in a simple way as the ratio "volume of box/water advection" while the plot in the bottom figure is calculated with additional harmonisation results from the CODE model. This model improvement leads to a better description of the "average" concentration with regards to potential variability and demonstrates that a combination of different models can be useful for final results.

2.2. An improvement of the NRPA dispersion model for the Baltic Sea.

The NRPA approach for box modelling includes terms describing the dispersion of radionuclides into oceanic space with time (Iosjpe et al., 2002; 2009). That is, the model considers that radionuclides cannot move from one box to another instantly. The model uses the times of availability for each box (the first times when box is open for dispersion of radionuclides). It is interesting to note that traditional box modelling is a particular case of the present approach when all times of availability are zero (more detailed description of the NRPA box approach is given in Appendix 2).

Under the course of the present project this modified approach was used for the description of the dispersion of radionuclides in the Barents Sea. Calculations show that this approach can significantly improve the modelling of the radionuclide dispersion, especially for the deep part of the Baltic Sea.

Sources for ^{137}Cs contamination of the Baltic Sea regions are shown in Figure 18 (COSEMA, 2014).

Comparison of the 137Cs concentration in the seawater for the Gulf of Finland and the deep waters of the Western and Eastern Baltic Sea are shown in Figures 19 and 20.

Figures 19 and 20 show the results of the model simulations for 137Cs contamination compared with the experimental data (EC, 2000 and HELCOM, 1995). The circles and quadrates show the average values, while the error bars show the minimum and maximum values of the experimental data. Figures 19 and 20 demonstrate that the model predictions are reasonably accurate.

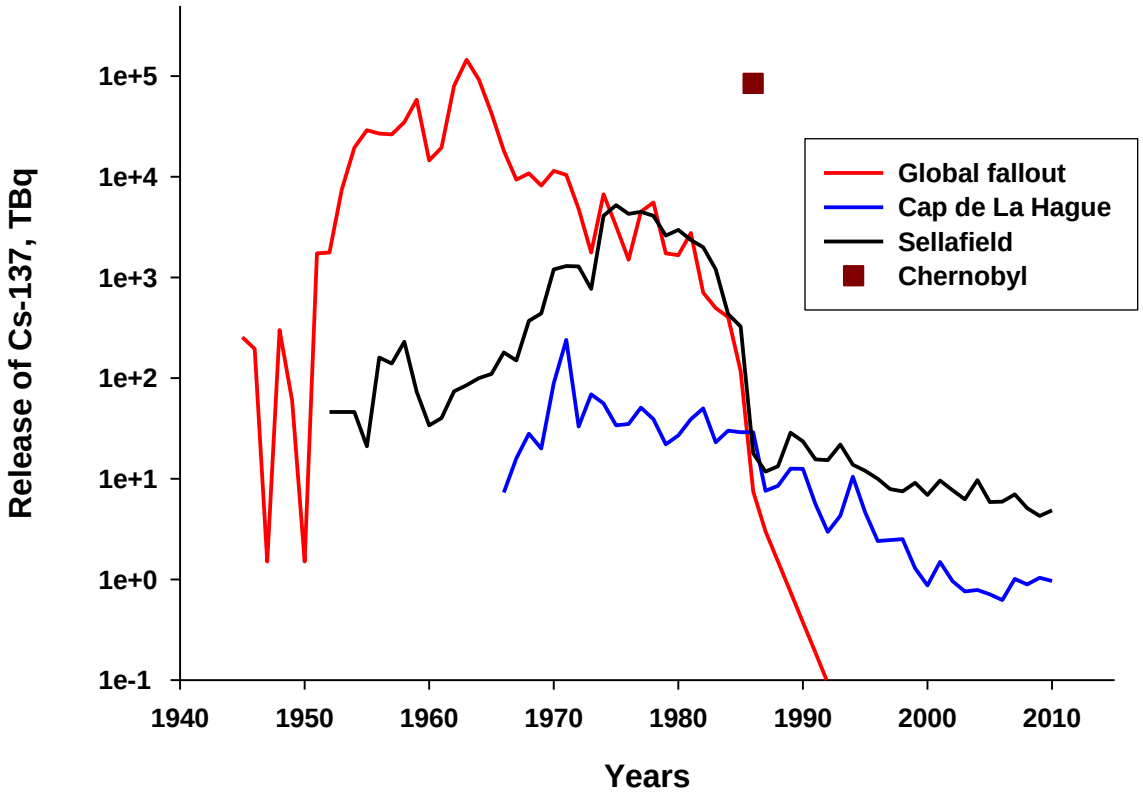

Figure 18. Sources of ^{137}Cs in the Baltic Sea.

It is clearly shown in Figure 20 that the NRPA box modelling modified approach can significantly improve the accuracy of the simulation of the radionuclide dispersion.

A good correlation between the results of model simulations of the ^{137}Cs concentration in seawater with the experimental data for the Gulf of Finland, provides a good opportunity for further testing of the bioaccumulation model.

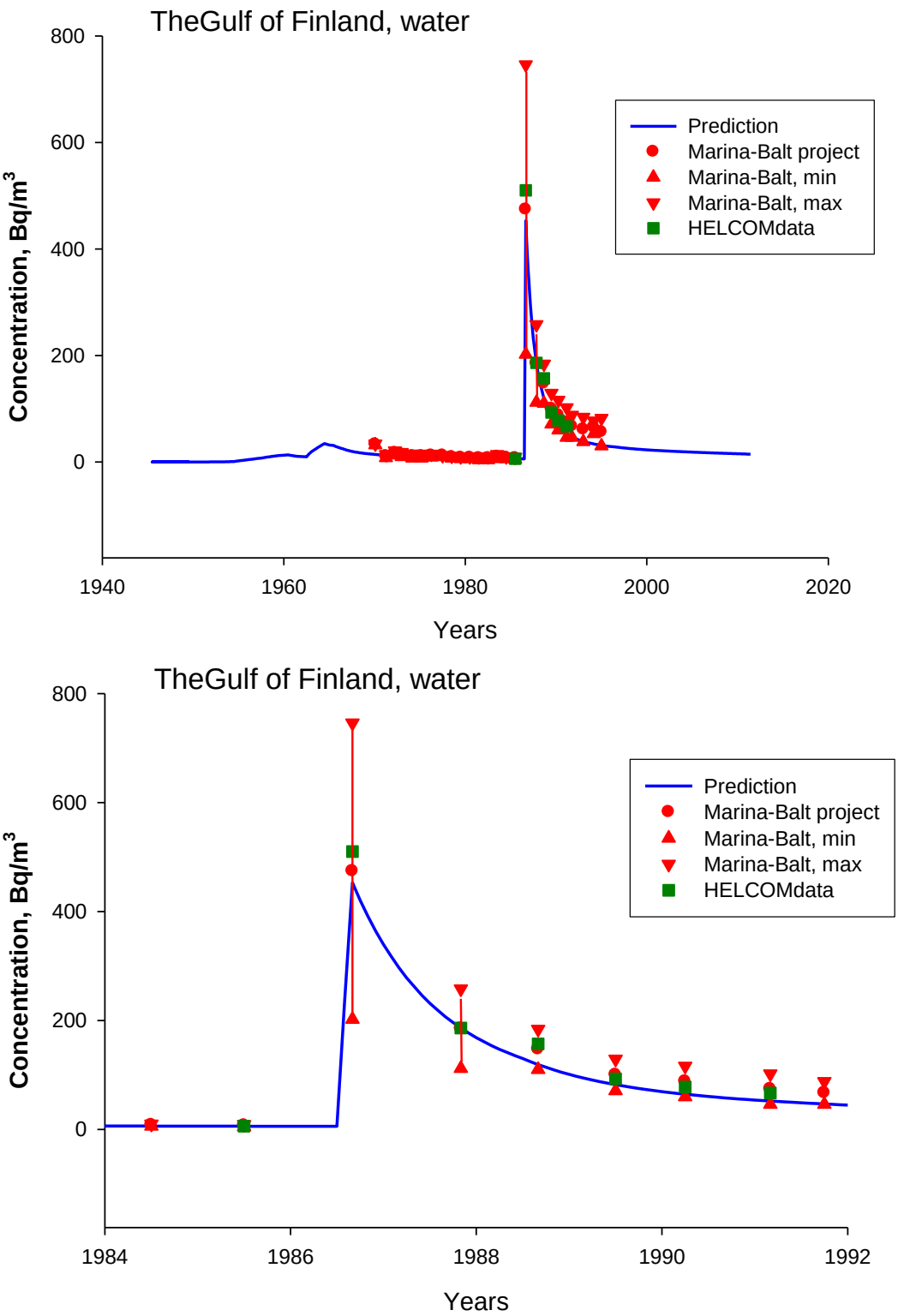

Figure 19. Comparison of the prediction of the concentration of ^{137}Cs in sea water with experimental data for the Gulf of Finland from 1945 (top) and for the Chernobyl accident (bottom).

Results of calculation outlined in Figures 19-20 clearly indicate a potential significance of the modified approach for box modelling (times of availability are evaluated according to the algorithm which is described in Appendix 2) for consequences after discharges of radionuclides into marine areas in comparison to traditional modelling, where times of availability are equal to zero.

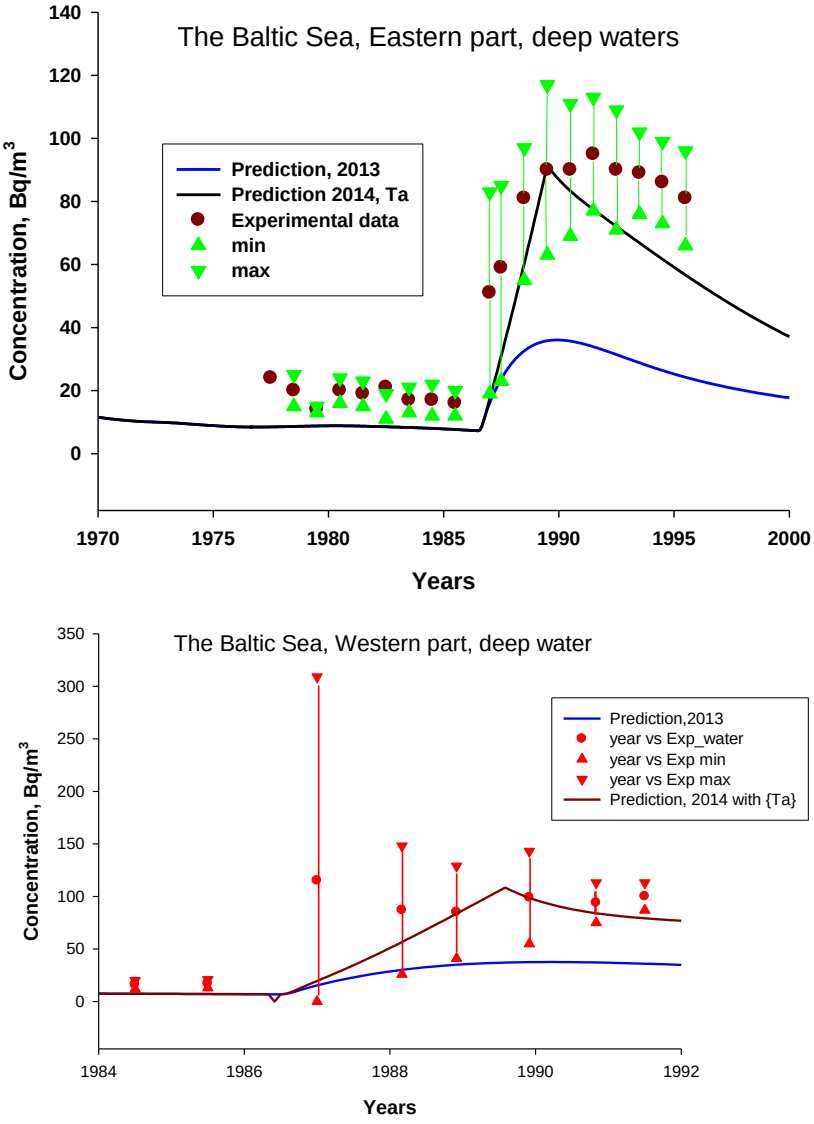

Figure 20. Comparison of modified (2014, Ta) and traditional approaches with experimental data for deep waters of the Baltic Sea after the Chernobyl accident.

3. Bioaccumulation modelling

3.1. Development and implementation of the bioaccumulation process into the NRPA box model

The NRPA model uses a modified approach for box modelling with non-instantaneous mixing of radioactivity in the marine environment (Iosjpe et al., 2002, 2009; see also Appendix 2 of the present report). The model includes site-specific information for the compartments, advection of radioactivity between compartments, sedimentation, diffusion of radioactivity through pore water in sediment, resuspension, mixing due to bioturbation, particle mixing, a burial process for radionuclides in deep sediment layers and radioactive decay. The contamination of biota is calculated from the known radionuclide concentrations in filtered seawater in the different water regions on the basis of constant concentration factors /ratios (CF approach). Doses to man are calculated on the basis of seafood consumption, in accordance with available data for seafood catches and assumptions about human diet in the respective areas. Dose to biota is calculated on the basis of radionuclide concentrations in marine organisms, water and sediment, using dose conversion factors.

3.1.1. Modelling of the bioaccumulation process

Figure 21 shows the schematic of the biokinetic model, which was selected as a basis for the EFMARE project. The model has been chosen after an analysis of existing models (Thomann, 1981; Heling et al., 2002; Brown et al., 2004; Vives i Batlle et al., 2008; Maderich et al., 2013). Parameters for the fish submodel for ^{137}Cs and ^{239}Pu are selected from (Thomann, 1981) with an additional assumption about the possibility of an uptake of radionuclides via zooplankton for large fish.

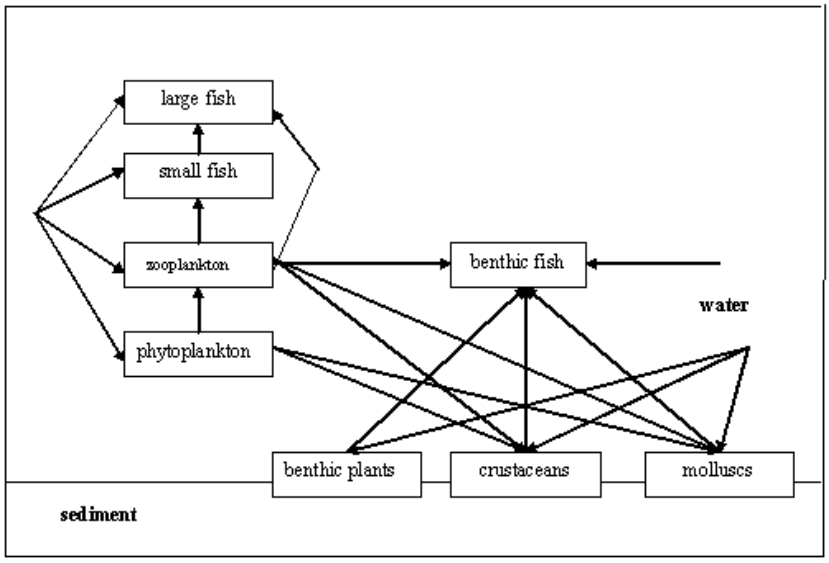

Figure 21. Schematic of the biokinetic model used in the present report.

The system of equations for the biokinetic model can be described by the followingexpressions:

$$\frac{dC_i^{(tl)}}{dt} = AE_i \cdot IR_i \cdot C_{i-1}^{(tl)} + k_{u,i} \cdot C_w - C_i^{(tl)} \cdot k_{e,i} \qquad (1)$$

Here $C^{(tl)}_i$ and $C^{(tl)}_{i-1}$ – concentrations of radionuclide in trophic levels "*i*" and "*i-1*"; C_W – concentration of radionuclide in water column; AE_i – the assimilation efficiency for trophic level "*i*", IR_i – ingestion per unit mass for trophic level "*i*"; $k_{u,i}$ – rate of the direct uptake of activity from water column for trophic level "i"; $k_{e,i}$ – the excretion rate for trophic level "i". Where the consumption for species in trophic levels "*i*" includes "*m"* different species in trophic levels "*i-1*", parameter $C^{(tl)}_{i-1}$ can be described as

$$C_{i-1}^{(tl)} = \sum_{j=1}^{m} w_j \cdot C_{i-1,j}^{(tl)}$$

Here the consumption for species in trophic level "*i*" includes *m* species in trophic levels

"*i-1*" with concentration of radionuclide in species *j* (*j=1,…,m*) of $C^{(tl)}_{i-1,j}$; w_j is a fraction of species *j* of all m species, where

$$\sum_{j=1}^{m} w_j = 1$$

The comparison of the activity concentration in biota between a constant concentration factor approach and a biokinetic modelling approach is shown in Figure 22. Calculation of the concentrations of radionuclides for phytoplankton is based on concentration factor approach. Results of the implementation of the kinetic model for bioaccumulation processes into the NRPA box model clearly demonstrated that there is a significant difference between the kinetic modelling approach and the approach based on constant concentration factors, especially during the initial time of dispersion. After some time an equilibrium is established, which can be successfully described by a constant concentration ratio approach.

Using constant concentration factors to describe the process of bioaccumulation has several advantages. Due to the large number of studies, there is a database for concentration factors for many radionuclides, which significantly exceeds the information about biokinetic coefficients needed for more complex models. Furthermore, biokinetic modelling is a more sophisticated method, when compared to the constant concentration ratio approach. Therefore, it often requires more detailed and specific data about the concentration of radionuclides in the marine environment, and this data may sometimes be difficult to measure or predict. This is because we often need to work with a complex marine environment, which is contaminated by many different sources of pollution, many of which interact with each other.

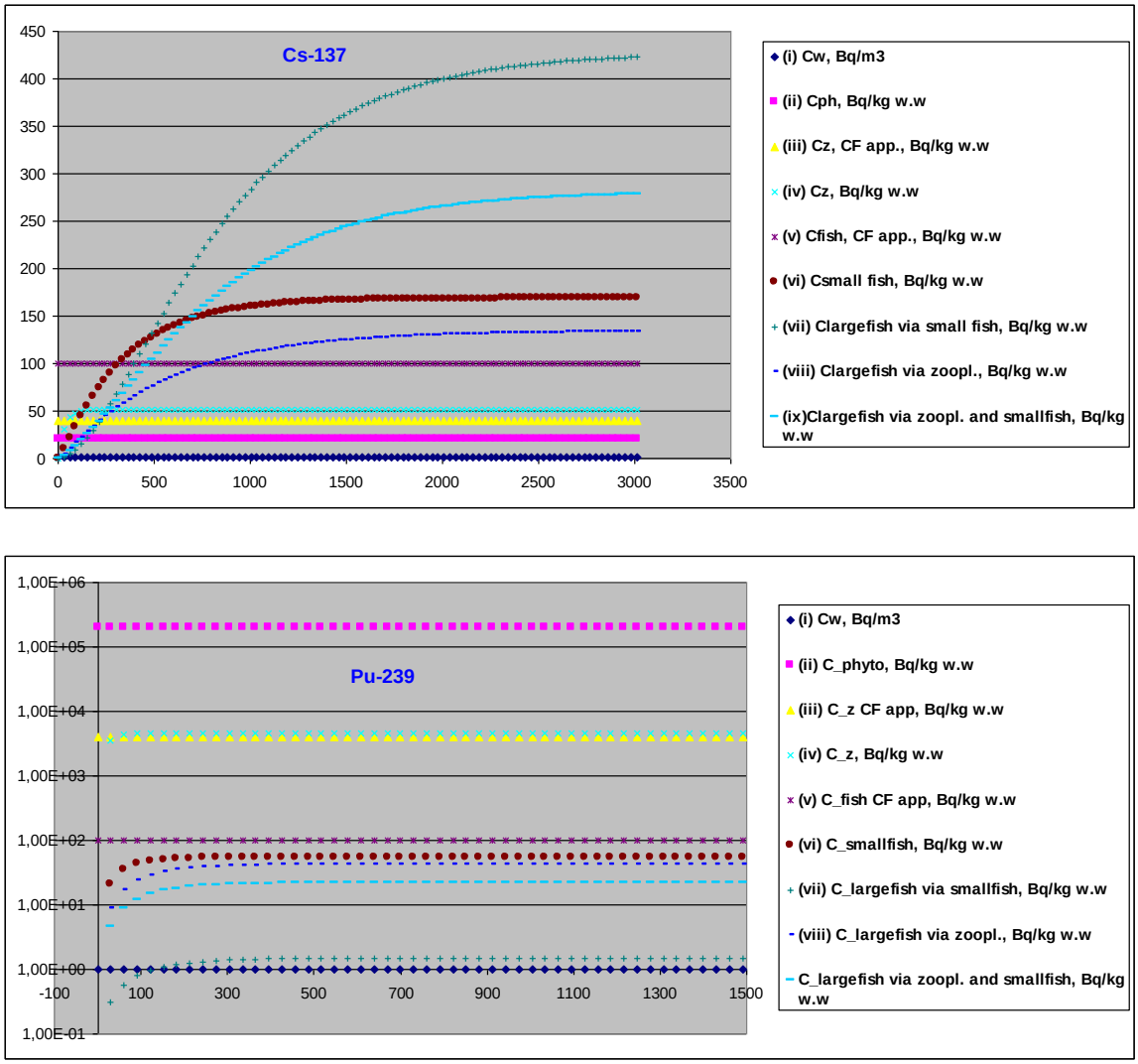

Figure 22. Comparison of the concentration of radionuclides in biota for both the constant concentration factor approach and the biokinetic modelling for ^{137}Cs (top) and ^{239}Pu (bottom) with the concentrations: (i) in water, (ii) in phytoplankton (iii) in zooplankton with the concentration factor approach, (iv) in zooplankton with biokinetic modelling, (v) in fish with the concentration factor approach, (vi) in small fish with biokinetic modelling, (vii) in large fish with biokinetic modelling and uptake via water and small fish, (viii) in large fish with biokinetic modelling and uptake via water and zooplankton, (ix) in large fish with biokinetic modelling and uptake via water, zooplankton and small fish.

Figure 23 indicates the complexity of some marine regions. In these regions the radionuclide dispersion after an atmospheric fallout, as well as releases from European and Russian nuclear facilities, has occurred for decades. The concentration factors/ratios for these marine environments are shown in

Figure 24 (experimental data was collected by Fróðskaparsetur Føroya and Technical University of Denmark over the course of the EFMARE project). Results of calculations indicate variability of the concentration factors/ratios for the same fish in different environments and times, as well as between different species. At the same time, the results can be described by concentration ratio 100 for fish (IAEA, 2004) with a relatively large variability, approximately a factor of 4. No clear patterns of change of concentration factor can be determined; rather we must speak about the influence of random factors related to the complexity of the migration of radionuclides in the marine environment and prolonged exposure to various sources of pollution.

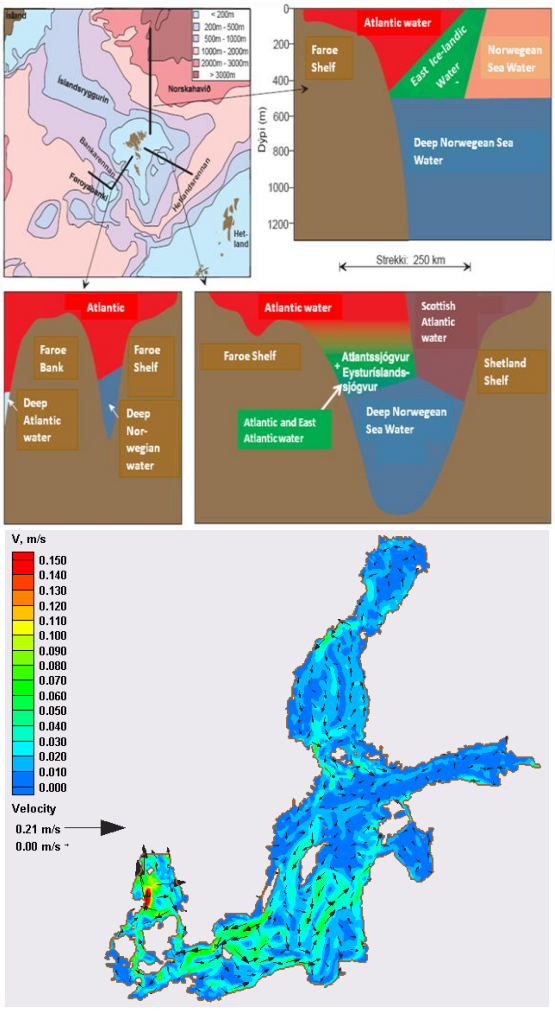

Figure 23. Water mass distribution for the Faroe region (top) and water currents for the Baltic Sea (bottom)

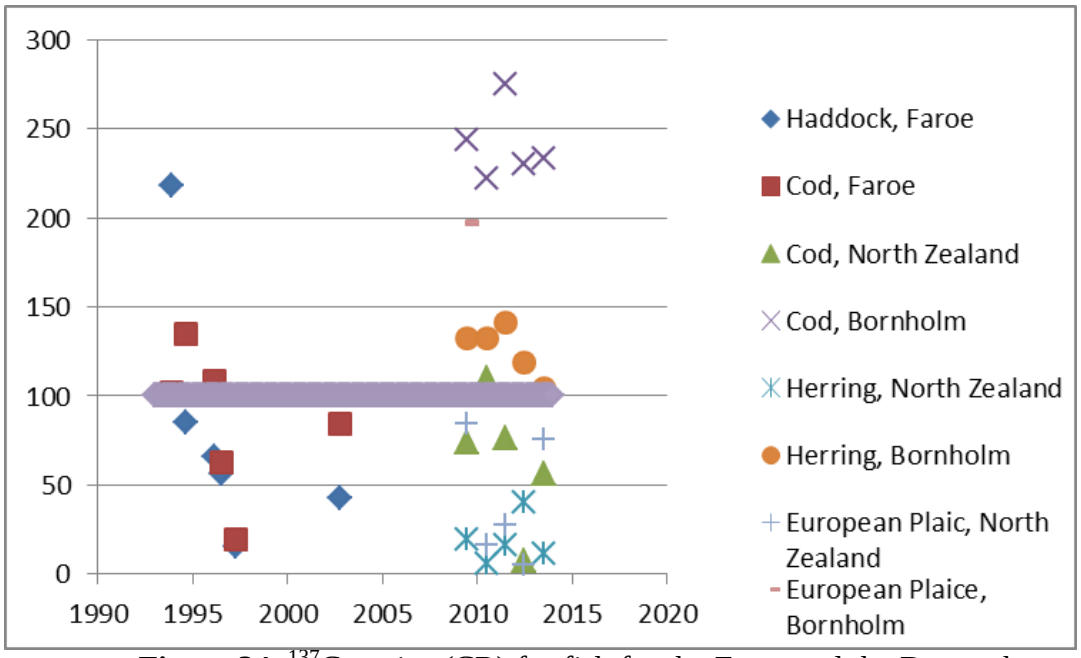

Figure 24. ^{137}Cs ratios (CR) for fish for the Faroe and the Denmark coastal waters.

On the other hand, Figure 22 shows that the bioaccumulation described using biokinetic modelling can be very important in an accidental release of radionuclides. This conclusion is confirmed by studies of the consequences of the Fukushima accident (Maderch, 2013). Because precisely these accident scenarios are considered in the EFMARE project, the biokinetic sub-model has been tested by applying it to the consequences after the Chernobyl accident in the Gulf of Finland (the Gulf of Finland was chosen due to the good correlation between the predicted and the measured data for ^{137}Cs concentration in the water, making it highly suitable to test the biokinetic submodel).

Results of biokinetic modelling approach were compared with experimental data on the basis of an improved version of the NRPA box model for the Baltic Sea (see Figure 25).

Blue and red lines in Figure 25 correspond with concentrations in water and fish (with concentration factor approach), correspondently. Therefore, these plots have the same shape. Biokinetic modelling describes the “delay” with the changing of concentration of radionuclides in water. It is a clear demonstration that the dynamic modelling of the bioaccumulation processes provides a more correct description of the concentration of radionuclides in biota (up to an order of magnitude) and, therefore, these results support one of the main ideas of the EFMARE project, namely that the biokinetic modelling approach is important when evaluating the consequences after accidental releases of radionuclides into a marine environment.

It is interesting to note that the results in Figure 25 demonstrate that present modelling predictions are borne out by the experimental data after Chernobyl accident (1986) because the modelling parameters correspond to data from 1981 (Thomann, 1981).

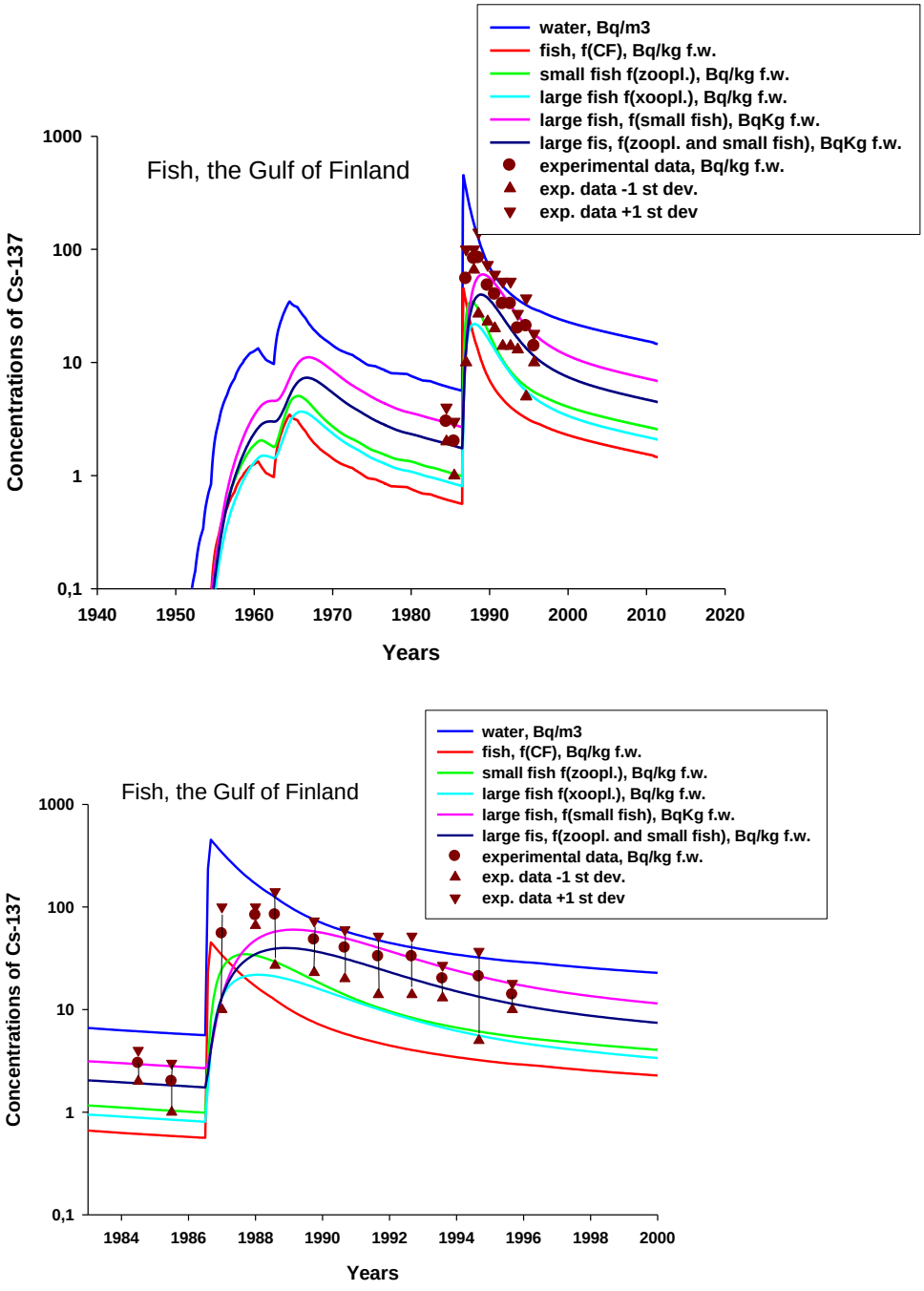

Figure 25. Comparison of the prediction of the concentration of ^{137}Cs in fish with experimental data for the Gulf of Finland for both the constant concentration factor approach and the biokinetic modelling from 1945 (top) and for the Chernobyl accident (bottom).

It is important to note that knowledge about biokinetic coefficients based on habitat, ingestion of food, diet and excretion of activity for studied species are crucial information for biokinetic modelling. Useful information can be found in Brown et al. (2004), Vives i Batlle (2008), Yankovich et al. (2010), Maderch et al. (2013) and Appendix 3 of the present report (data in Appendix 3 was collected by University of Gothenburg over the course of the EFMARE project).

3.2. Bioaccumulation model application of the DETRA computer code of VTT

The conceptual compartmental dispersion model consists of dynamic models for marine basin and for fish food chain (Figure 26). The DETRA computer code can be applied for radionuclides transfer analyses as well as for parametric sensitivity studies.

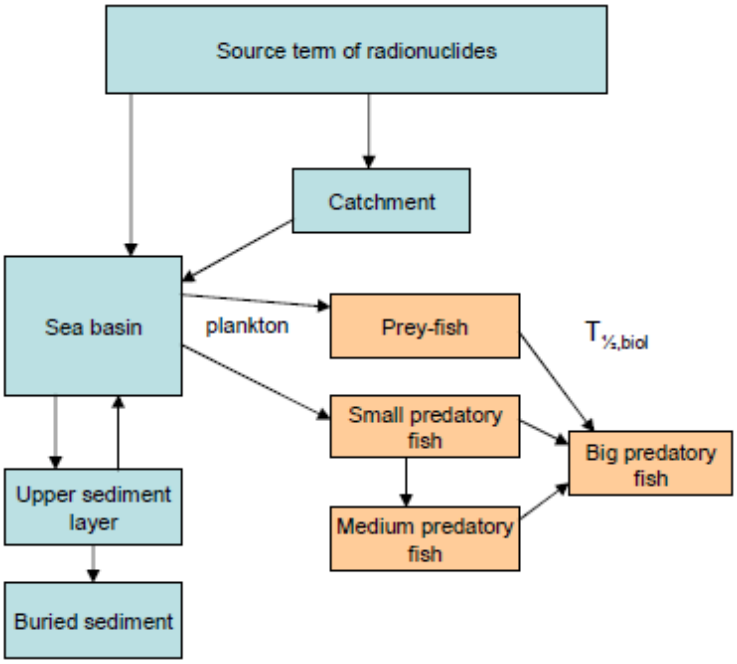

Figure 26. Conceptual bioaccumulation model for marine environment.

In each of the model compartments sufficient homogenization of concentrations are assumed to be reached. Radionuclides transfer between compartments is modelled with convective carry flows of water and

suspended sediment material. As consideration of radionuclides transfer, the main flow rates are generally related to seawater turnover and to sedimentation of suspended material from seawater to the bottom sediment layer. Additionally, there are also other important transfer mechanisms like erosion from catchment towards sea. This erosion is caused by runoff and by wind induced erosion where radionuclides are first dispersed into the atmosphere, and further deposited onto seawater.

Mechanisms which tend to dilute (e.g. seawater turnover) or on the other hand mechanisms which tend to concentrate (e.g. radionuclides uptake to fish or sedimentation) are essential factors when estimating the build-up of radionuclide concentrations in various parts of the considered marine ecosystem. Additionally, the element specific sorption characteristics determine the final distribution between water phase and solid matter. Therefore, the soluble nuclides are mainly carried with seawater and strongly sorbing nuclides are mainly carried with solid matter (sedimentation).

The concentration responses of prey fish occur quite soon, whereas the maximum of predatory fish concentration will be obtained in the later phase. Predatory fish is placed later in the food chain than prey fish and biological half-life of predatory fish is longer compared to prey fish (Table 2).

Table 2. Biological half-lives estimates used for Caesium in the fish chain model.

Fish type	$T_{½, b}$ (day)
Prey fish	100
Perch(S) (15-20 g)	200
Perch(M) (25-100 g)	250
Pike	300

Calculation results of the bioaccumulation model application of DETRA are presented later related to hypothetical severe release scenarios to sea water in the Baltic area.

4. Severe accident source term and consequences. Effects of kinetic modelling of bioaccumulation process to radioecological assessments

4.1. The Baltic Sea (DETRA computer code)

The source term estimates for Fukushima accident are considered in the reference of UNSCEAR 13-85418. Estimates for direct release in Fukushima to the ocean is 3 to 6 PBq and indirect release to the ocean 5 to 8 PBq for Cs-137. With the Fukushima reactors inventories this corresponds to a release fraction of about 2% for Cesium.

Considering this reference release fraction data for severe accident, consequences for a 3000 MWth release scenario to the Baltic Sea environment is calculated (Figure 27).

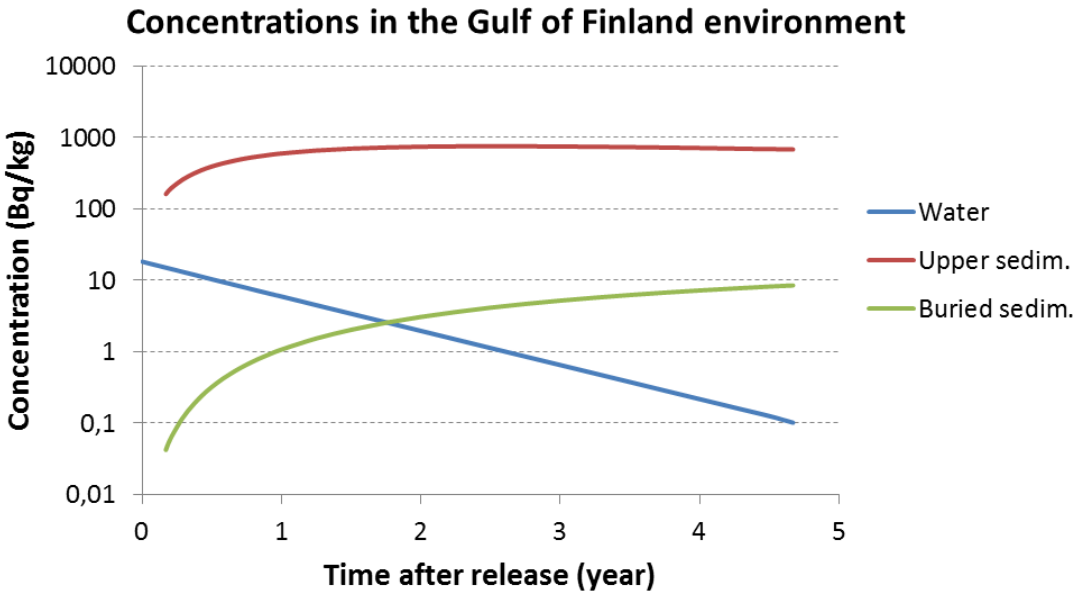

Figure 27. Estimated Cs-137 concentrations in the Gulf of Finland after a 10 PBq(Cs-137) release to the sea water.

In the study, dynamic contamination of various fish types i.e. fish food chain was considered and modelled. In nature, prey fishes and small predatory fishes eat plankton and their metabolism is faster compared to

larger predatory fishes. In the case of radioactive contamination in sea plankton, the prey fish concentrations will increase first and contamination of predatory fishes are obtained until in the later phase.

Consequences of two severe hypothetical release scenarios have been considered: release to the Gulf of Finland and release to the Baltic Proper (Figures 28 and 29). It can be noticed that in the Baltic Proper area water turnover rate is slower and radioactivity may accumulate toward predatory fish types during longer period.

It should be emphasized that model calculation results presented here are based on approximated fish metabolic data and the results are preliminary. Further research on the subject is necessary. However, the results indicate remarkable differences in temporal behaviour of concentrations between prey fish and predatory fish types. This phenomenon has been obtained already earlier and is familiar also from the measurements performed after radioactive depositions to aquatic environments.

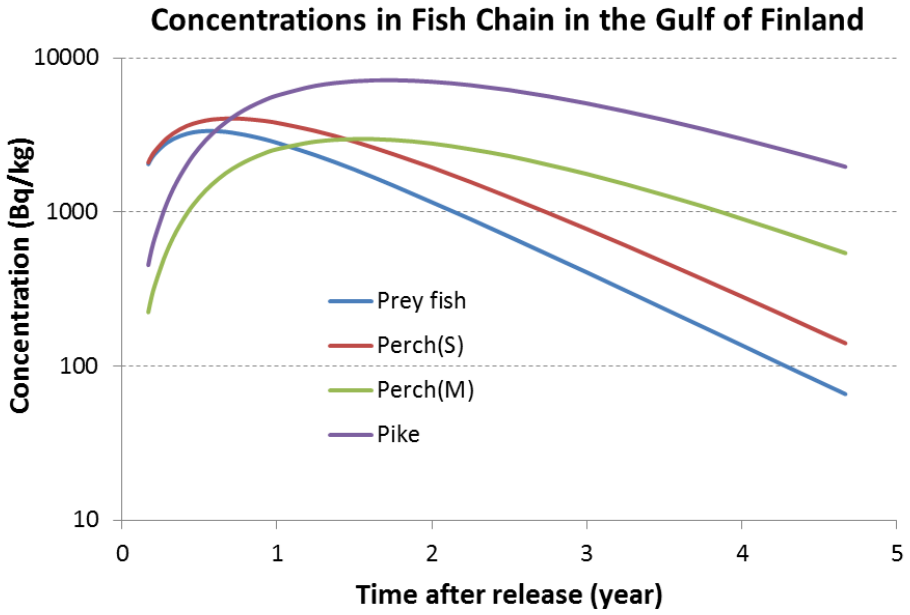

Figure 28. Estimated Cs-137 concentrations in fish chain after a hypothetical severe release of 10 PBq to the Gulf of Finland sea water.

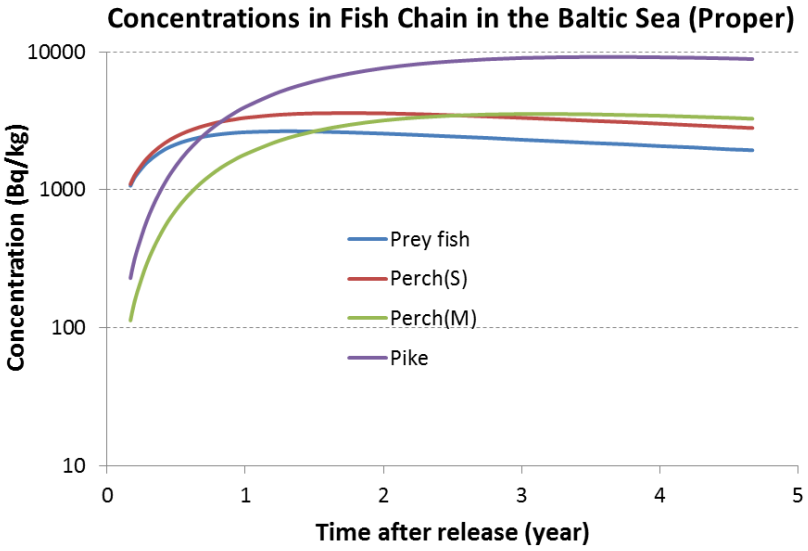

Figure 29. Estimated Cs-137 concentrations in fish chain after a hypothetical severe release of 10 PBq(Cs-137) to the Baltic Proper water.

Comparison of two release scenarios: release from the Finnish coast and release from the Sw edish coast is presented in Figure 30 (Cs-137 concentrations in the Baltic proper after release). According to calculations, the concentration in the Baltic appear earlier in case of a release from the Swedish coast. The maximum Cs-137 concentration in the Baltic seawater is about 1 Bq/liter.

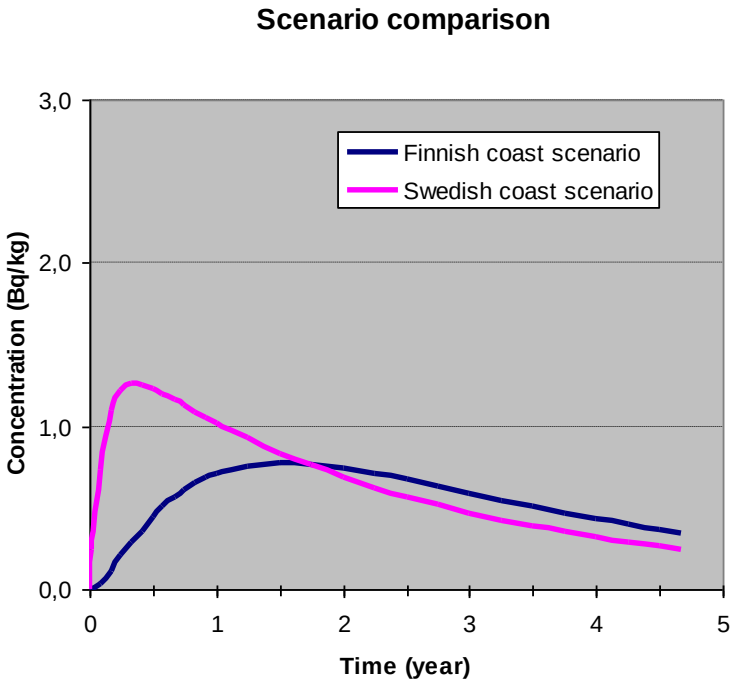

Figure 30. Comparison of estimated Cs137 concentrations in the Baltic sea between the 'Finnish coast' and the 'Swedish coast' release scenarios.

4.2. The Iceland coastal waters (NRPA regional box model)

4.2.1. Release Scenario

The total and the individual releases of the radionuclides that had the most significant effect on the release rates during the initial and later phases of accidental releases are presented in Figure 31. As expected, the maximum release occurs during the initial period after the accident (the instant release fraction) with maximum values of $1.6 \cdot 10^{18}$ Bq at the beginning of release. Figure 31 shows that short-lived radionuclides of iodine and barium are

most significant during the initial phase of release according to the present scenario, while ^{90}Sr and ^{137}Cs dominates in the final period of release.

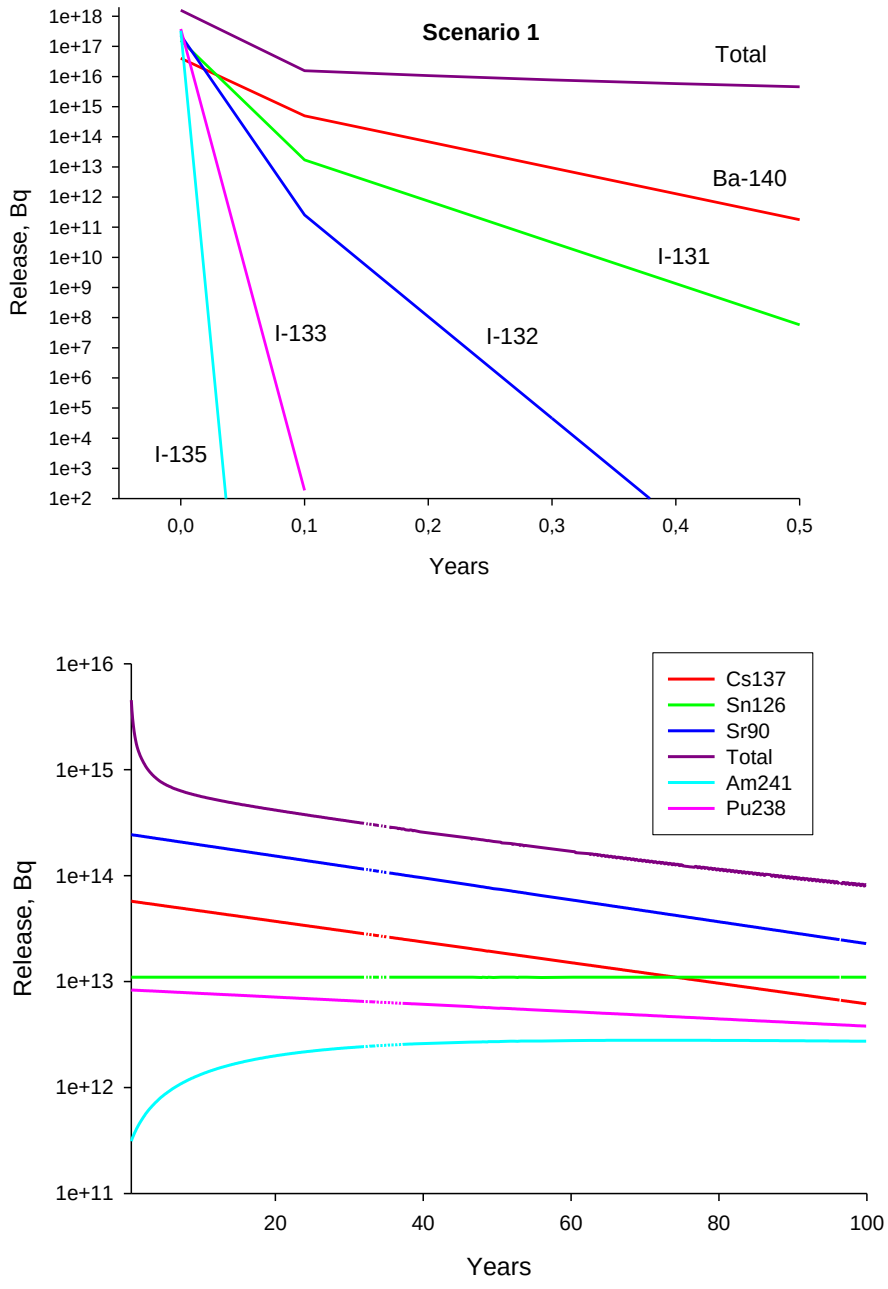

Figure. 31. The release scenario for the initial time of 0-0.5 year (top) and for the time 0.5-100 years (bottom)

Effects of dynamic behaviour of Nordic marine environment to radioecological assessments will be provided on the base of results presented in the COSEMA project (COSEMA, 2014; Appendix 4 of the present report).

4.2.2 Caesium

^{137}Cs and ^{134}Cs isotopes are most important for radioecological dose assessment for the present scenario. A dose to the critical group is dominated by the doses from fish contaminated by these isotopes (Appendix 4).

4.2.2.1 ^{137}Cs

A release scenario for the hypothetical accident with a nuclear submarine in the Icelandic coastal waters is described in detail in (COSEMA, 2014). According to this scenario, about 25 PBq of ^{137}Cs was released into the marine environment. The dynamics of the releases of ^{137}Cs for ten years is shown in Figure 31.

Parameters for equation (1) for zooplankton, small fish and large fish are adopted from Thomann (1981). Parameters for molluscs and crustaceans are adopted from PREPARE 2015. Phytoplankton and benthic plants have been calculated on the basis of the concentration factor (IAEA, 2004).

Figure 32 shows calculation of ^{137}Cs concentration (box 2, see Fig. A2.1, Appendix 2) in seawater and fish according to this scenario, corresponding to the accident location. The results in Figure 32 show the same shape for the water concentration plots with a maximal value at the initial time (a red line) and all kinds of fish, calculated on the basis of the constant concentration factor (green line), whereas the use of the biokinetic model leads to another shape of the curves with a gradual increase followed by a decrease of the fish concentration similar to the results in Figure 22 (blue and brown lines).

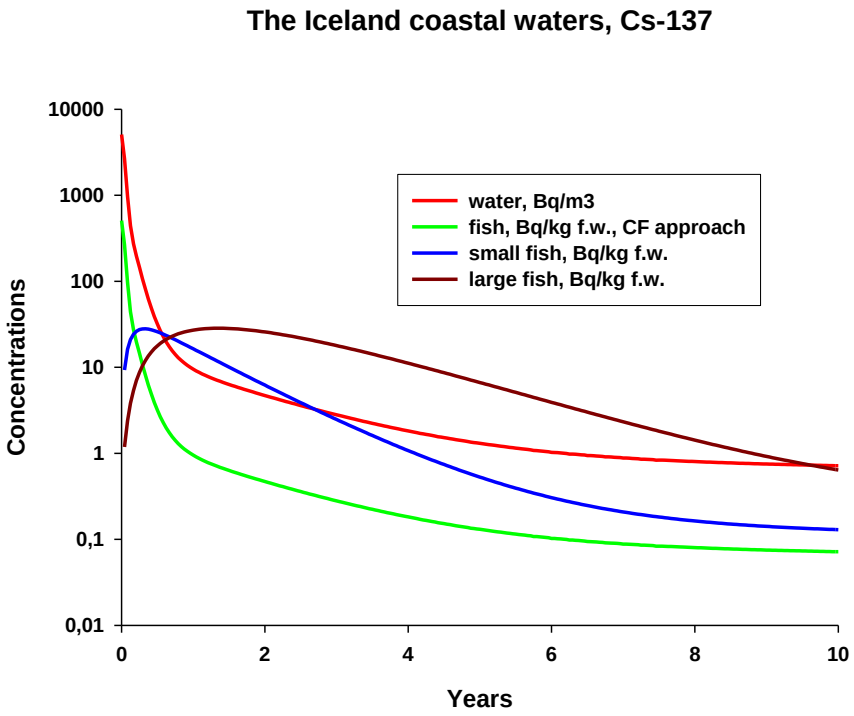

Figure 32. Concentrations of ^{137}Cs in seawater and fish.

The results regarding the ^{137}Cs concentration with the constant concentration ratio approach leads to different dose distribution for the critical group (the group of high consumption of seafood) compared to the biokinetic modelling approach. Results in Figure 33 shows that when the concentration ratio approach is used, the maximum is reached in the first year (26 μSv) and the concentration becomes almost insignificant in subsequent years. The use of the biokinetic approach for doses to the critical group for large fish, results in a distribution with the maximum dose corresponded to the second year (16 μSv), with slight decreases in subsequent years. At the same time, the total dose after ten years for the concentration ratio approach and for the biokinetic modelling approach are equal to 27 μSv and 60 μSv, respectively.

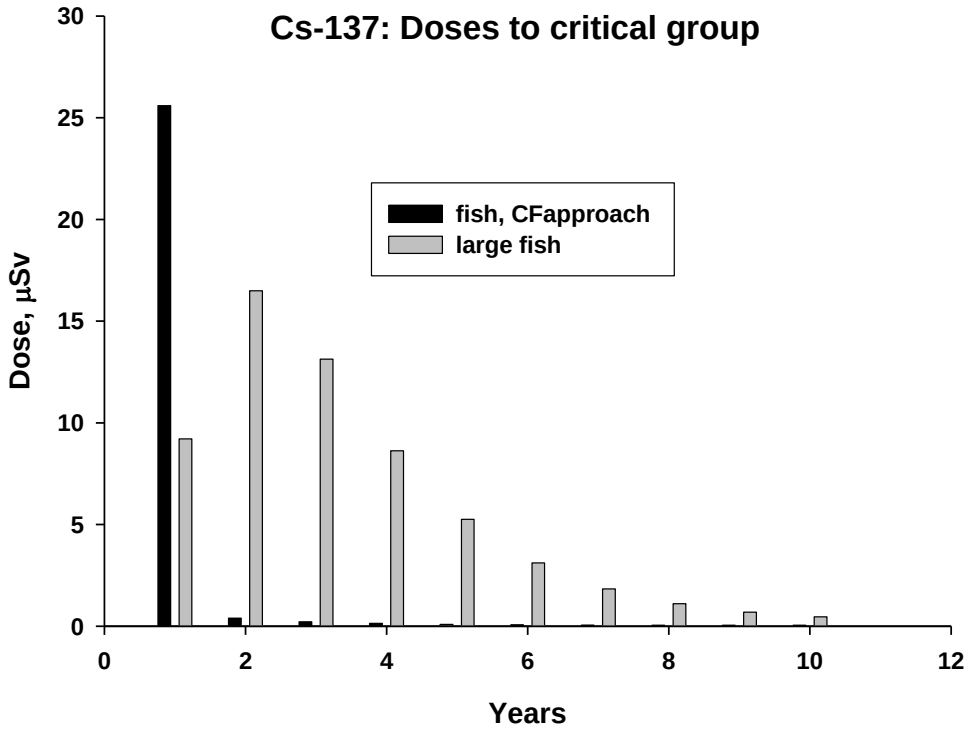

Figure 33. Doses the critical group from fish consumption.

4.2.2.2 ^{134}Cs

The dynamics of the releases of ^{134}Cs for ten years is shown in Figure 34.

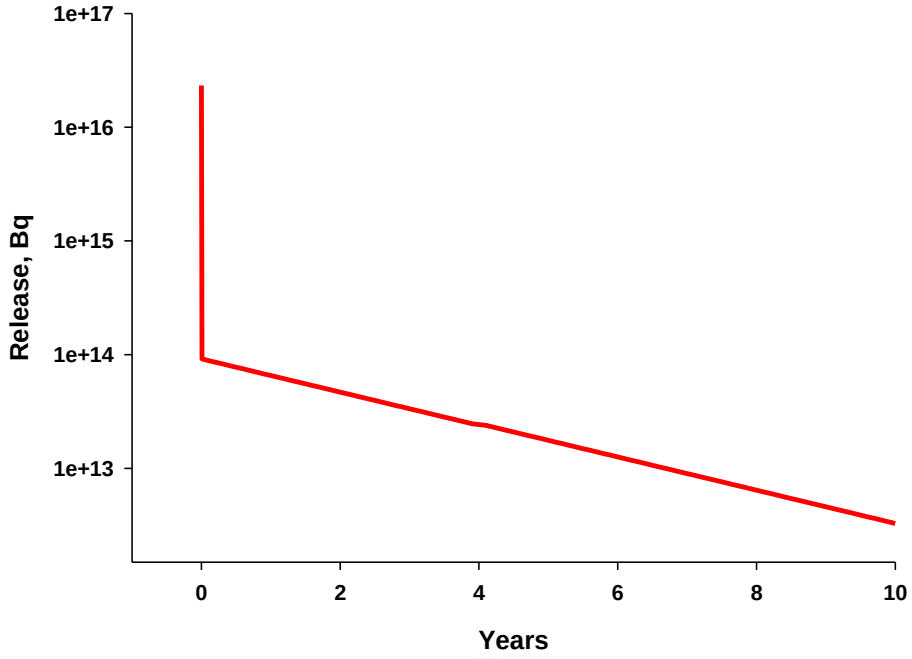

Figure 34. ***Release of ^{134}Cs into seawater***

Parameters for trophic level "*i*": the assimilation efficiency (AE_i), ingestion per unit mass (IR_i), rate of the direct uptake of activity from the water column ($k_{u,i}$) are the same as for ^{137}Cs.

The excretion rate of trophic level "i" ($k_{e,i}$) for ^{134}Cs is calculated by expression (2):

$$k_{e,i} = k_{e,i}^{(0)} + \ln 2\left[\frac{1}{T_{1/2,i}} - \frac{1}{T_{1/2,i}^{(0)}}\right], \qquad (2)$$

where $k_{e,i}^{(0)}$ is an excretion rate of trophic level "i" for ^{137}Cs, $T_{1/2,i}$ and $T_{1/2,i}^{(0)}$ are radionuclide half-life for ^{134}Cs and ^{137}Cs, correspondently.

Expression (2) has used an assumption that difference between excretion rates for ^{134}Cs and ^{137}Cs is based on differences of radionuclides physical

half-life components in the biological half-life for marine organisms with the same physiology and metabolism for caesium isotopes.

Similar to results for ^{137}Cs, the results regarding the ^{134}Cs concentration with the constant concentration ratio approach leads to different concentration in fish and different dose distribution for the critical group (the group of high consumption of seafood) compared to the biokinetic modelling approach (Figures 35-36).

The use of the biokinetic approach for doses to the critical group for large fish, results in a distribution with the maximum dose corresponded to the second year (27 μSv), with slight decreases in subsequent years. At the same time, the total dose after ten years for the concentration ratio approach and for the biokinetic modelling approach are equal to 50 μSv and 75 μSv, respectively.

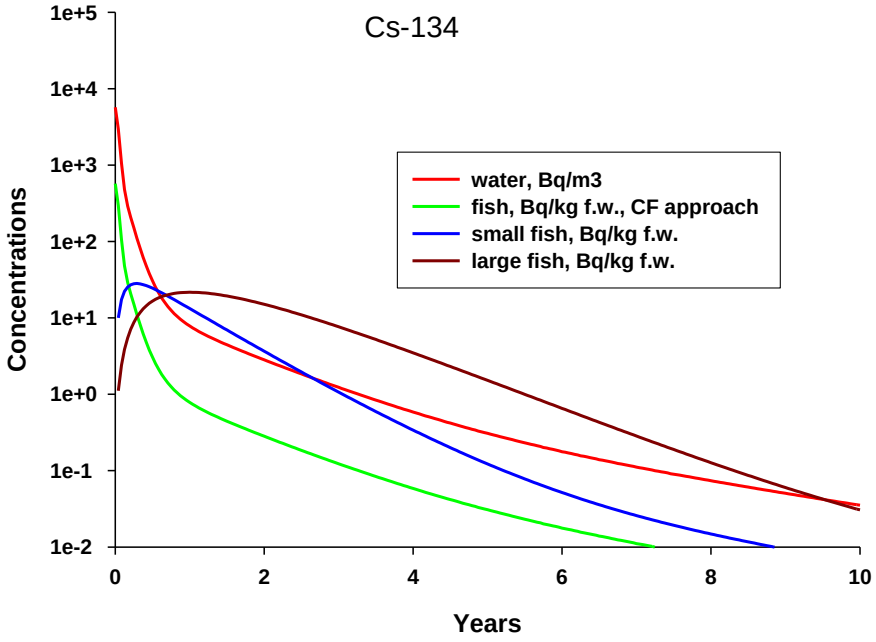

Figure 35. Concentrations of ^{134}Cs in seawater and fish.

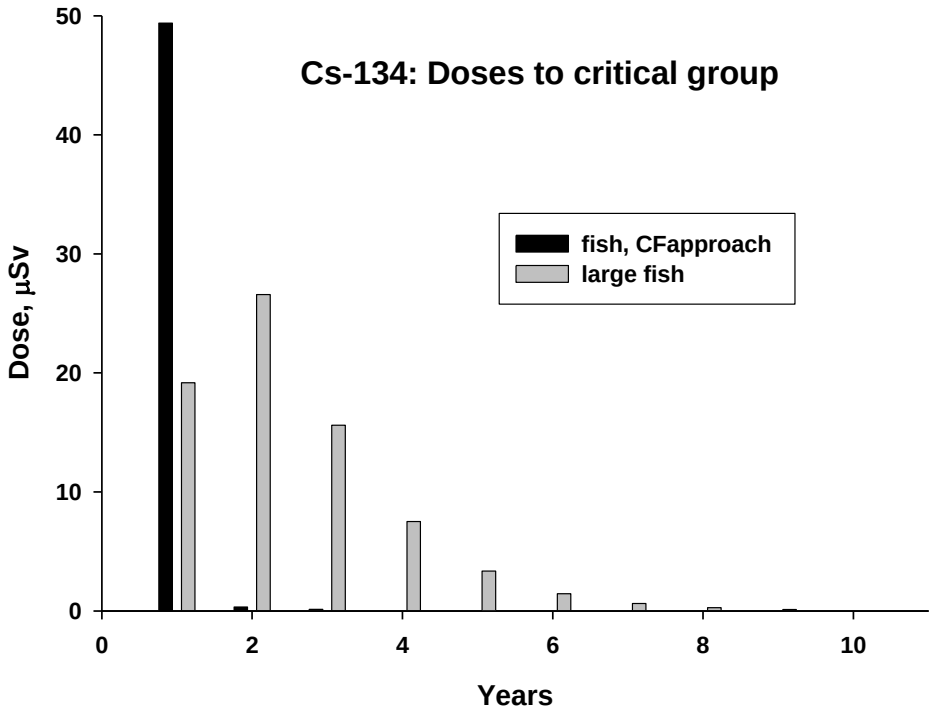

Figure 36. Doses the critical group from fish consumption.

4.2.3 Plutonium -238

Bioaccumulation of isotopes of plutonium is especially significant for molluscs (IAEA, 2004; COSEMA, 2014; Figure A4.2 in Appendix 4 of the present report). In particular, ^{238}Pu dominates contamination in molluscs according to the present release scenario (Appendix 4), but food chain considered by Thomann (1981) has no molluscs component, and parameters for molluscs in PREPARE (2015) do not pay special attention to ^{238}Pu. Therefore, it is impossible to use equation (1) for molluscs without additional assumptions.

Assume that equilibrium state provided by equation (1), when $t \to \infty$ correspond to average concentration in molluscs, which can be defined due the concentration factor.

When $t \to \infty$ equation (1) for molluscs can be written as

$$0 = AE_m \cdot IR_m \cdot C_m^* + k_{u,m} C_w - k_{e,m} \cdot C_m, \quad \textbf{(3)}$$

where concentration of ^{238}Pu in mulluscs C_m and concentration of ^{238}Pu in food consumption of molluscs $C^{(*)}_m$ will be calculated due the concentration factor under.

The ingestion rate for molluscs IR_m = 0.06 d^{-1} can be adopted from PREPARE (2015) with following food consumption: 60% of phytoplankton, 20% of zooplankton and 20% of macroalgae (Bezhenar et al., 2016).

Input parameters for ^{239}Pu from Thomann (1981) have been adopted for ^{238}Pu in the present report. Parameters are shown in Table 3

Table 3. Input parameters from Thomann (1981)

Biota	Assimilation rate AE_i	Excretion rate $k_{e,i}$	Water direct uptake rate $k_{u,i}$
Zooplankton	0.01	0.05	18,7
Small fish	0.01	0.02	0.3
Large fish	0.01	0.01	0.01

In order to use the equations (1) and (3), it is necessary to make additional assumptions. Considering that AE_i = 0.01 for all trophic levels, we assume here that assimilation rate for molluscs is equal to zero: AE_m = 0.

An allometric relationship demonstrates decreasing of the excretion rates with increasing of the biota mass (US DOE, 2002; Vives i Battle et al., 2009). An assumed weight for small fish lies within the broad range between 0.005 and 50 g f.w. (Thomann, 1981). The weight for benthic molluscs can be within the range between $2 \cdot 10^{-3}$ and 10 g f.w. (Jaiswar and Kulkarni, 2002; Vives i Batlle et al., 2008). Therefore, it is possible to assume that an excretion rate for molluscs $k_{e,m}$ will lie within the range between 0.02 and 0.05 d^{-1} (the value of $k_{e,m}$ is likely closer to 0.02 than to 0.05 according to weight comparison of the animals)

It is necessary to note that according to expression (3)

$$k_{e,m} > [AE_m \cdot IR_m \cdot C_m^{(*)}] / C_w . \quad (4)$$

Further, $C_m^{(*)} = 0.6 \cdot C_p + 0.2 \cdot C_z + 0.2 \cdot C_a$, where $C_{p,}$ C_z and C_a are concentrations in phytoplankton, zooplankton and macroalgae, respectively. $C_{p,}$ C_z and C_a are calculated with the concentration factors from IAEA (2004), where C_w=1 Bq/l. Considering the expression (4) with, $k_{e,m}$ will lie within the range between 0.025 and 0.05 d^{-1}.

The value of 0.025 d^{-1} for $k_{e,m}$ is selected for the following calculation in the present report.

And finally, the rate of the direct uptake of activity from water column ($k_{u,m}$) may be written in form

$$k_{u,m} = [AE_m \cdot IR_m \cdot C_m^{(*)} - C_m \cdot k_{e,m}] / C_w$$

and $k_{u,m}$ = 2.04 d^{-1}, where $k_{e,m}$ = 0.025 d^{-1}.

Figure 37 shows concentration ^{238}Pu in molluscs, where the concentration in water is of 1Bq/l for biokinetic modelling. According to present modelling approach concentrations in water and molluscs come to equilibrium after one hundred days, approximately

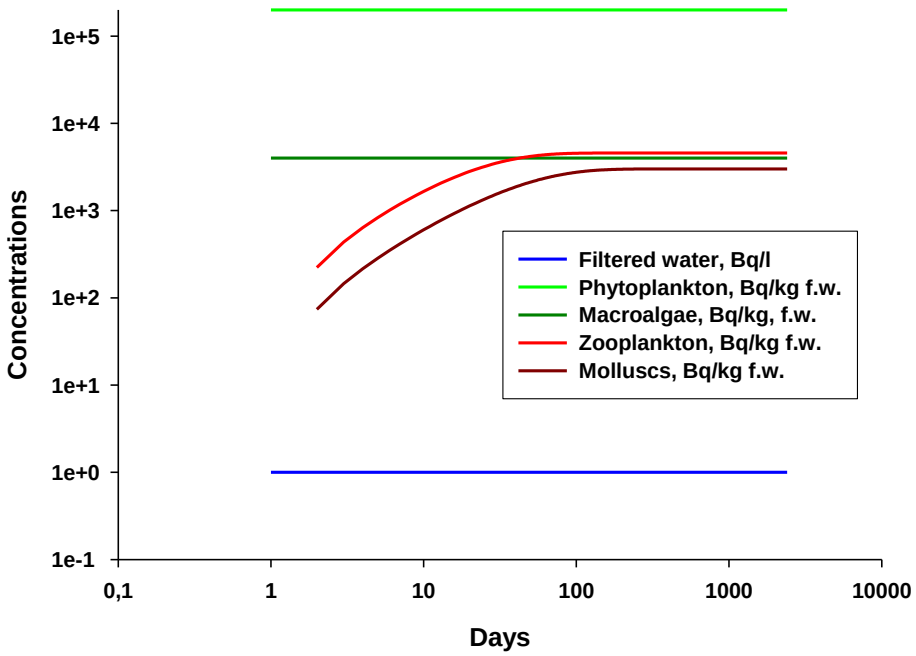

Figure 37. Concentration of ^{238}Pu in water and different trophic levels

Figure 38 shows calculation of ^{238}Pu concentration (box 2, see Fig. A2.1, Appendix 2) in seawater and molluscs according to this scenario, corresponding to the accident location. The results in Figure 38 show the same shape for the graphs for water concentration and concentration in molluscs, calculated on the basis of the constant concentration factor, whereas the use of the biokinetic model leads to another shape of the curves with a gradual increase followed by a decrease of the mollusc concentration. It is interesting to note that concentration in molluscs according to the present approach does not exceed the Guideline level for the Group 1 of radionuclides that can be important for design makers.

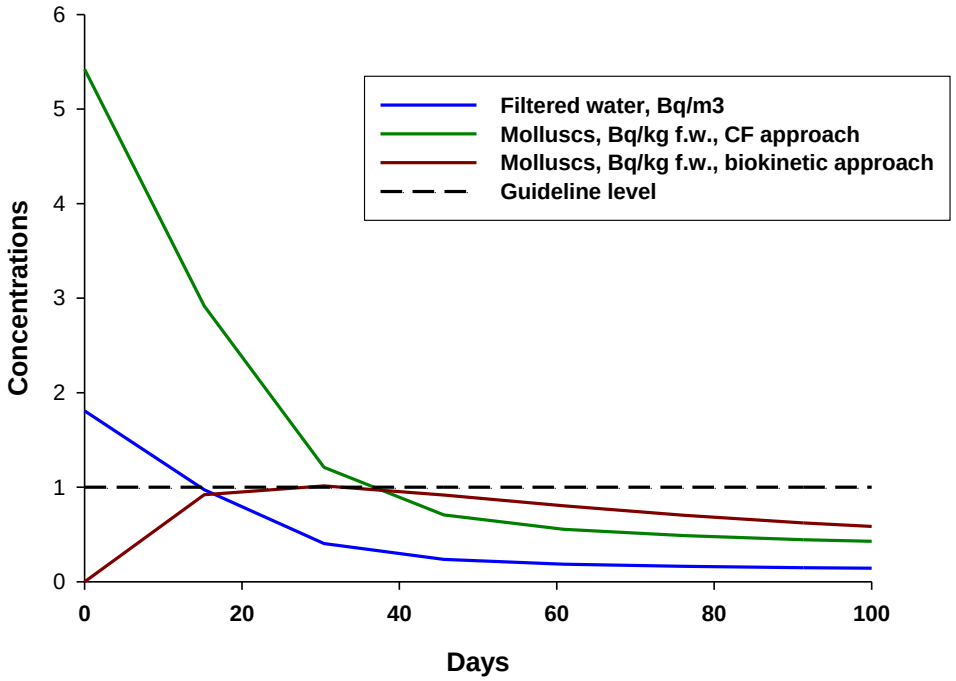

Figure 38. Concentration of ^{238}Pu in water and molluscs (the submarine scenario)

4.2.4. Tellurium -132

Concentration of ^{132}Te in biota in Figure A4.3 (COSEMA, 2014; Appendix 4) significantly exceeds (up to two orders of magnitude) the guideline level for this group of radionuclides during an initial time of radionuclide release, but dose to the critical group from ^{132}Te is negligible (Appendix 4). Therefore, a hypothesis that evaluation of concentration of radionuclides in biota on the basis of the concentration factor approach is too conservative for ^{132}Te has to be evaluated.

Unfortunately, information, which can be used for evaluation of kinetic coefficients, is very poor.

There is limited information in ICRP (1993) that assimilation rates for tellurium isotopes for several animal species can lies within the range between 0.2 and 0.5. Additionally, values of 0.3 and 0.6 may be adopted for adults and infants, respectively.

For following calculations, the value of 0.2 is selected for the zooplankton assimilation rate because this value corresponds to water soluble fractions of radionuclide (ICRP, 1993). For all other biota, it is selected conservative value of 0.6 for assimilation rates. The selection of conservative value can potentially lead to the faster accumulation process.

There is no information concerning excretion rates or biological half-lifes for ^{132}Te, but we can again select a conservative approach and define excretion rates as

$$k_{e,i} = \frac{\ln 2}{T_{1/2}^{(*)}},$$

where $T_{1/2}^{(*)}$ is radioactive half-live for ^{132}Te (3.26 d).

With methodology from section 4.2.3, parameters for equation (1) have been selected. Selected parameters are shown in Table 4.

Table 4. Input parameters from equation (1)

Biota	Assimilation rate AE_i	Excretion rate $k_{e,i}$	Water direct uptake rate $k_{u,i}$
Zooplankton	0.2	0.25	40.
Small fish	0.6	0.22	220
Large fish	0.6	0.213	208

Figure 39 shows concentration of ^{132}Te in fish, where the concentration in water is of 1Bq/l. According to present modelling approach concentrations in water and fish come to equilibrium after ten days, approximately

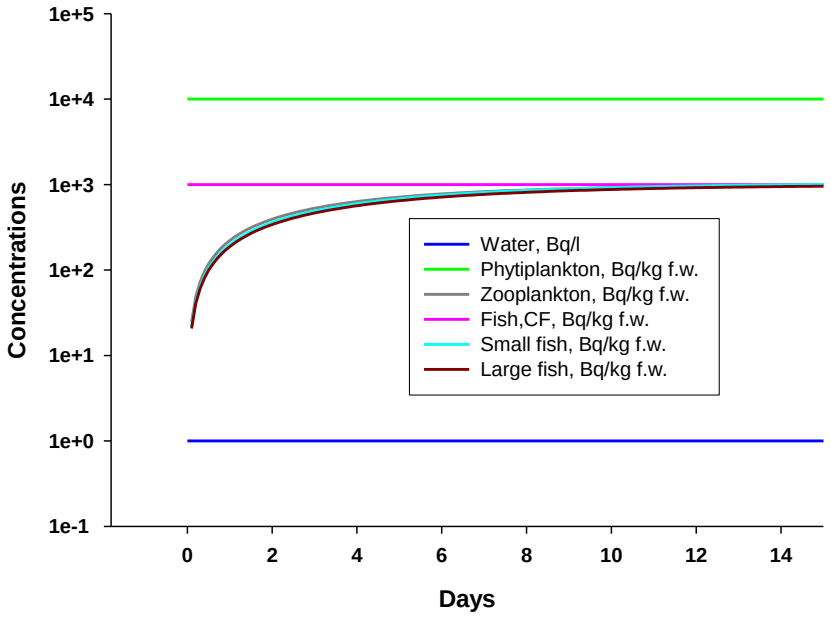

Figure 39. Comparison of the concentration of radionuclides in biota for ^{132}Te.

Figure 40 shows calculation of ^{132}Te concentration (box 2, see Fig. A2.1, Appendix 2) in seawater and fish according to the submarine accident scenario. Figure 40 shows the same shape for the graphs for water concentration and concentration in fish, calculated from the constant concentration factor, whereas the use of the biokinetic model leads to another shape of the curves with a dramatic decreasing of ^{132}Te concentration in fish (up to orders of magnitude). Small and large fish have very similar shape under this selection of parameters. It is important to note that concentration in fish according to the present approach does not exceed the Guideline level for the Group 3 of radionuclides. Such results can be important for design makers, have better harmonisation with doses to humans and, in spite of lack of information for closer approximation of necessary parameters, provide more logical description of the bioaccumulation processes than approach based on use of constant concentration factors.

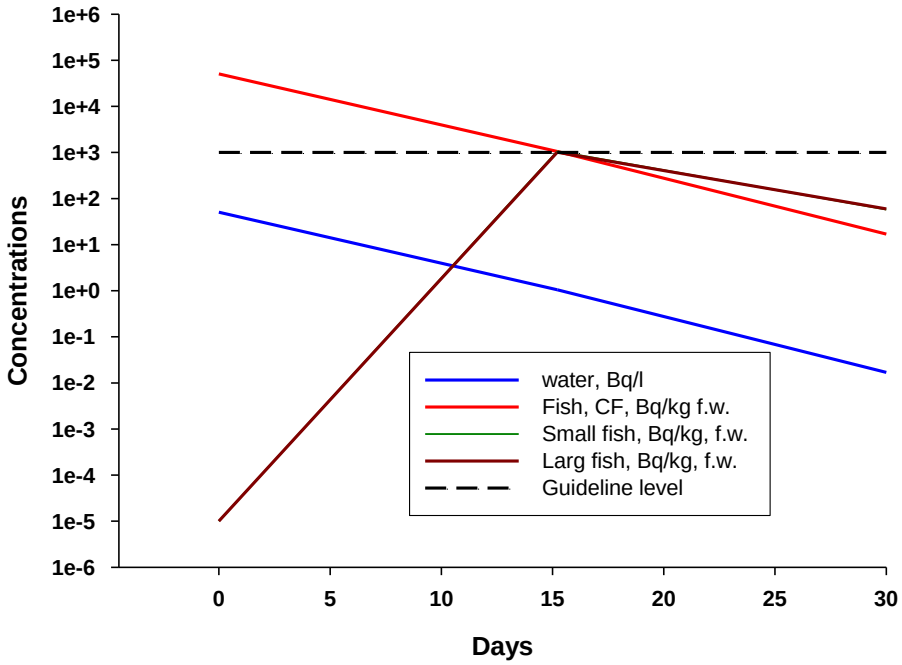

Figure 40. Comparison of the concentration of radionuclides in biota for ^{132}Te for the Submarine scenario

5. Conclusions

The results of the implementation of the kinetic model for bioaccumulation processes into the NRPA box model and the DETRA computer code clearly demonstrated that there is a significant quantitative difference between the kinetic modelling approach and the approach based on the constant concentration rates.

The modelling results were compared with experimental data on the basis of improved version of the NRPA box model for the Baltic Sea. It clearly shows that dynamic modelling of the bioaccumulation processes can provide a more correct description of the concentration of radionuclides in biota. Therefore, these results support the main goal of the EFMARE project.

It is important to note that the improved modelling approach for radioecological assessment indicates significant differences between results based on constant concentration factors (CF) and the description of bioaccumulation process with a kinetic submodel. Also, kinetic modelling of bioaccumulation processes leads to a better harmonisation between the differenct calculations (for example, between doses to the critical group

and concentrations in marine organisms for short-life radionuclides) and also to better logical explanations of the results.

With a numerical case study the temporal variability of pollutant dispersal in Icelandic waters was demonstrated and discussed. The simulations, which contain a pollution source in Denmark Strait northwest of Iceland, are based on flow and turbulence fields provided by the CODE operational ocean model. The results show a spreading directed mainly eastwards over the north Icelandic shelf with the North Icelandic Irminger Current. Another path leads into the southward directed East Greenland Current. The dispersal into both branches shows a high inter-seasonal variability whereas the role of the seasonal signal is, at least in certain areas, only of minor importance. The results emphasize the necessity to use operational hydrodynamic ocean models in order to forecast pollutant dispersal in Icelandic waters.

The use of particle density can be used for comparison with simulations from the NRPA box model.

Our study of the temporal variability of pollutant dispersal in Icelandic waters shows that simultaneous use of different models (eg hydrodynamic and box models) can significantly improve the description of dispersion of radionuclides in the marine environment.

The recalculation of the results for the NPP in the Baltic Sea region has been carried out based on corrected information concerning the source term from the Fukushima accident.

It is shown that the concentration in the Baltic appear earlier in case of release from the Swedish coast. Preliminary results show that the maximum Cs-137 concentration in seawater is about 1 Bq/l.

References

Bezhenar R., Jung K. T., Maderich V., Willemsen S., Govert de With, F. Qiao (2016). Transfer of radiocaesium from contaminated bottom sediments to marine organisms through benthic food chain in post-Fokushima and post-Chernobyl periods. Biogeosciences, under review, personal communications

Brown J., Børretzen P., Dowdall M., Sazykina T., and Kryshev I., 2004. The derivation of transfer parameters in the assessment of radiological impacts on Arctic marine biota. Arctic, 57, No. 3, 279-289.

COSEMA, 2014. Consequences of severe radioactive releases to Nordic marine environment. Final report for the NKS-B COSEMA activity 2013, Contract AFT/B(13)3.

EC (2000). The radiological exposure of the population of the European Community to radioactivity in the Baltic Sea, Marina-Balt Project. European Commission, Luxembourg, EUR 19200.

Fowler S., Heyraud M. and Beasley T.M., 1975. Experimental studies on plutonium kinetics in marine biota. In Impacts of nuclear releases into the aquatic environment. Proceedings of an intornational symposium on radiological impacts of releases from nuclear facilities into aquatic environments, p. 157-176, IAEA, Vienna, Austria.

HELCOM, 1995. Radioactivity in the Baltic Sea 1984-1991. Baltic Sea Environment Proceedings 61, 182 pp.

Heling R., Koziy I., Bulgakov V., 2002. On the dynamic uptake model developed for the uptake of radionuclides in marine organisms for the POSEIDON-R model system. Radioprotection 37 (C1), 833-838.

IAEA, 2004. *Sediment distribution coefficients and concentration factors for biota in the marine environment.* IAEA Technical reports series no. 422. Vienna: International Atomic Energy Agency, IAEA.

ICRP, 1993. Age-depended doses to members of the public from intake of radionuclides: Part 2, Ingestion dose coefficients, ICRP Publications 67. Annals of the ICRP vol. 23, No. 3/4.

Iosjpe, M., J. Brown & P. Strand, 2002. Modified approach for box modeling of radiological consequences from releases into marine environment, Journal of Environmental Radioactivity 2002, 60, 91–103.

Iosjpe M., M. Karcher, J. Gwynn, I. Harms, R. Gerdes and F. Kauker (2009). Improvement of the dose assessment tools on the basis of dispersion of the ^{99}Tc in the Nordic Seas and the Arctic Ocean. *Radioprotection*, vol. **44**, n^{o} 5, 531-536.

Jaiswar A. K. and Kulkarni B. G., 2002. Length-weght relationship of intertidal mollusscs from Mumbai, India, Journal of the Indian Fisheries Association, 29, 55-63

Logemann, K., J. Ólafsson, Á. Snorrason, H. Valdimarsson, and G. Marteinsdóttir (2013): The circulation of Icelandic waters – a modelling study, Ocean Sci., 9, 931-955, doi:10.5194/os-9-931-2013, 2013.

Maderch V., Bezhenar R., Heling R., G. de With, Jung K.T., Myoung J.G., Cho Y.-K., Qiao F., Robertson L., 2013. Regional long-term model of radioactivity dispersion and fate in the Fukushima Dai-ichi accident. Journal of Environmental Radioactivity 2013, www.elsevier.com/locate/jenvrad.

PREPARE, 2015. Design document for POSEIDON model integration. Deliverable D 5.2, PREPARE(WP5)-(1)-01.

Thomann R.V., 1981. Equilibrium model of fate of microcontaminants in diverse aquatic food-chains. Canadian Journal of Fisheries and Aquatic Sciences 38:280-296.

UNSCEAR 2013 Report. Volume I, Scientific Annex A: Levels and effects of radiation exposure due to the nuclear accident after the 2011 great east-Japan earthquake and tsunami. UNSCEAR 13-85418.

US DOE, 2002. A graded approach for evaluating radiation doses to aquatic and terrestrial biota. Technical standart DOE-STD-1153-2002, Washington D.C., U.S. Department of Energy.

Vives i Batlle J., Wilson R.C., Watts S.J., Jones S.R., McDonald P., Vives-Lynch S., 2008. Dynamic model for assessment of radiological exposure to marine biota. Journal of Environmental Radioactivity 99, 1711-1730.

Vives i Batlle J., Wilson R.C., Watts S.J., McDonald P., Craze A. 2009. Derivation of allometric relationships for radionuclides in marine phyla. Radioprotection, 44, 47-52.

Yankovich T.L. et al., 2010. Whole body to tissue concentration ratios for use in biota dose assessments for animals. Radiat. Environ. Biophys. 49, 549-565.

Appendix 1. Graphics of particle density

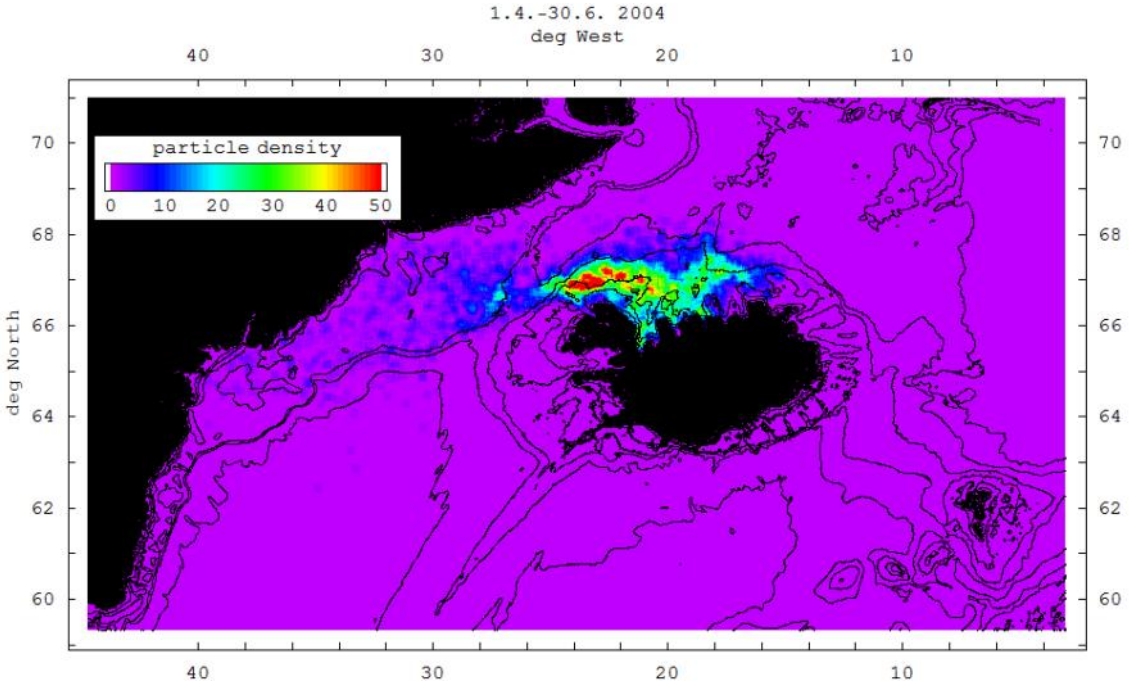

Fig. A1.1: Particle density at the end of the spring 2004 simulation.

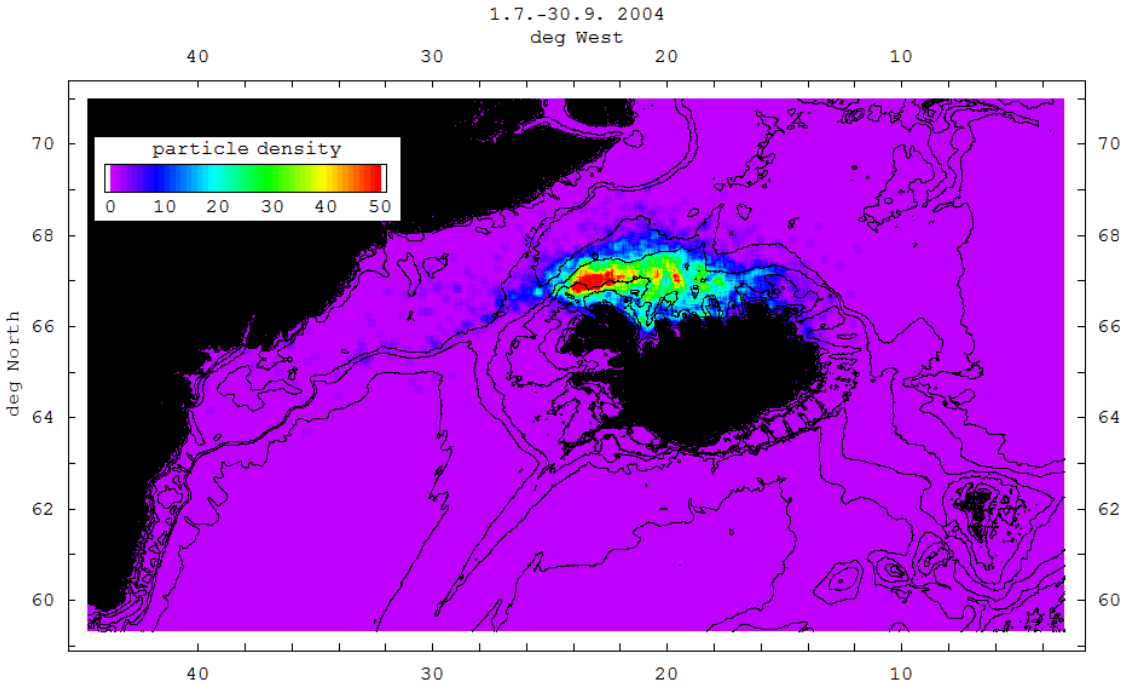

Fig. A1.2: Particle density at the end of the summer 2004 simulation.

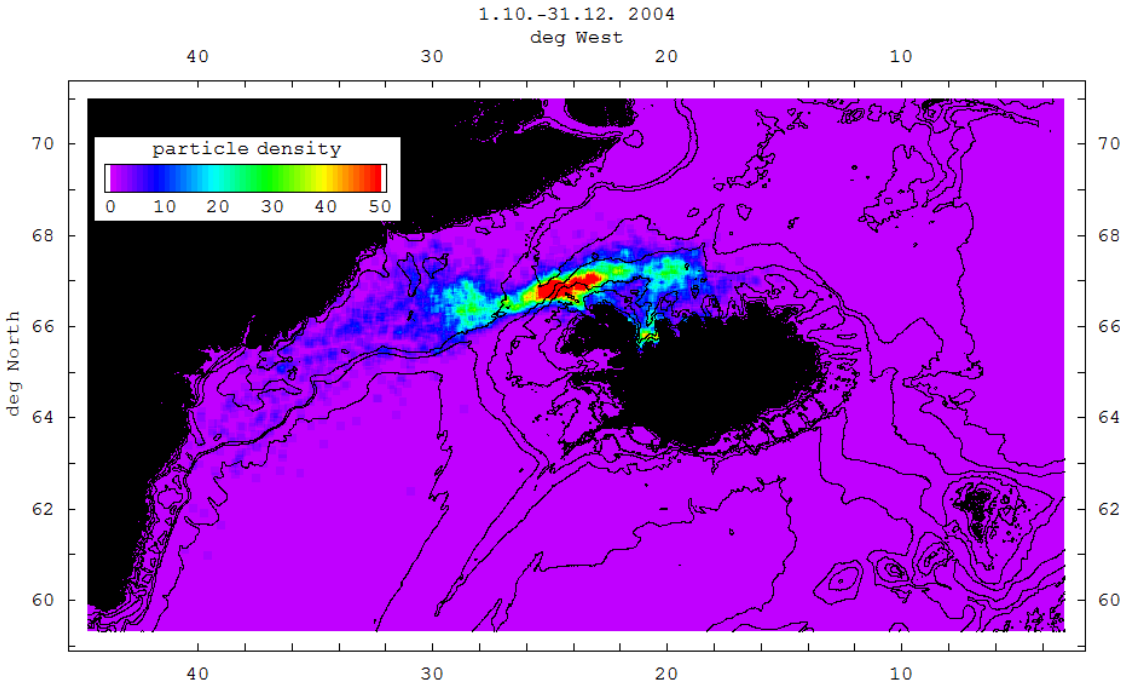

Fig. A1.3: Particle density at the end of the autumn 2004 simulation.

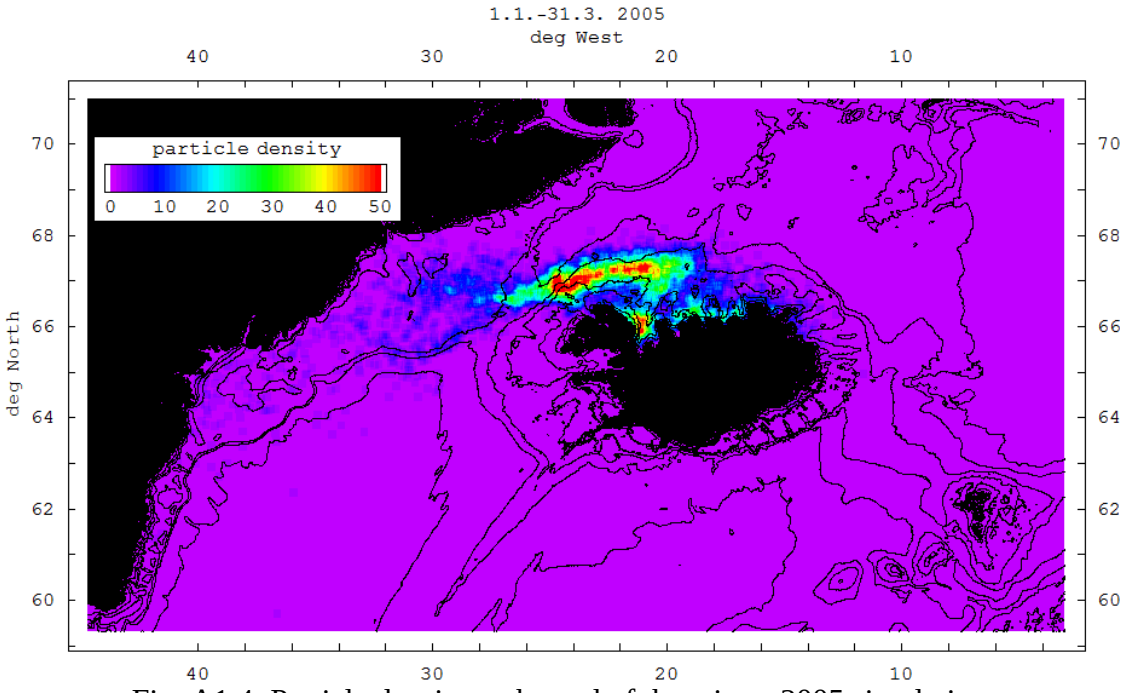

Fig. A1.4: Particle density at the end of the winter 2005 simulation.

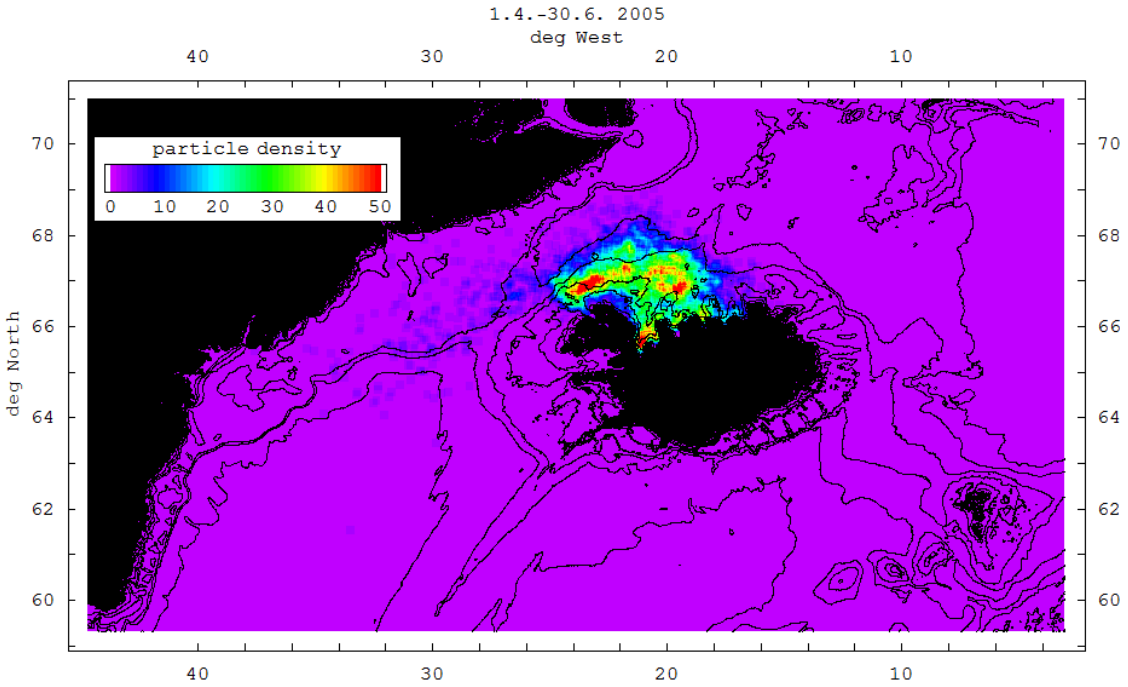

Fig. A1.5: Particle density at the end of the spring 2005 simulation.

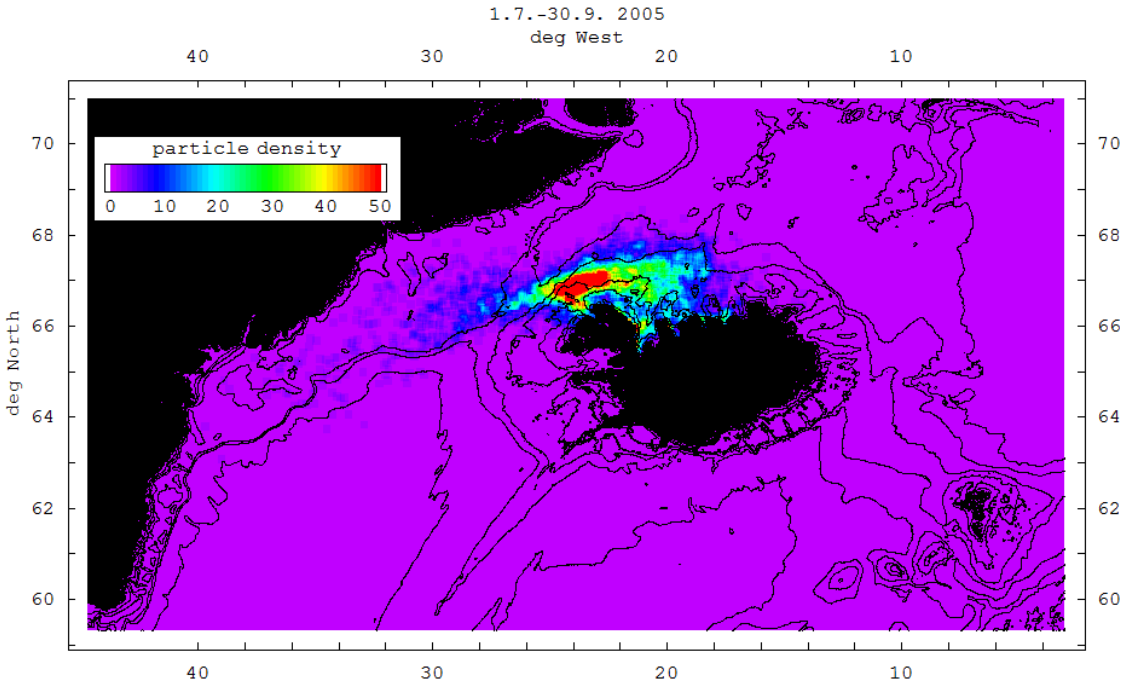

Fig. A1.6: Particle density at the end of the summer 2005 simulation.

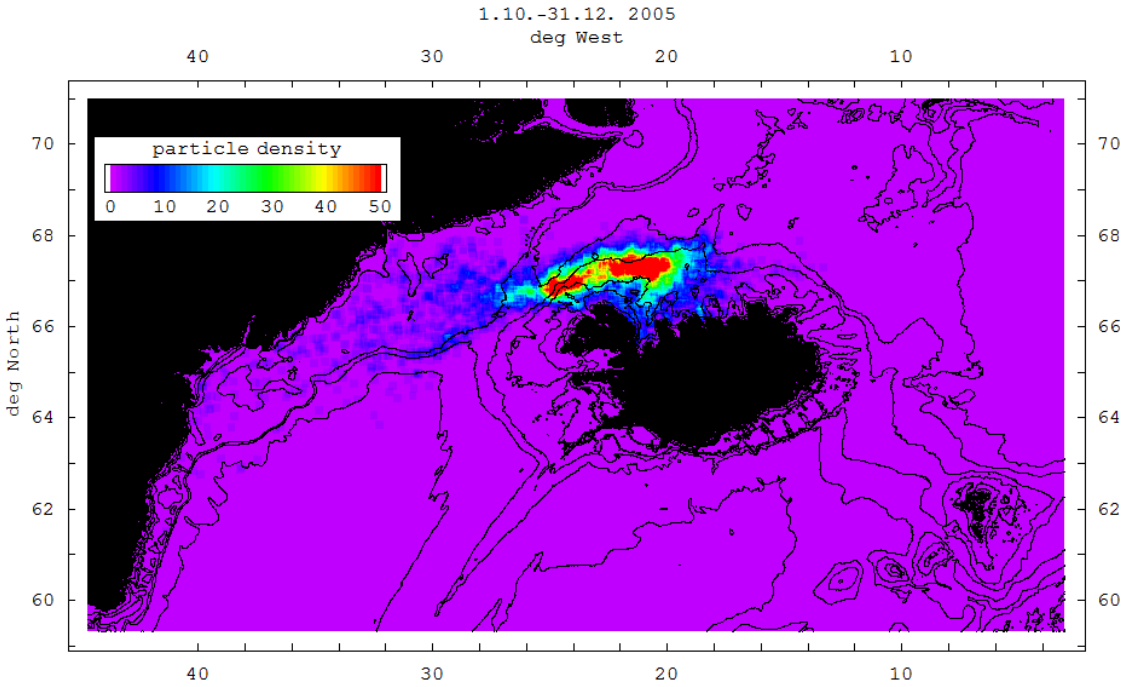

Fig. A1.7: Particle density at the end of the autumn 2005 simulation.

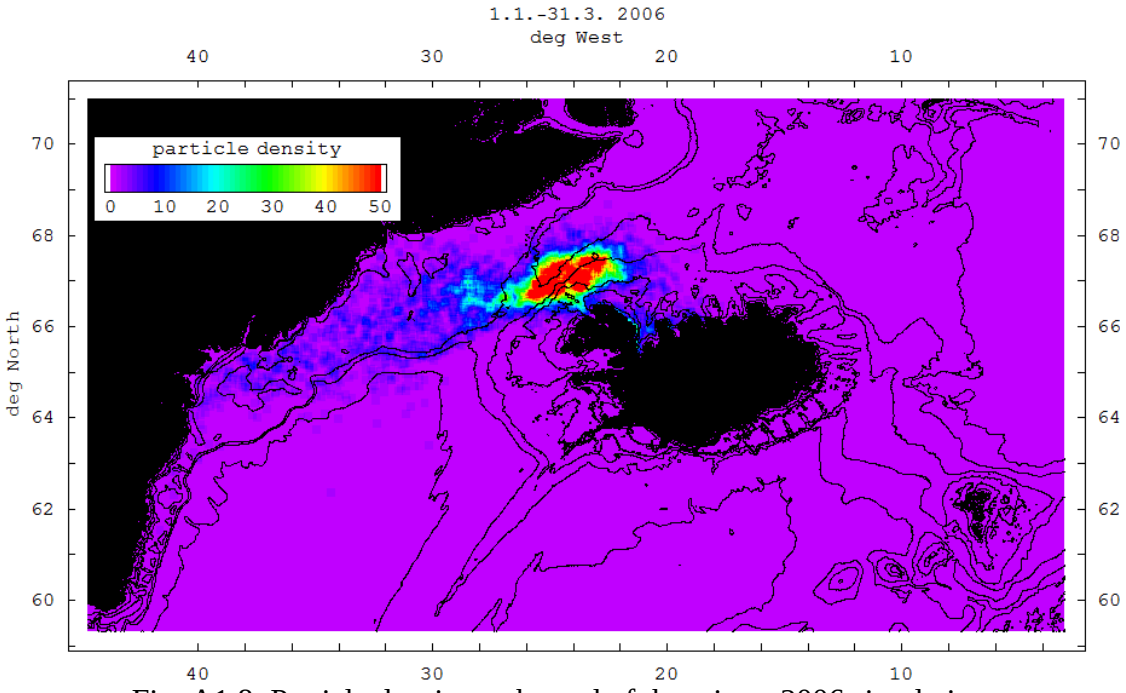

Fig. A1.8: Particle density at the end of the winter 2006 simulation.

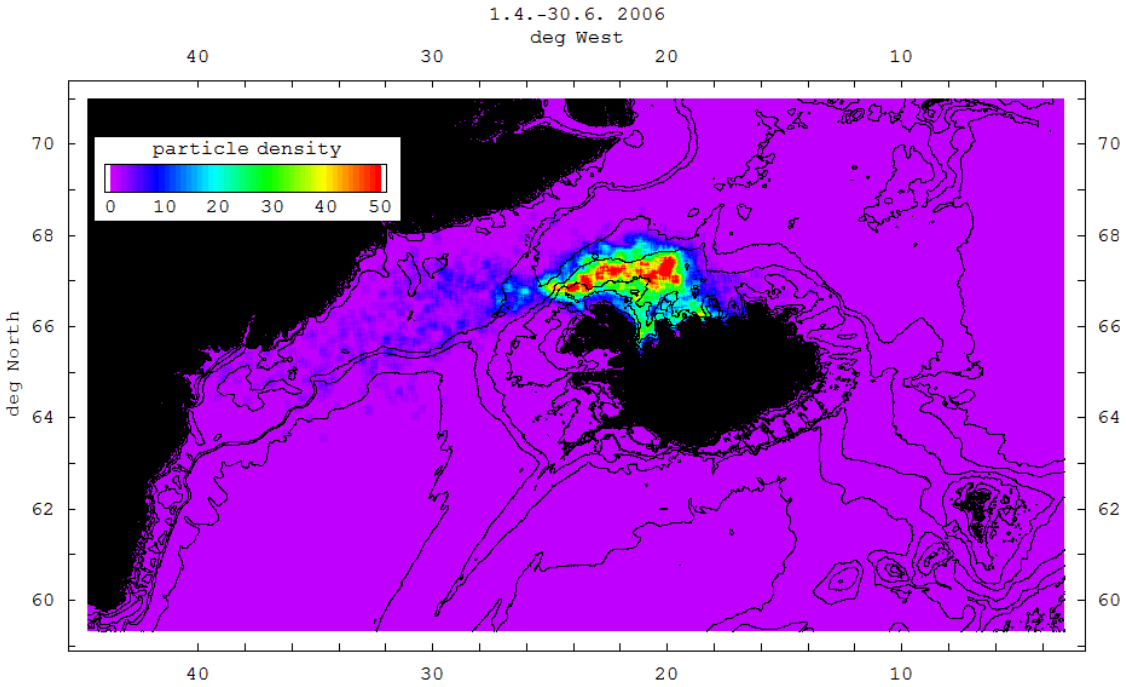

Fig. A1.9: Particle density at the end of the spring 2006 simulation.

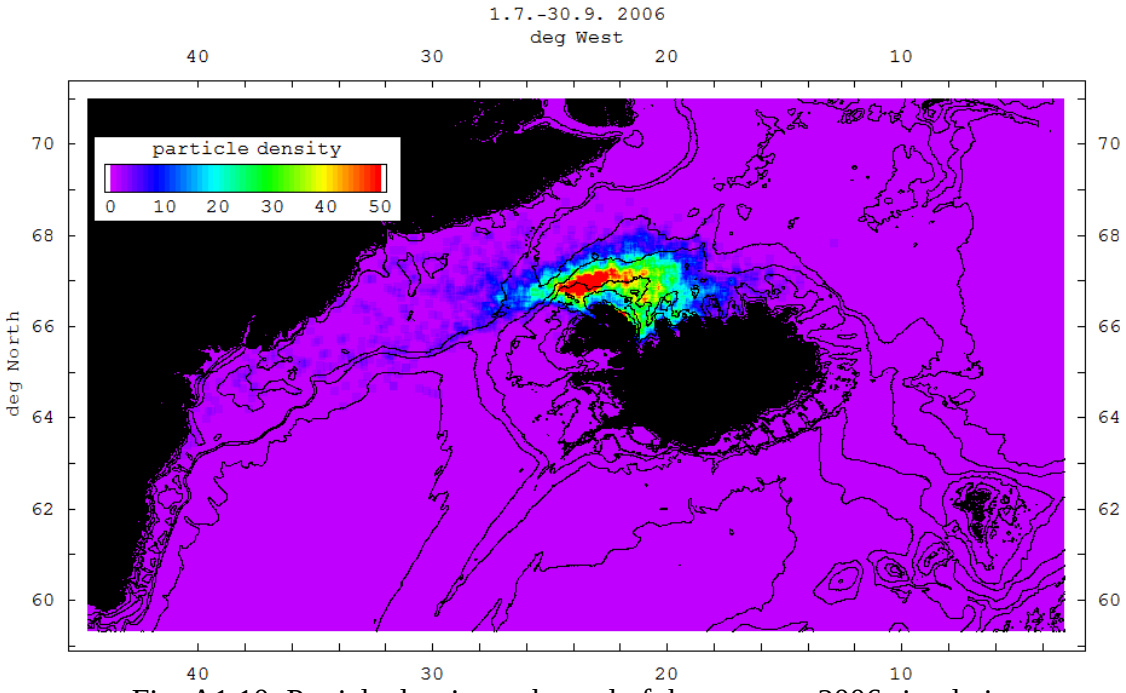

Fig. A1.10: Particle density at the end of the summer 2006 simulation.

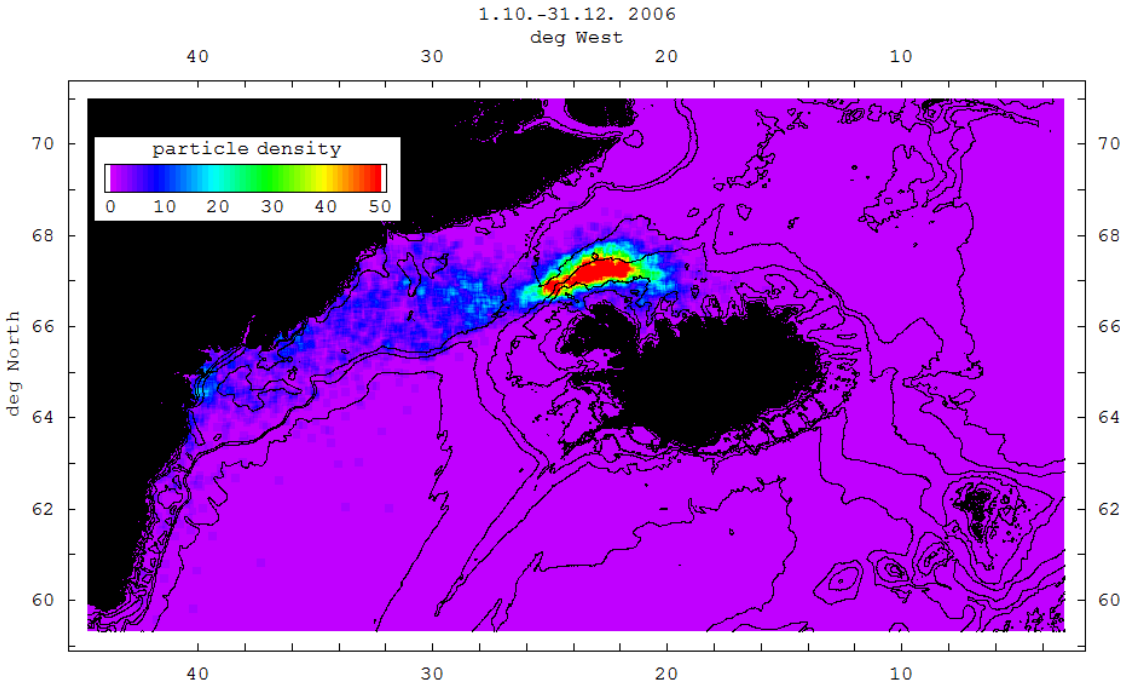

Fig. A1.11: Particle density at the end of the autumn 2006 simulation.

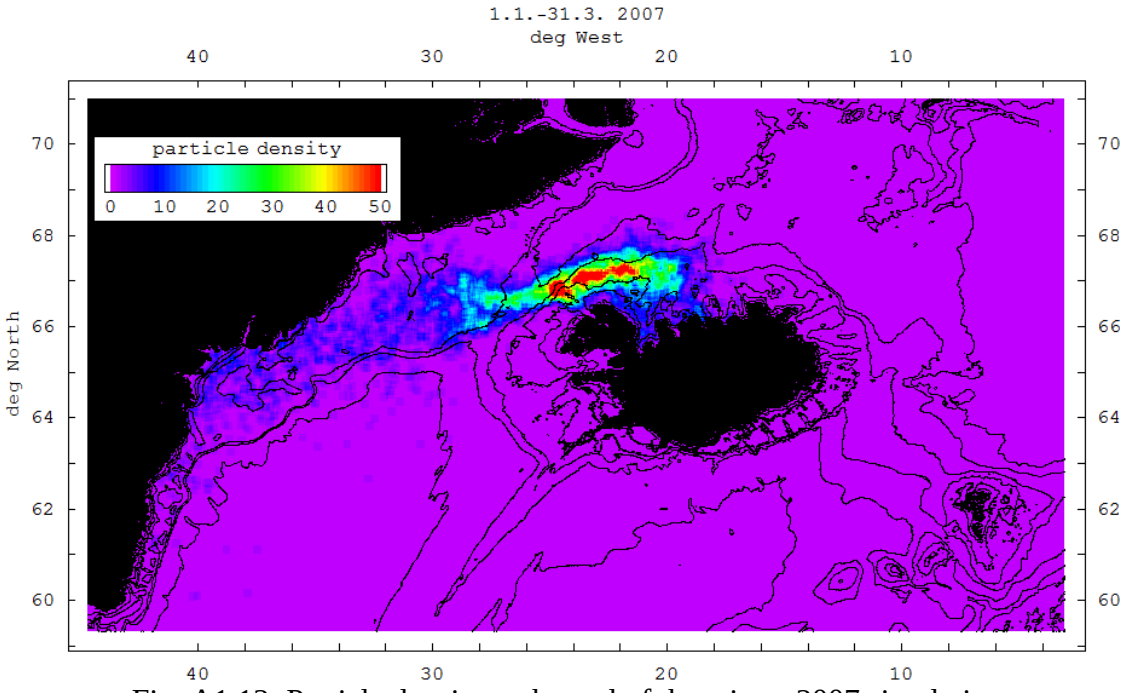

Fig. A1.12: Particle density at the end of the winter 2007 simulation.

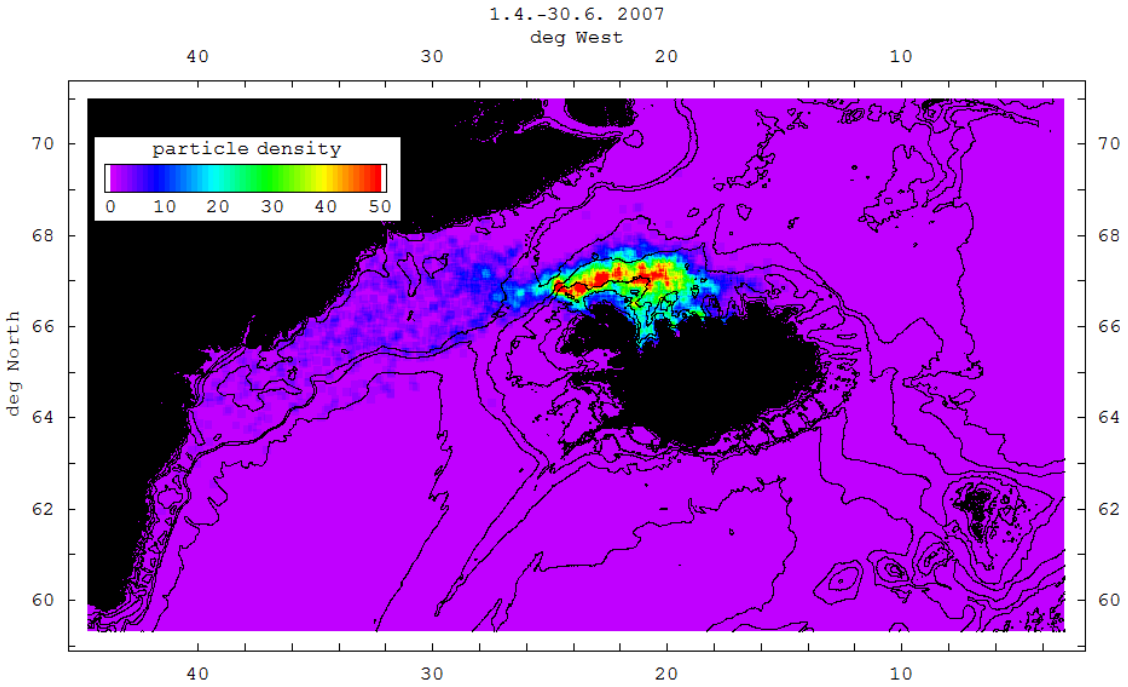

Fig. A1.13: Particle density at the end of the spring 2007 simulation.

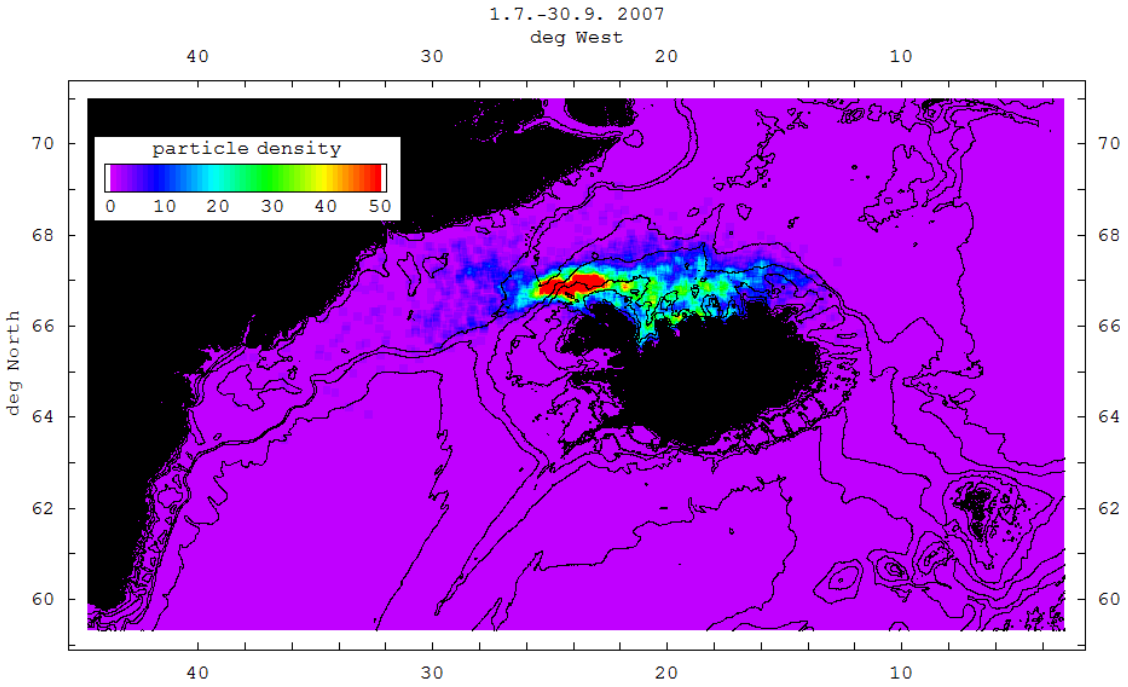

Fig. A1.14: Particle density at the end of the summer 2007 simulation.

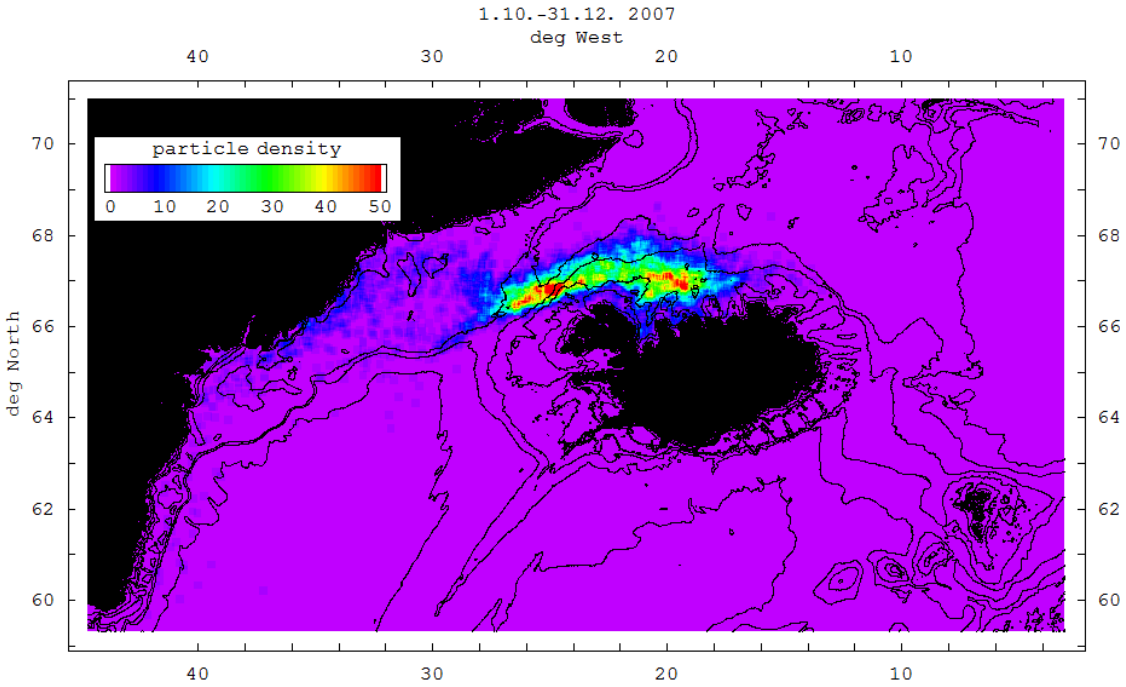

Fig. A1.15: Particle density at the end of the autumn 2007 simulation.

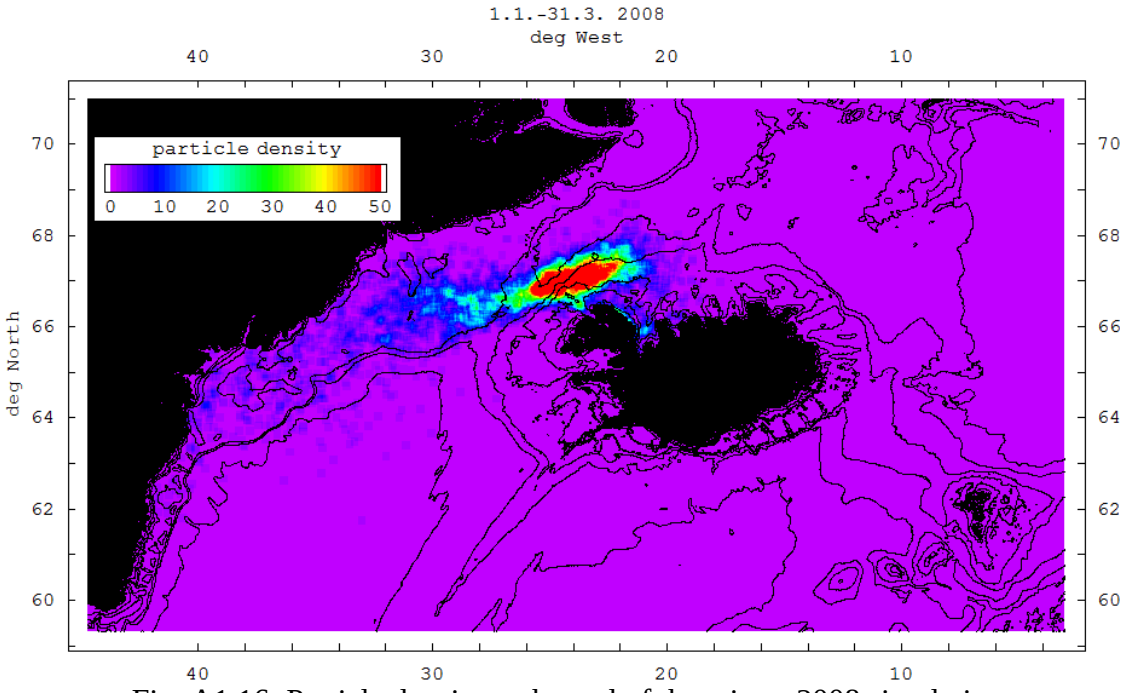

Fig. A1.16: Particle density at the end of the winter 2008 simulation.

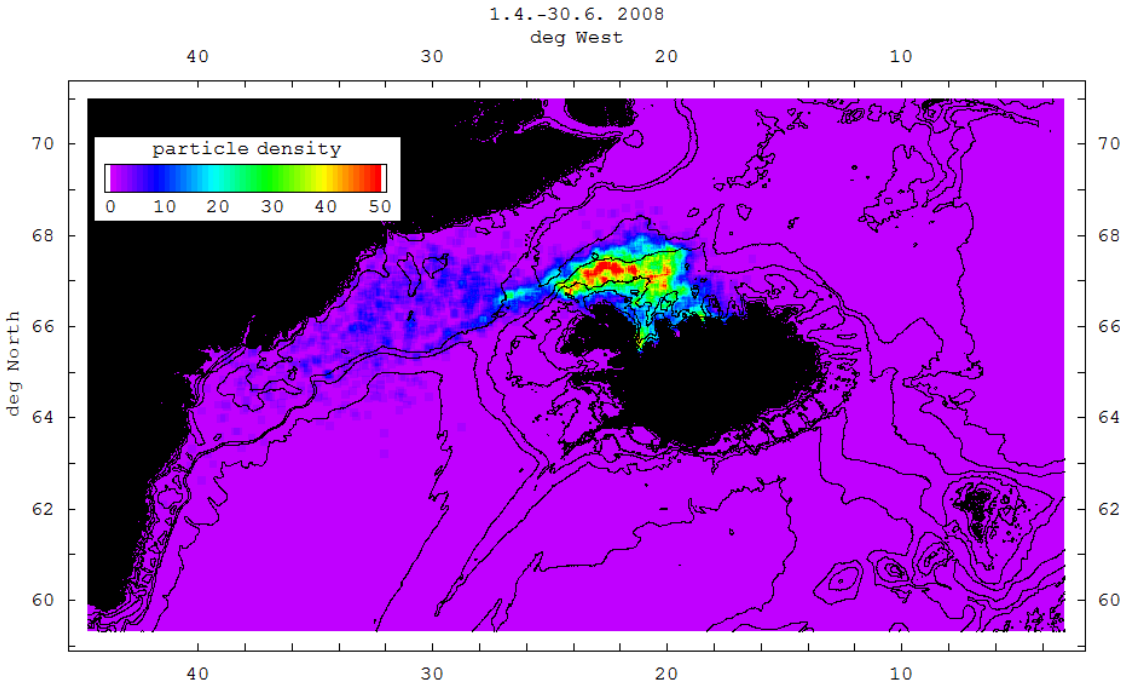

Fig. A1.17: Particle density at the end of the spring 2008 simulation.

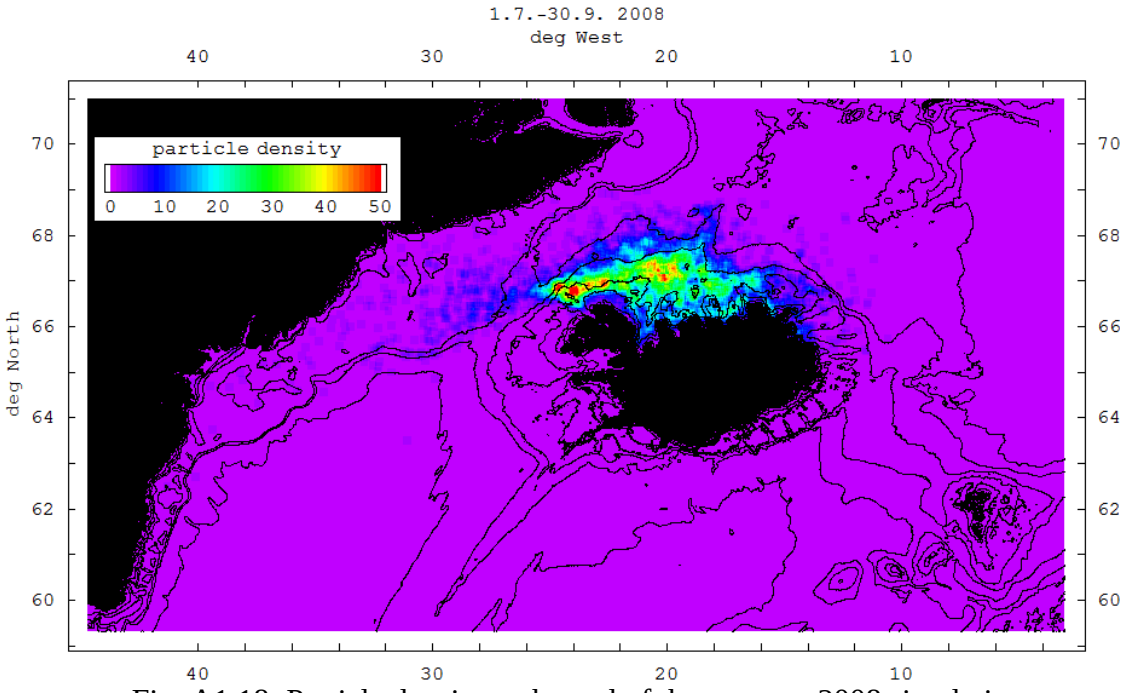

Fig. A1.18: Particle density at the end of the summer 2008 simulation.

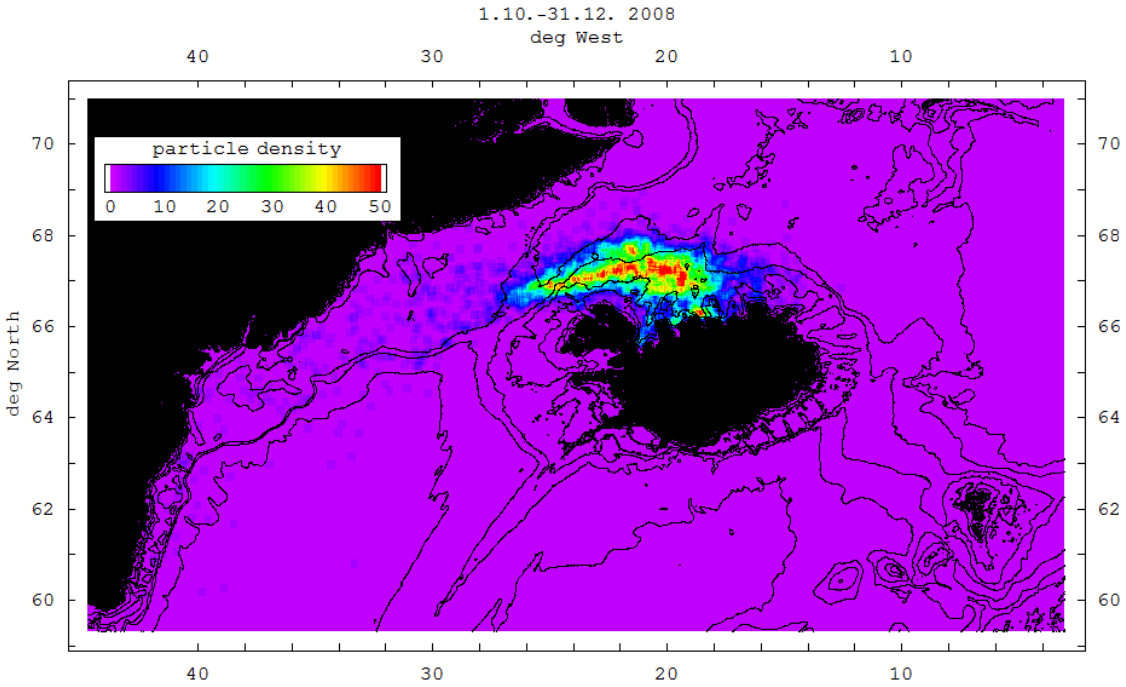

Fig. A1.19: Particle density at the end of the autumn 2008 simulation.

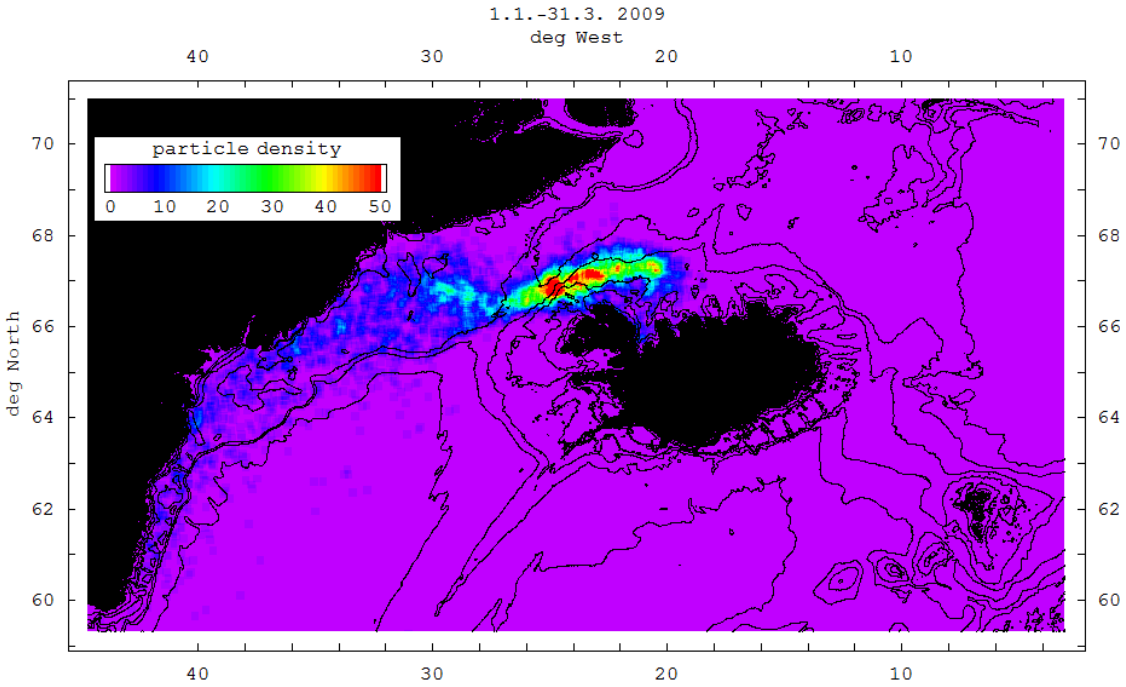

Fig. A1.20: Particle density at the end of the winter 2009 simulation.

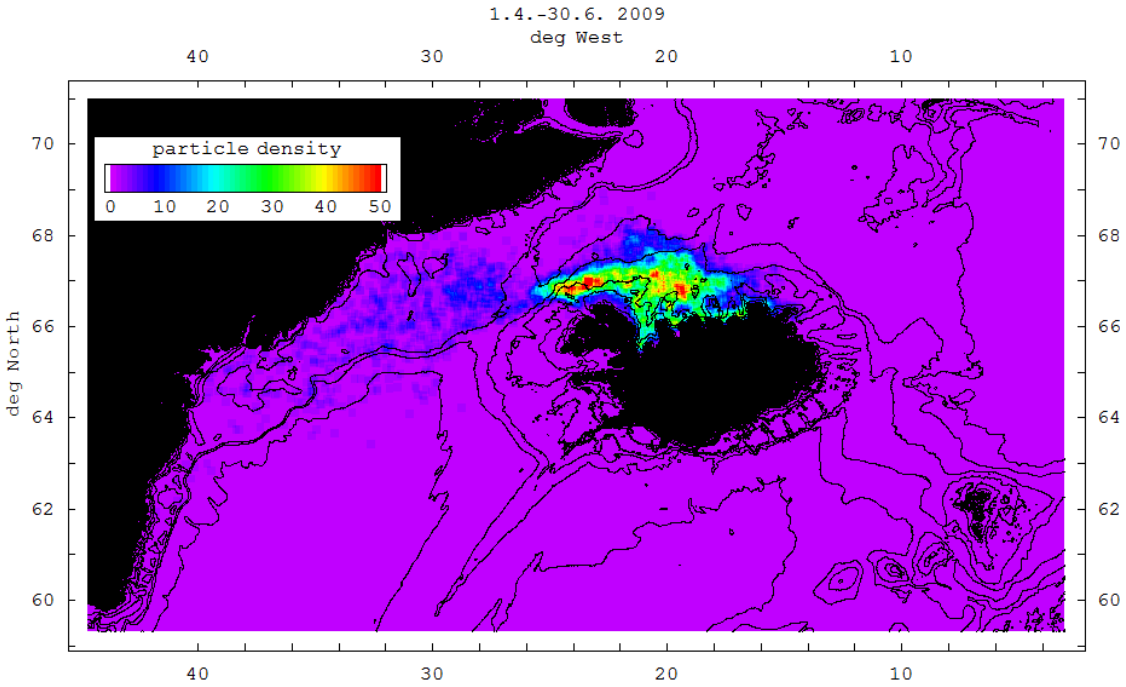

Fig. A1.21: Particle density at the end of the spring 2009 simulation.

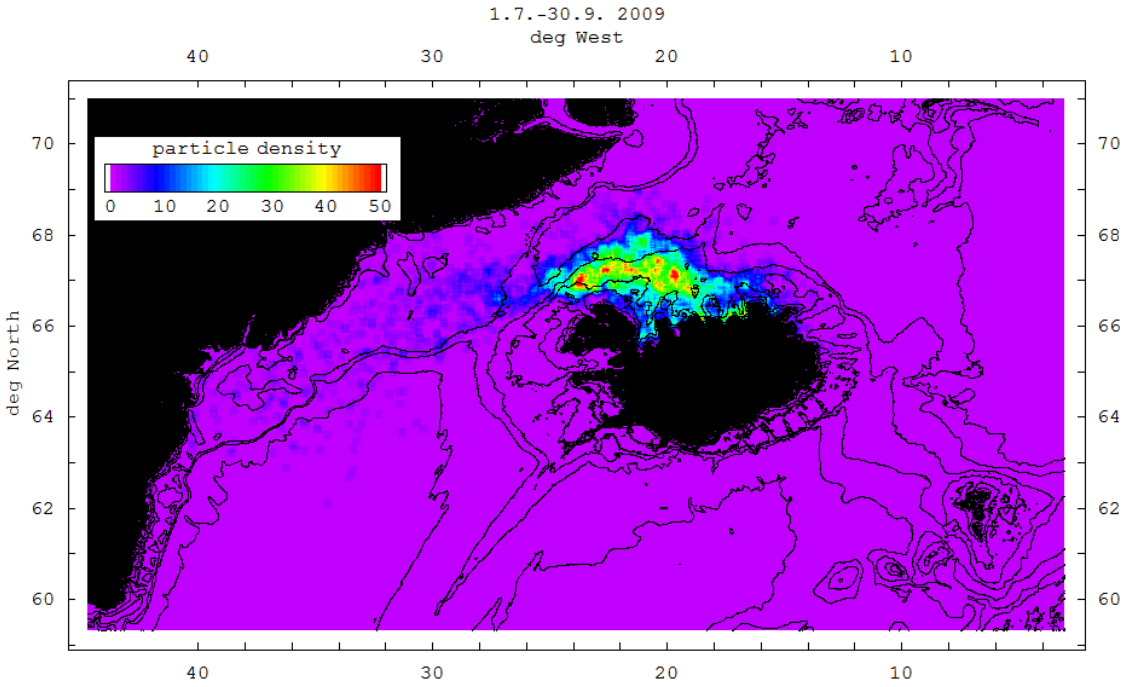

Fig. A1.22: Particle density at the end of the summer 2009 simulation.

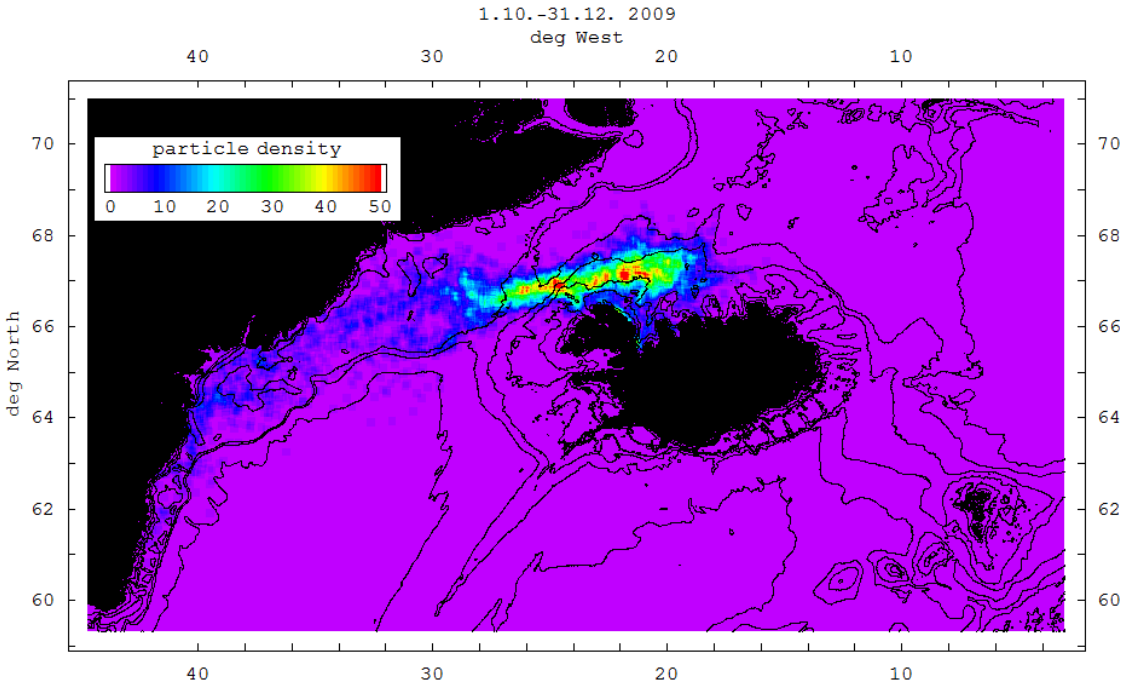

Fig. A1.23: Particle density at the end of the autumn 2009 simulation.

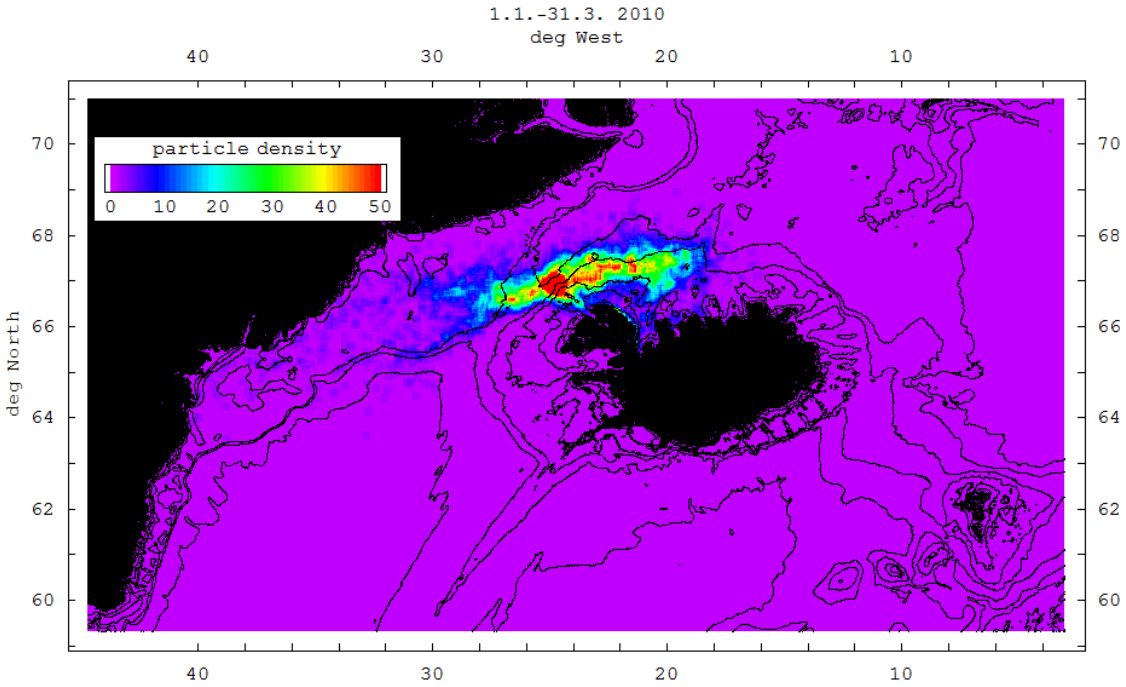

Fig. A1.24: Particle density at the end of the winter 2010 simulation.

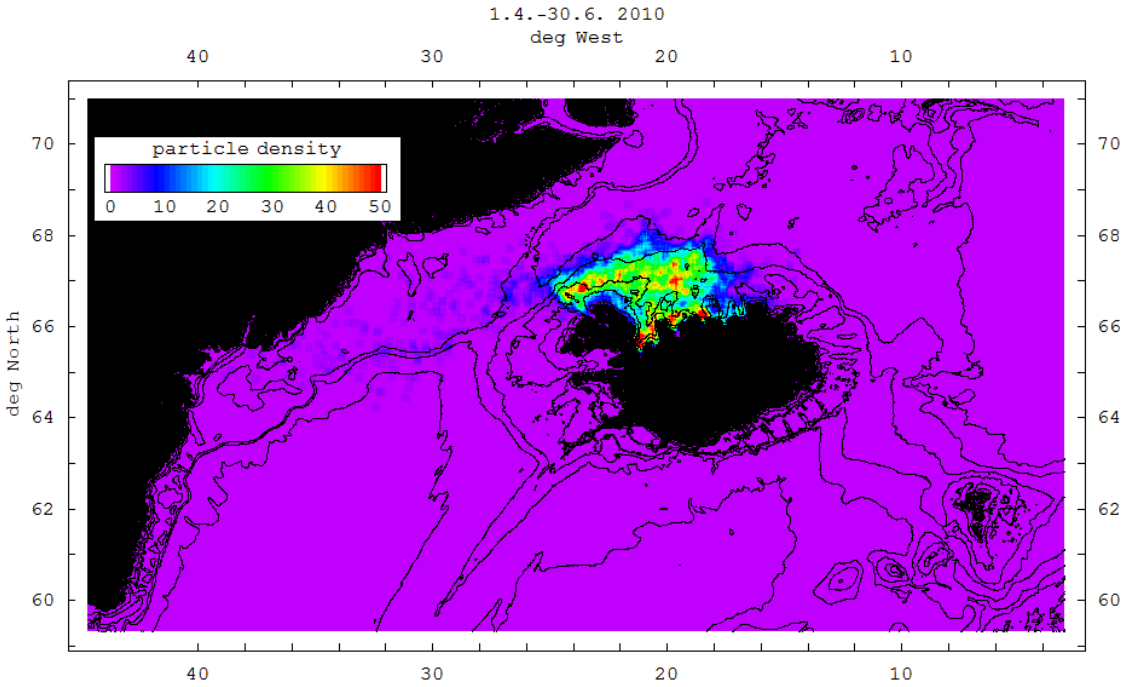

Fig. A1.25: Particle density at the end of the spring 2010 simulation.

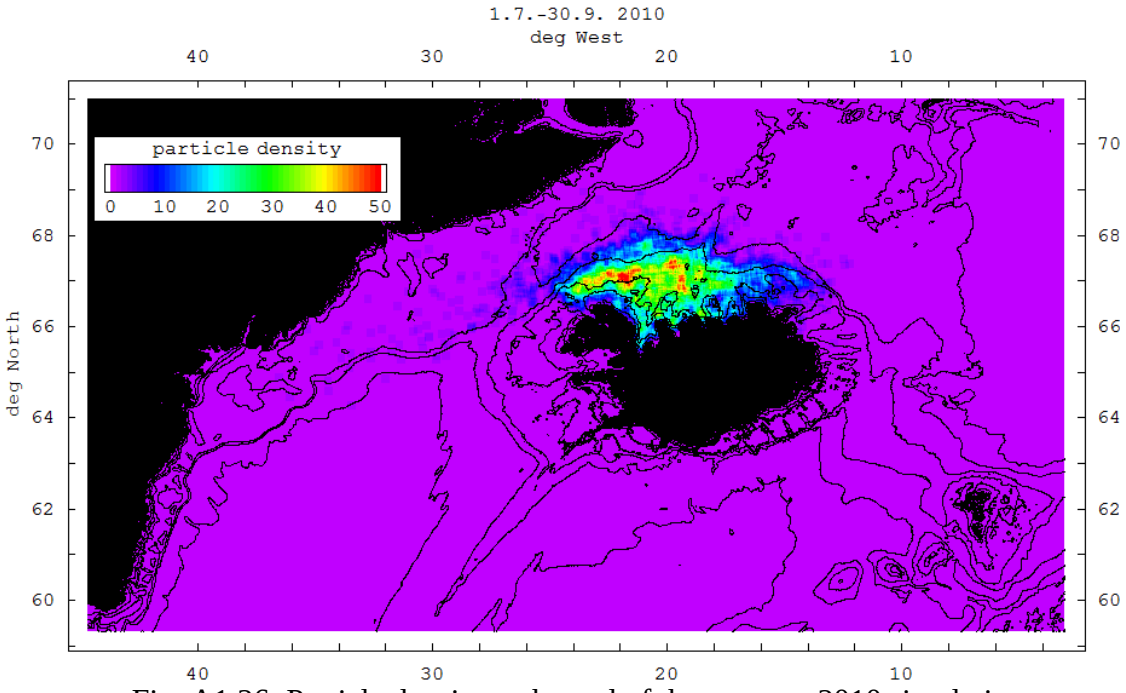

Fig. A1.26: Particle density at the end of the summer 2010 simulation.

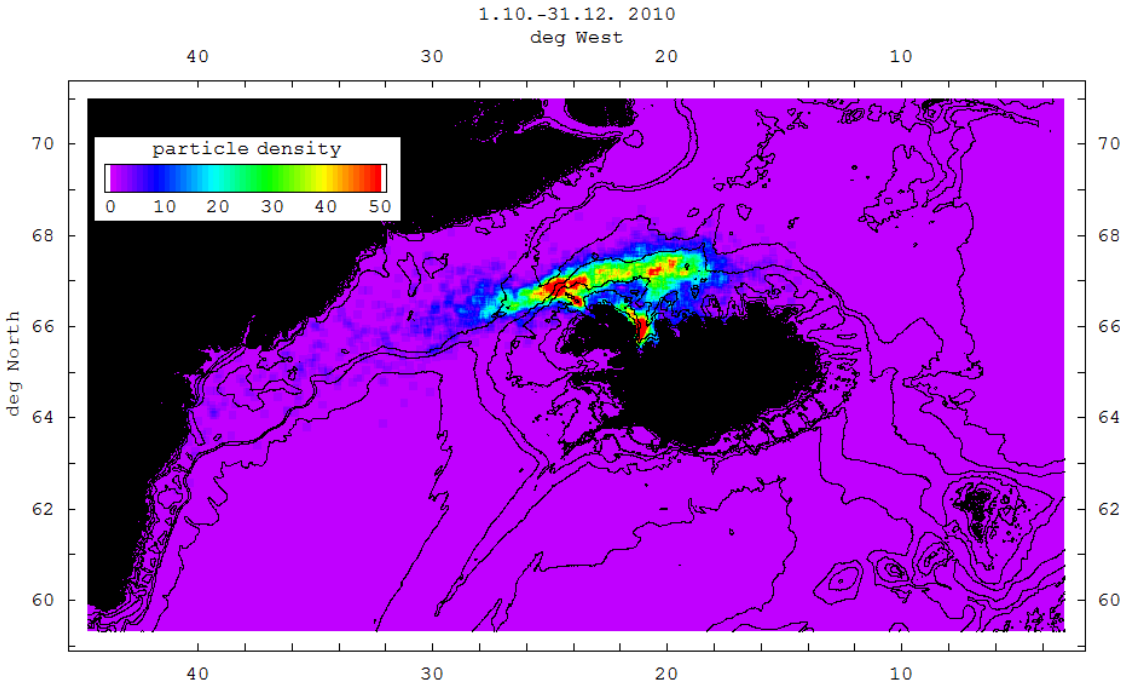

Fig. A1.27: Particle density at the end of the autumn 2010 simulation.

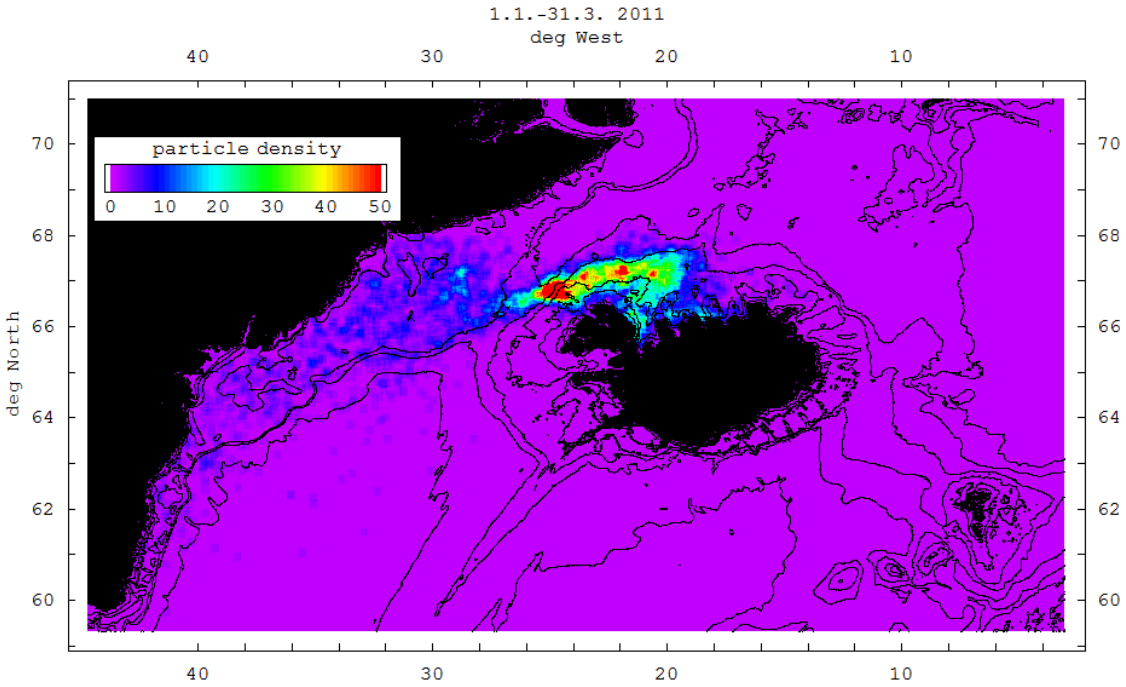

Fig. A1.28: Particle density at the end of the winter 2011 simulation.

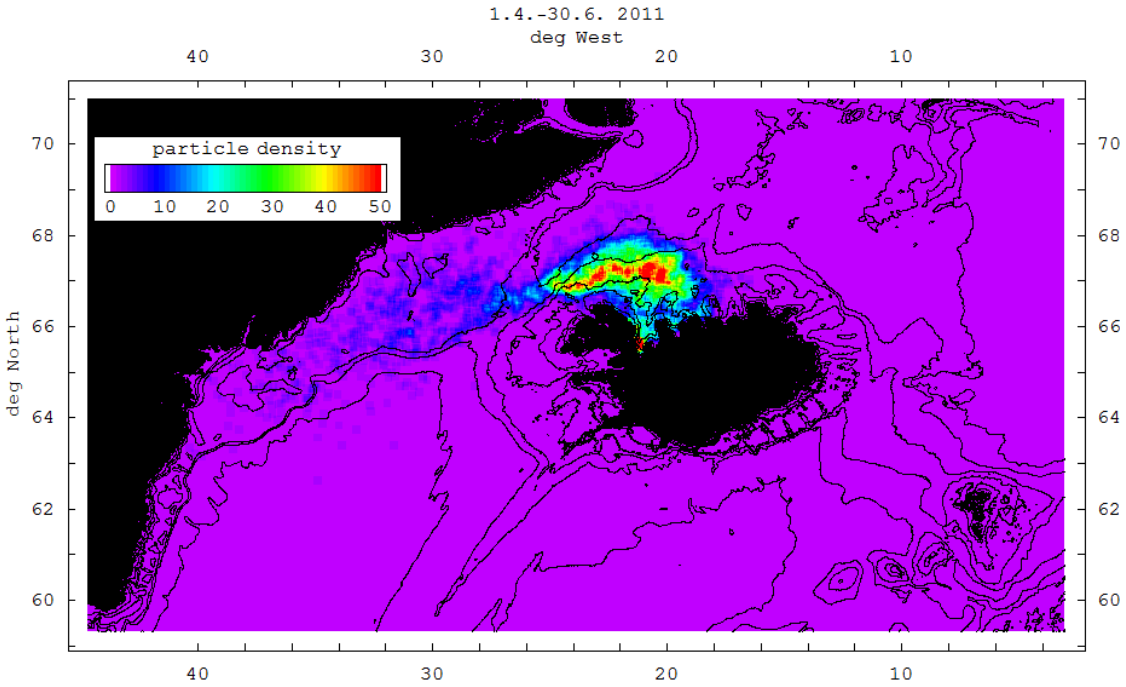

Fig. A1.29: Particle density at the end of the spring 2011 simulation.

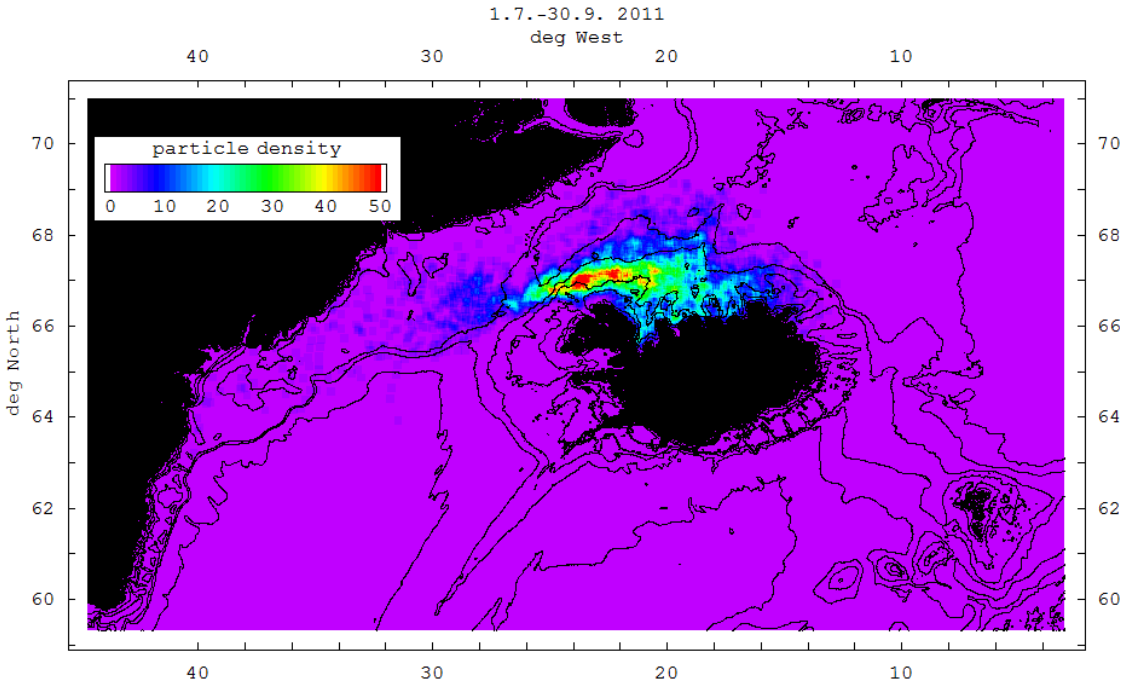

Fig. A1.30: Particle density at the end of the summer 2011 simulation.

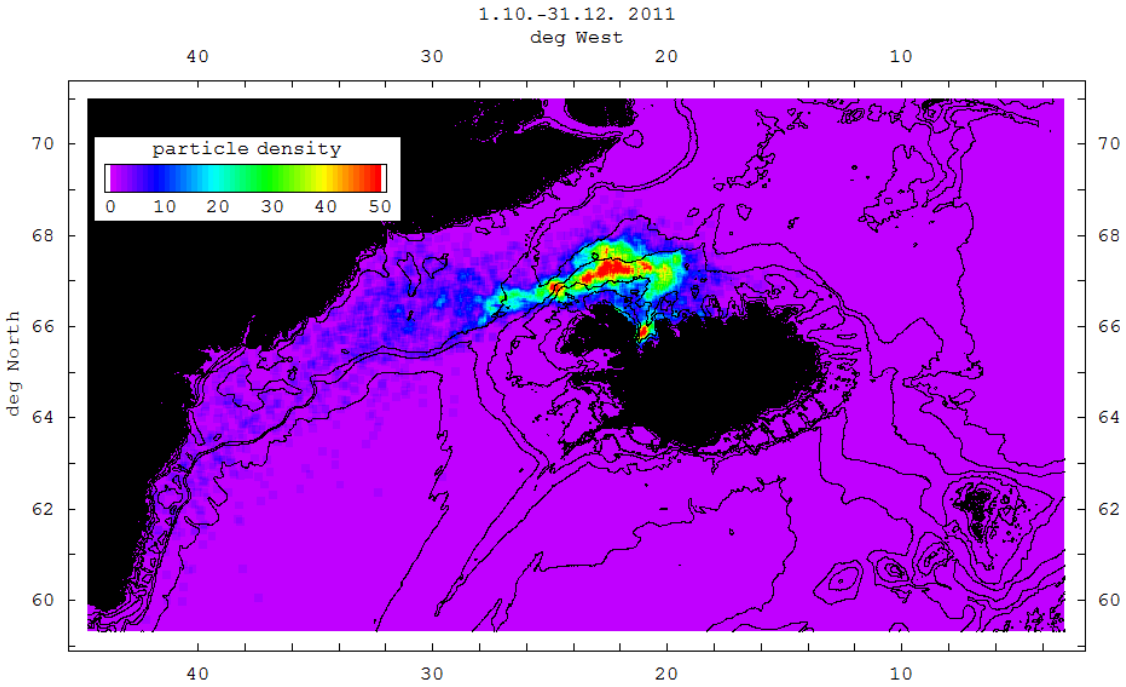

Fig. A1.31: Particle density at the end of the autumn 2011 simulation.

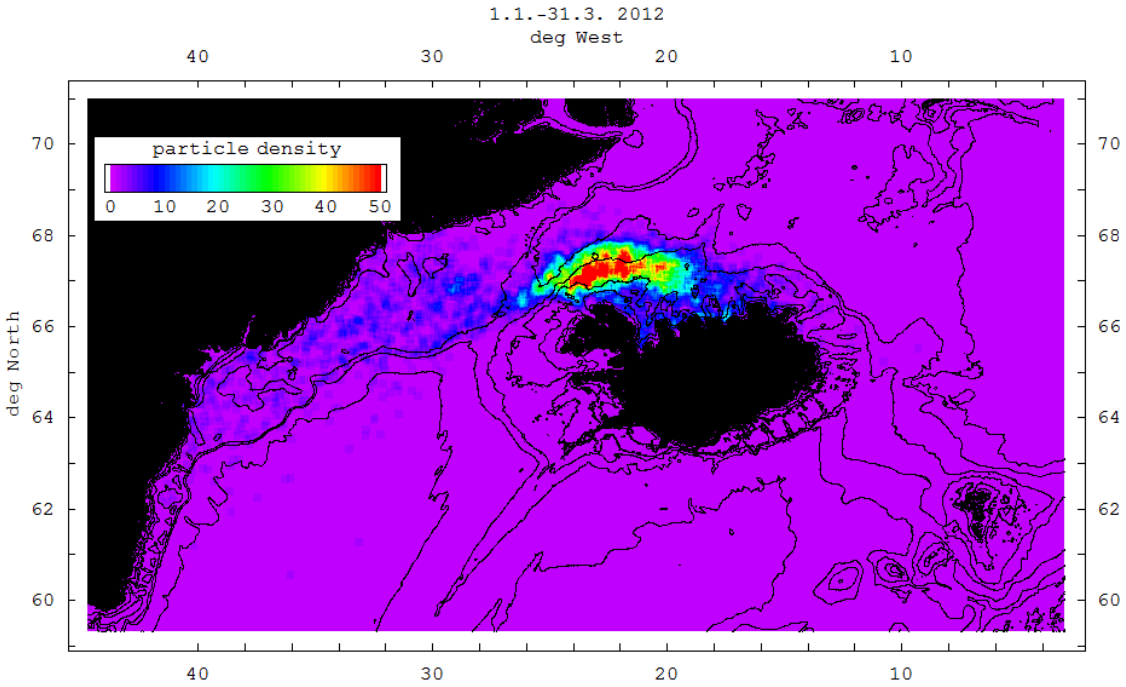

Fig. A1.32: Particle density at the end of the winter 2012 simulation.

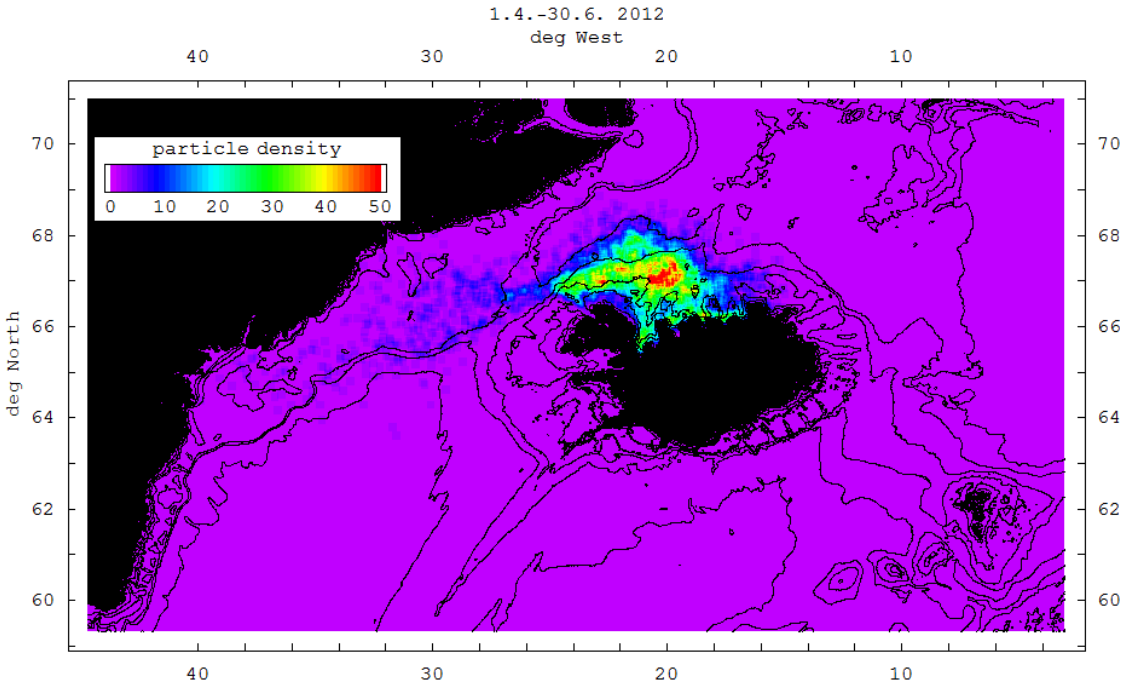

Fig. A1.33: Particle density at the end of the spring 2012 simulation.

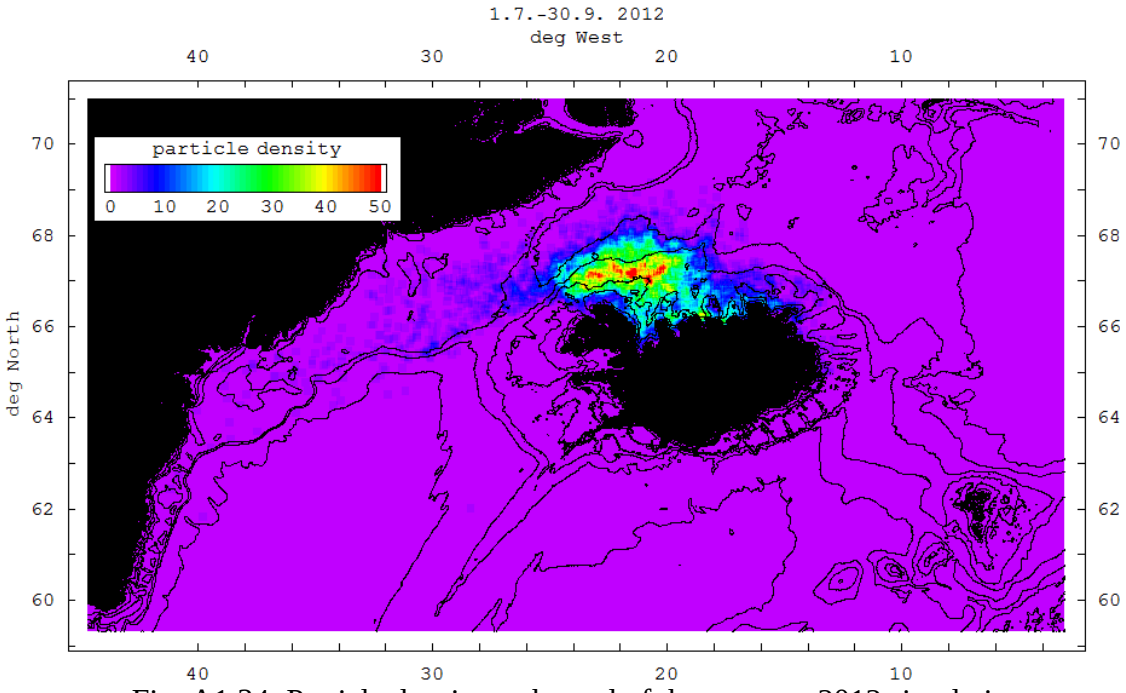

Fig. A1.34: Particle density at the end of the summer 2012 simulation.

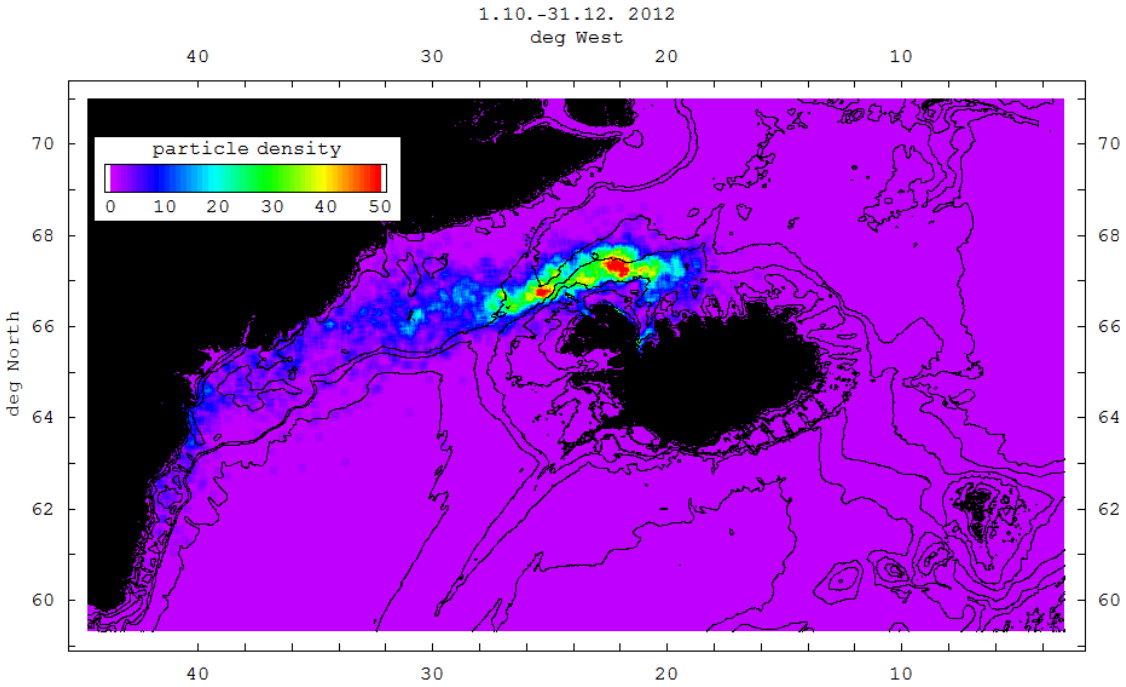

Fig. A1.35: Particle density at the end of the autumn 2012 simulation.

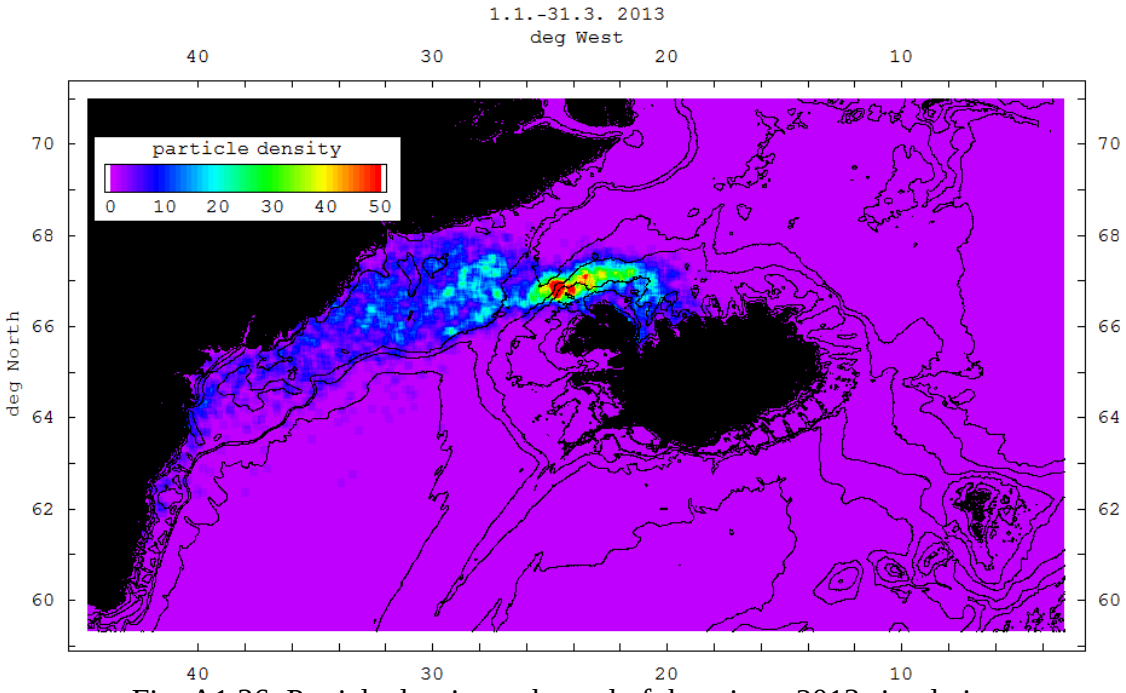

Fig. A1.36: Particle density at the end of the winter 2013 simulation.

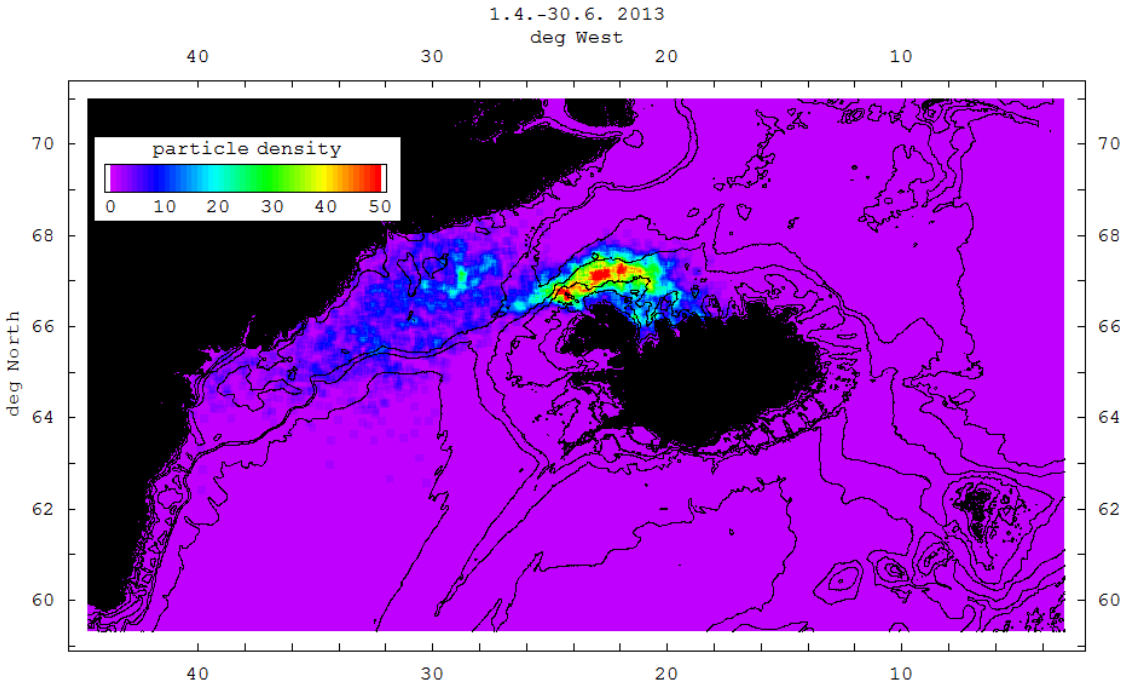

Fig. A1.37: Particle density at the end of the spring 2013 simulation.

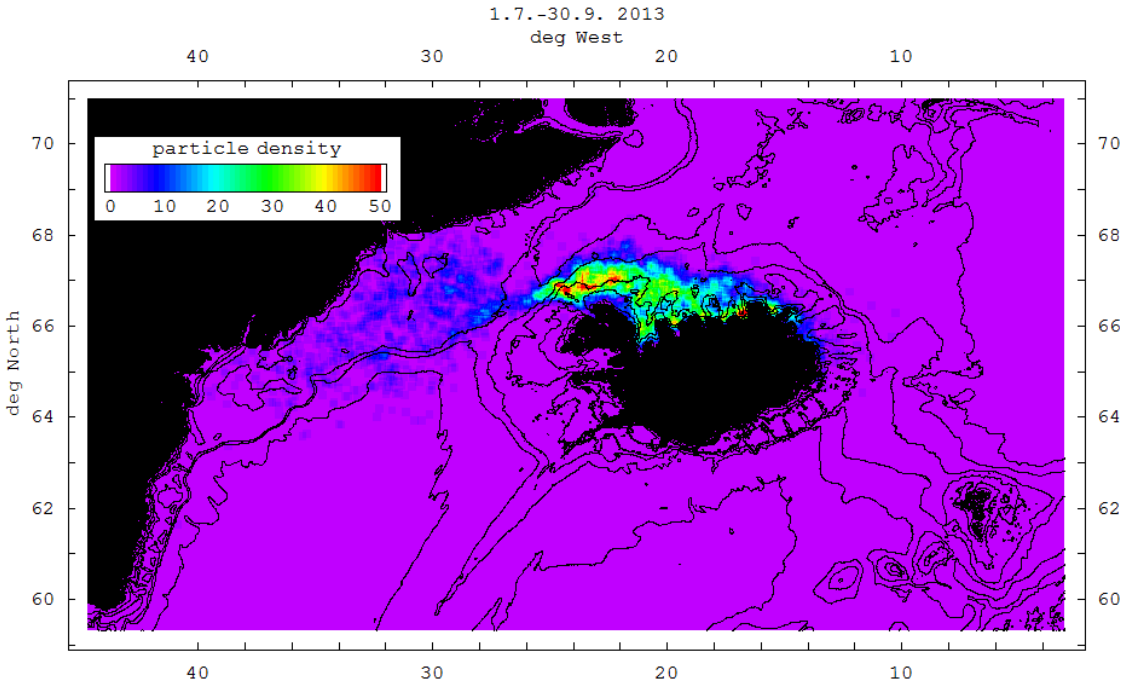

Fig. A1.38: Particle density at the end of the summer 2013 simulation.

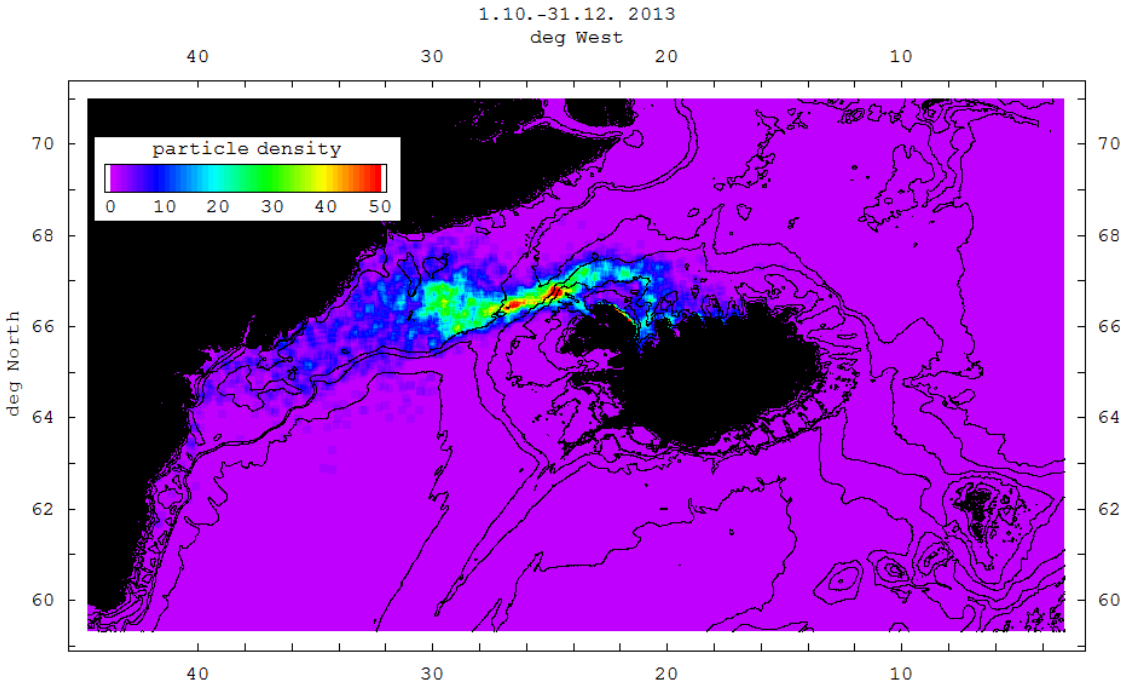

Fig. A1.39: Particle density at the end of the autumn 2013 simulation.

Appendix 2. NRPA box model description

The present model uses a modified approach for compartmental modelling (Iosjpe et al., 2002, 2009; Iosjpe, 2006) which allows the study of dispersion of radionuclides over time (non-instantaneous mixing in the oceanic space). The box structures for surface, mid-depth and deep water layers have been developed based on the description of polar, Atlantic and deep waters in the Arctic Ocean and the Northern Seas and site-specific information for the boxes generated from the 3D hydrodynamic model NAOSIM (Karcher and Harms, 2000). Surface structure is presented in Fig. A2.1.

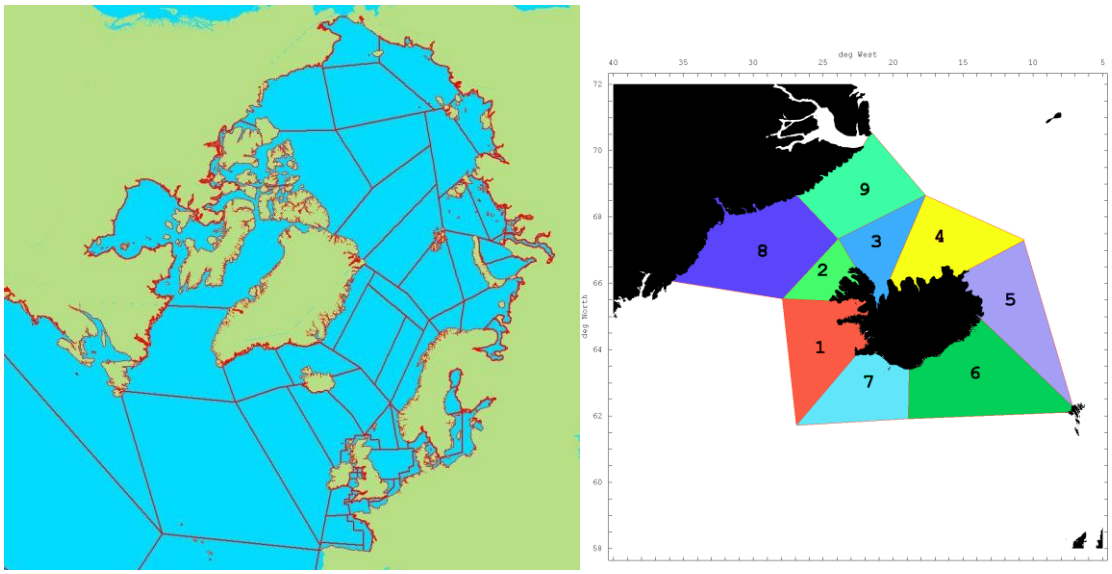

Figure A2.1. The structure of the surface water boxes for the NRPA box model and for the regional model for the Iceland coastal waters (COSEMA model).

The box model includes the processes of advection of radioactivity between compartments, sedimentation, diffusion of radioactivity through pore water in sediments, particle mixing, pore water mixing and a burial process of radioactivity in deep sediment layers. Radioactive decay is calculated for all compartments. Accumulation of contamination by biota is further calculated from radionuclide concentrations in filtered seawater in different water regions. Doses to humans are calculated on the basis from given seafood consumptions, based on available data for seafood catches and assumptions about human diet in the respective areas. Dose rates to biota are developed on the basis of calculated radionuclide concentrations in marine organisms, water and sediment, using dose conversion factors. Its structure is presented in Fig. A2.2.

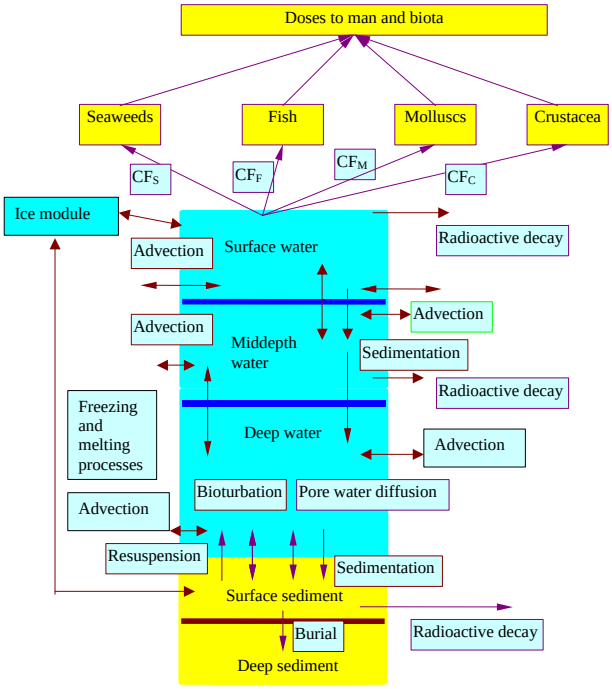

Figure A2.2. A schematic structure of the processes involved in modelling.

The equations of the transfer of radionuclides between the boxes are of the form:

$$\frac{dA_i}{dt} = \sum_{j=1}^{n} k_{ji} A_j \gamma[t \geq (T_j + w_{ji})] - \sum_{j=1}^{n} k_{ij} A_i \gamma[t \geq (T_i + w_{ij})] - k_i A_i \gamma(t \geq T_i) + Q_i, \; t \geq T_i$$

$$A_i = 0, \; t < T_i \qquad , \qquad (A1)$$

where $k_{ii}=0$ for all i, A_i and A_j are activities (Bq) at time t in boxes i and j; k_{ij} and k_{ji} are rates of transfer (y^{-1}) between boxes i and j; k_i is an effective rate of transfer of activity (y^{-1}) from box *i* taking into account loss of material from the compartment without transfer to another, for example radioactive decay; Q_i is a source of input into box i (Bq y^{-1}); n is the number of boxes in the system, T_i is the time of availability for box i (the first times when box i is open for dispersion of radionuclides) and γ is an unit function:

$$\gamma(t \geq T_i) = \begin{cases} 1, \; t \geq T_i \\ 0, \; t < T_i \end{cases}.$$

The times of availability T_i

$$T_i = \min_{\mu_m(v_0,v_i)\in M_i} \sum_{j,k} w_{jk}$$

are calculated as a minimized sum of the weights for all paths $\mu_m(v_0,...,v_i)$ from the initial box (v_0) with discharge of radionuclides to the box i on the oriented graph G=(V, E) with a set V of nodes v_j correspondent to boxes and a set E of arcs e_{jk} correspondent to the transfer possibility between the boxes j and k (graph elements as well as available paths are illustrated by Figure A2.3). Every arc e_{jk} has a weight w_{jk} which is defined as the time required before the transfer of radionuclides from box j to box k can begin (without any way through other boxes). Weight, w_{jk}, is considered as a discrete function F of the water fluxes f_{jk}, f_{kj} between boxes j and k, geographical information g_{jk} and expert evaluation X_{jk}. M_i is a set of feasible paths from the initial box (v_0) to the box i (v_i).

It is interesting to note that traditional box modelling is a particular case of the present approach when all times of availability in (A1) are zero: $\{T_i\} = 0, i = 1,\ldots, n.$

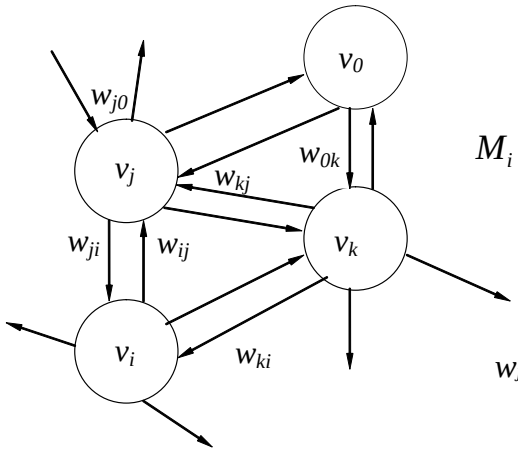

$$M_i = \begin{cases} \mu_1(v_0, v_j, v_i) \\ \mu_2(v_0, v_k, v_i) \\ \mu_3(v_0, v_j, v_k, v_i) \\ \mu_4(v_0, v_k, v_j, v_i) \end{cases}$$

$$w_{jk} = F(f_{jk}, f_{kj}, g_{jk}, X_{jk})$$

Figure A2.3. Graph elements.

Expressions for the transfer rates of radioactivity between the bottom water and sediment compartments will be useful in the present analysis (the transfer rates are shown in Figure A2.4):

NKS-B EFMARE

$$k_{WS} = \frac{SR \cdot k_d}{d \cdot (1 + k_d \cdot SSL)} + \frac{D}{d \cdot h_S (1 + k_d \cdot SSL)} + \frac{R_T \cdot \omega \cdot h_S}{d \cdot (1 + k_d \cdot SSL)} + \frac{R_W \cdot \rho \cdot k_d \cdot (1 - \omega)}{d \cdot (1 + k_d \cdot SSL)}$$

$$k_{SW} = \frac{D}{h_S^2 \cdot [\omega + k_d \cdot \rho \cdot (1 - \omega)]} + \frac{R_T \cdot \omega}{\omega + k_d \cdot \rho \cdot (1 - \omega)} + \frac{R_W \cdot \rho \cdot k_d \cdot (1 - \omega)}{h_S \cdot [\omega + k_d \cdot \rho \cdot (1 - \omega)]}$$

$$k_{SM} = \frac{D \cdot \omega}{h_S^2 \cdot [\omega + k_d \cdot \rho \cdot (1 - \omega)]} + \frac{k_d \cdot SR}{h_S \cdot [\omega + k_d \cdot \rho \cdot (1 - \omega)]}$$

$$k_{MS} = \frac{D \cdot \omega}{h_S \cdot h_{SM} \cdot [\omega + k_d \cdot \rho \cdot (1 - \omega)]}$$

$$k_{MD} = \frac{k_d \cdot SR}{h_{SM} \cdot [\omega + k_d \cdot \rho \cdot (1 - \omega)]}.$$

Here k_{WS} is composed of expressions describing the transfer of activity by sedimentation, molecular diffusion, pore water mixing and particle mixing, respectively. Similarly, k_{SW} is composed of expressions describing the transfer of radioactivity by molecular diffusion, pore water mixing and particle mixing. k_{SM} is composed of expressions describing the transfer of radioactivity by sedimentation and molecular diffusion. k_{MS} corresponds to the transfer by molecular diffusion. Finally, k_{MD} corresponds to the transfer of radioactivity by sedimentation. R_W (m y^{-1}) is the sediment reworking rate; R_T (y^{-1}) is the pore-water turnover rate; k_d (m^3 t^{-1}) is the sediment distribution coefficient; *SSL* (t m^{-3}) is the suspended sediment load in the water column; *SR* (t m^{-2} y^{-1}) is the sedimentation rate; *D* (m^2 y^{-1}) is the molecular diffusion coefficient, h_S (m) and h_{SM} (m) are the surface and middle sediment thickness respectively; ω is the porosity of the bottom sediment; ρ (t m^{-3}) is the density of the sediment material and *d* is the depth of the water column.

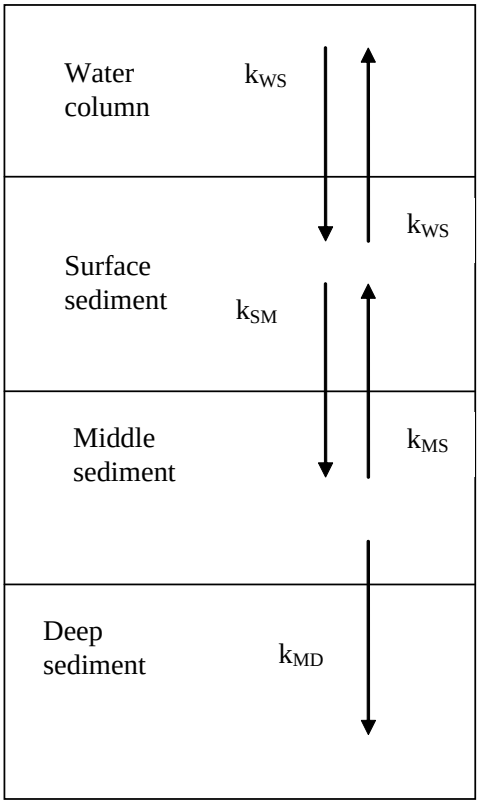

Figure A2.4. Generic vertical structure of the water-sediment compartments.

References

Iosjpe M., 2006. Environmental Modelling: Modified Approach for Compartmental Models. In: Radionuclides in the Environment. Edd. P.P. Povinec, J.A. Sanchez-Cabeza. Radioactivity in the Environment, vol. 8, Series Editor: M.S. Baxter, 2006, 463-476.

Iosjpe M., Brown J. & Strand P. (2002). Modified Approach for Box Modelling of Radiological Consequences from Releases into Marine Environment, Journal of Environmental Radioactivity, Vol. 60, No 1-2, 91-103.

Iosjpe M., M. Karcher, J. Gwynn, I. Harms, R. Gerdes and F. Kauker (2009). Improvement of the dose assessment tools on the basis of dispersion of the ^{99}Tc in the Nordic Seas and the Arctic Ocean. *Radioprotection*, vol. **44**, n^{o} 5, 531-536.

Karcher M.J. and Harms I.H., 2000. Estimation of water and ice fluxes in the Arctic for an improved box structure of the NRPA box model. In: Iosjpe M. (Ed.): Transport and fate of contaminants in the Northern Seas, NRPA, 2000.

Appendix 3. The biological half-life for species and effective half-life of Cs-137 for the Baltic Sea

The biological half-life of Cs-137 in primary producers and the effective half-lives of Cs-137 in surface water in different basins of the Baltic Sea are shown below.

Table A3.1. Effective half-lives of Cs-137 in surface water. Data is taken from HELCOM MORS Baltic Sea Environment Proceedings No. 135.

Baltic Sea Region	1986-1988	1993-2006	1993-2010
Bothnian Bay	-	10	9
Bothnian Sea	2.5	9	9
Gulf of Finland	0.8	13	11
Baltic Sea proper	-	15	11

Table A3.2. The biological half-life of Cs-137 in primary producers. Data taken from U.S. Environmental Protection Agency 1986 520/1-85-015. (algae)

Organism	Biological half-life in days
Ulva lactuca	5
Codium decorticatum	15
Fucus vesiculosus	8
Porphyra umbilicalis	3
Chondrus crispus	2
Gracilaria foliifera	12
Agardhiella tenera	21
Halimeda incrassata	3

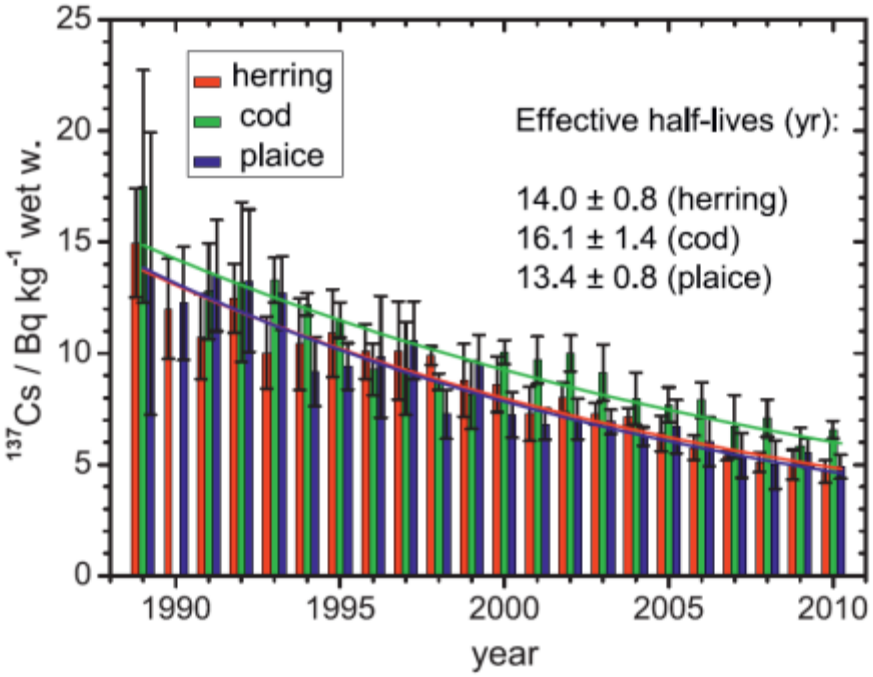

Figure A3.1. Effective half-lives for fish for the Poland coastal waters.

Bentic fish consumption.

It is estimated that the fish consumption consist of 80% zooplankton, 10% benthic plants, 5% benthos and 5% grazing macrofauna (Kumblad et al., 2003).

References

Kumblad L., Gilek M., Næslund B., Kautsky U. (2003). An ecosystem model of the environmental transport and fate of carbon-14 in a bay of the Baltic Sea, Sweden, Ecological modelling 166 (3), 193-210, 2003.

Appendix 4. Some results of radiological analysis for the Icelandic coastal waters from the COSEMA project

A4.1 Doses to the critical group

The total dose to the critical group is of 110 µSv y^{-1} The dose from Te-132 to the critical group is of; 8E-07 µSv y^{-1}

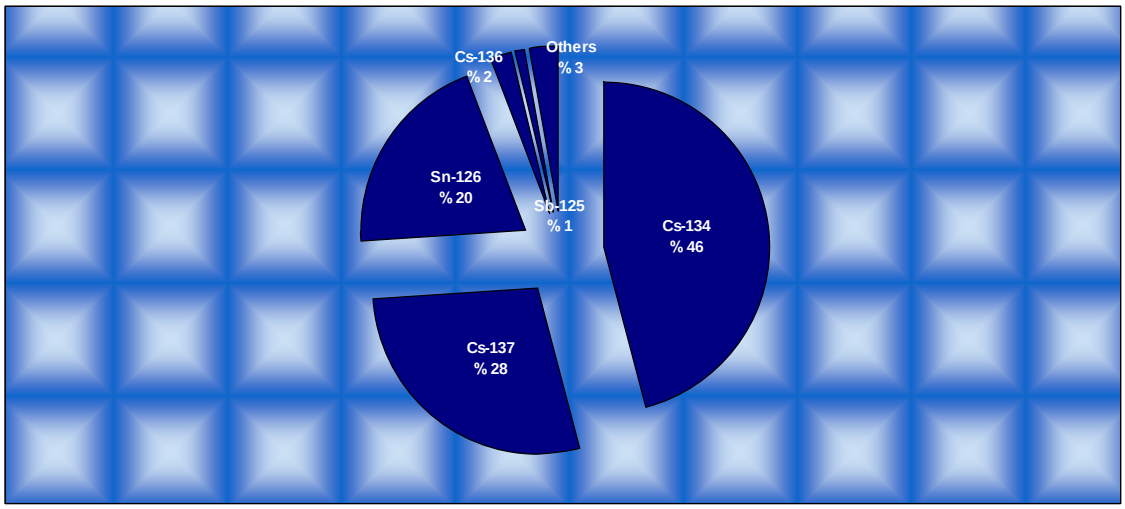

Figure. A4.1. Potential dose impact to the critical group from fish

A4.2 Concentrations of radionuclides in seafood

The Food and Agriculture organisation of the United Nations and World Health Organisation have provided recommendations (guideline levels) for the maximum permissible concentration of radionuclides in foods, when contaminated after an accidental release of radionuclides (CAC, 2006). According to the Codex Alimentarius Commission (CAC, 2006) radionuclides can be separated into four groups. Examples of some typical radionuclides for each group are presented in Table A4.1.

Table A4.1 Examples of international guideline levels for radionuclides in food.

Radionuclides in Foods		Guideline Level (Bq/kg)	
		Infant Foods	Other Foods
Group 1	^{238}Pu, ^{239}Pu, ^{241}Am	1	10
Group 2	^{90}Sr, ^{106}Ru, ^{129}I	100	100
Group 3	^{60}Co, ^{134}Cs, ^{137}Cs	1000	1000
Group 4	^{3}H, ^{14}C, ^{99}Tc	1000	10000

Following the CAC (2006) recommendations, the model calculations for fish, crustaceans and molluscs are provided separately for each group of radionuclides presented in Table A4.1.

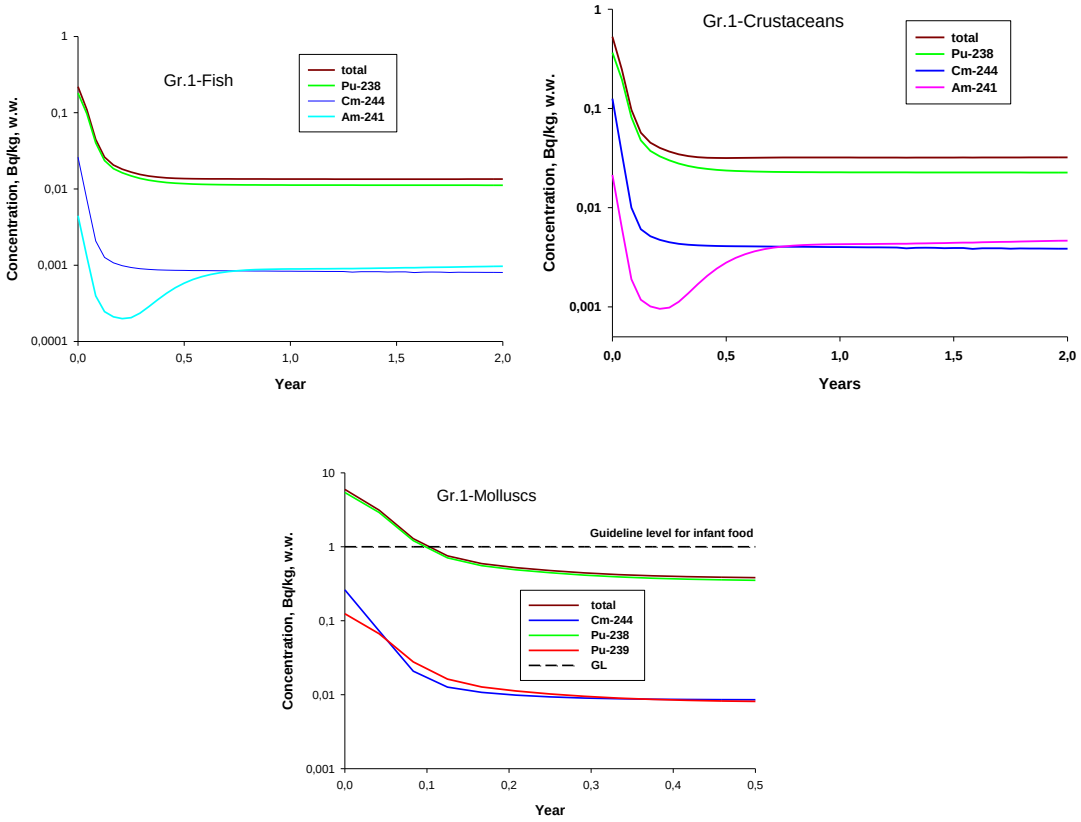

Figure A4.2. Predicted concentration of radionuclides (Group 1) in sea food.

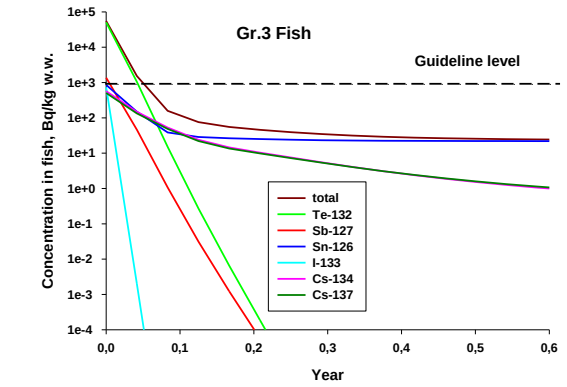

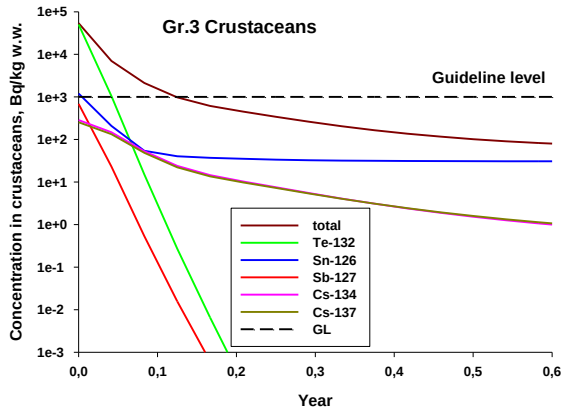

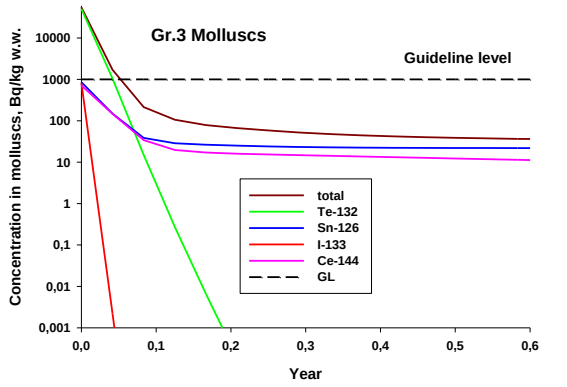

Figure A4.3. Predicted concentration of radionuclides (Group 3) in seafood.

Referances

COSEMA, 2014. Consequences of severe radioactive releases to Nordic marine environment. Final report for the NKS-B COSEMA activity 2013, Contract AFT/B(13)3.

Bibliographic Data Sheet **NKS-358**

Title	Effects of dynamic behaviour of Nordic marine environment to radioecological assessments
Author(s)	Iosjpe[1] M., Isaksson[2] M., Joensen[3] H. P., Jonsson[4] G., Logemann[5] K., Roos[6] P., Suolanen[7] V., Thomas[2] R.
Affiliation(s)	1 Norwegian Radiation Protection Authority, Norway 2 University of Gothenburg, Sweden 3 Fróðskaparsetur Føroya, Faroe Islands 4 Geislavarnir Rikisins, Iceland 5 University of Iceland, Iceland 6 Technical University of Denmark, Denmark 7 Technical Research Centre of Finland, Finland
ISBN	978-87-7893-442-0
Date	February 2016
Project	NKS-B / EFMARE
No. of pages	82
No. of tables	7
No. of illustrations	87
No. of references	27

Abstract
max. 2000 characters

The goal of the EFMARE project is an analysis of consequences of radioactive releases into marine environment with special attention to the effects of the dynamic behaviour of the Nordic seas to radioecological assessments.

The main goals for the EFMARE project is development and implementation of the bioaccumulation process into the models, improvement of the models, comparison with previous results and testing of the influence of the time of an accident for the radioecological consequences.

Results of implementation of the kinetic model for bioaccumulation processes into the NRPA box model and the DETRA computer code clearly demonstrated that there is a significant quantitative difference between the kinetic modelling approach and the approach based on the constant concentration rates.

Results of modelling were compared with experimental data on the basis of improved version of the NRPA box model for the Baltic Sea. It is clear demonstration that dynamic modelling of the bioaccumulation processes can provide a more correct description of the concentration of radionuclides in biota and, therefore, these results support the main goal of the EFMARE project.

It is shown that the improved modelling approach for radioecological assessment indicates significant differences between results based on constant concentration factors (CF) and the description of bioaccumulation process with a kinetic submodel. Also, kinetic modelling of bioaccumulation processes leads to a better harmonisation between the different end points calculations (for example, between doses to the critical group and concentrations in marine organisms for short-life radionuclides), and also to better logical explanations of the results.

With a numerical case study the temporal variability of pollutant dispersal in Icelandic waters was demonstrated and discussed. The results emphasize the necessity to use operational hydrodynamic ocean models in order to forecast pollutant dispersal in Icelandic waters.

The use of particle density can be used for comparison with simulations from the NRPA box model.

Key words marine environment, hydrodynamic and box modelling, bioaccumulation submodel, accidents, radioecological consequences

Available on request from the NKS Secretariat, P.O.Box 49, DK-4000 Roskilde, Denmark.
Phone (+45) 4677 4041, e-mail nks@nks.org, www.nks.org